Ingress of External Contaminants into Buildings – A Review

D.J. Hall, A.M. Spanton
Envirobods Ltd.

December 2012

ABSTRACT

This review follows a request by ADMLC to examine models and methods for predicting the ingress of external contaminants into buildings. The primary interest is in internal exposure to releases of hazardous materials over relatively short time periods (up to about 24 hours) from a single source and of the nature of that exposure. Intentional or accidental release of airborne contaminants can have important impacts on buildings and pose a significant threat to their occupants. Conversely, buildings can also be used as 'shelters' from external exposure, depending on the nature of the rate of the internal air interchange with the outside.

The review examines the whole chain of processes from the external release of a contaminant, its dispersion and possible exposure of a building, the factors controlling the ingress of the contaminant, the ingress process itself, infiltration through gaps and cracks in the structure, the time dependent response of the ingress and internal losses of the contaminant. It also reviews calculation methods briefly.

This study was funded by the UK Atmospheric Dispersion Modelling Liaison Committee.

EXECUTIVE SUMMARY

This review follows a request by ADMLC to examine models and methods for predicting the ingress of external contaminants into buildings. The primary interest is in internal exposure to releases of hazardous materials over relatively short time periods (up to about 24 hours) from a single source and of the nature of that exposure. Intentional or accidental release of airborne contaminants can have important impacts on buildings and pose a significant threat to their occupants. Conversely, buildings can also be used as 'shelters' from external exposure, depending on the nature of the rate of the internal air interchange with the outside.

The subject has been partly covered in previous ADMLC reviews, by Robins and Macdonald(2000), Colville et al(1997) and Milner et al(2004), but there has been no previous attempt to cover the whole process in an integrated way, as here. There have also been further developments in methodology and the availability of more diverse experimental data since this earlier work.

Exposure within a building to an external contaminant is the end result of a chain of processes from the original release to the ultimate internal exposure. The main parts of this chain are:

- The dispersion of the source of contaminant towards the building.
- The probability of the building being exposed to the release.
- The pattern of the contaminant concentration on the building façade.
- The building ventilation and infiltration processes that carry the material indoors.
    - This is driven by a mixture of buoyancy forces, from internal/external temperature differences, wind pressure patterns and any mechanical ventilation process that may be in action.
- The process of ingress of contaminant, which depends on a combination of the concentration and pressure patterns on the building envelope and the nature of the openings in the building envelope.
- The time dependence of the process of ingress and egress of contaminant, which partly governs internal exposure to time dependent releases.
- Internal losses either by external reaction or to the building's internal surfaces by absorption and deposition.

These processes are covered in turn in this review, to provide a full description of the process of contaminant ingress and internal exposure so that they can be viewed in perspective. All of these matters are also minor or major disciplines in their own right and have a significant literature. It has not therefore been possible to cover any specific matter in detail and this review has chosen to highlight the more critical matters important here, leading to the eventual internal exposure.

The review has also covered calculation and modelling methods. Since these too are major disciplines in their own right, and have been partly covered in previous reviews, they are again dealt with only briefly here.

CONTENTS

1 NOTATION

A	Surface area of openings in building envelope.
A_f	Building floor area.
A_{Total}	Total external surface area of all or part of a building.
ACH	Air changes per hour, commonly used for expressing building ventilation rate.
ACH_{50}	Air changes per hour in building when pressurized to 50 Pa.
C	Local concentration.
C_e	Local external concentration on building surface.
C_i	Internal concentration (inside building).
C_o	External concentration (outside building).
C_p	Pressure coefficient.
C_{pi}	Internal pressure coefficient (inside building).
D	Deposition rate.
ELA	Effective leakage area on building surface.
g	Gravitational acceleration.
h	Height.
H	Building height.
I_R	Risk index.
k	Discharge coefficient.
K	Dimensionless concentration.
L	Dimensional scale, usually of a building size.
M	Rate of contaminant ingress.
n	Exponent in surface ventilation or infiltration rate calculation.
NL	Normalised leakage.
p	Pressure.
p_h	Pressure at height h inside building.
p_i	Internal pressure inside building.
p_{ref}	Reference pressure.

p_0	Total (stagnation) pressure.
Δp	Pressure difference.
Q	Source emission rate of contaminant.
$R_{a,b,s}$	Particle deposition resistances; aerodynamic, sublayer and surface respectively.
sgn	'Signum' function, giving the sign of a number or function.
T	Temperature.
T_h	Temperature at height h inside building.
T_0	Temperature at the ground or external to a building.
u_*	Aerodynamic friction velocity.
U	Wind speed.
v_d	Deposition velocity.
v_s	Gravitational settling velocity.
V	Volume flow rate.
V_b	Total air ingress volume flow rate.
V_{50}	Volume flow rate at 50 Pa pressure difference in airtightness test.
W	Width of courtyard.
z_0	Aerodynamic surface roughness length.
ρ	Air density.
τ	Characteristic time response of building ventilation.
$\Delta\rho$	Air density difference from ambient.

2 INTRODUCTION

This review follows a request by ADMLC to examine models and methods for predicting the ingress of external contaminants into buildings. The primary interest is in internal exposure to releases of hazardous materials over relatively short time periods (up to about 24 hours) from a single source and of the nature of that exposure. Intentional or accidental release of airborne contaminants can have important impacts on buildings and pose a significant threat to their occupants. Conversely, buildings can also be used as 'shelters' from external exposure, depending on the nature of the rate of the internal air interchange with the outside.

This is one of two main current concerns over the impact of external contaminants on the internal environment. The second is the broader-based relationship between indoor and outdoor air quality and the way in which indoor exposure is controlled by the combination of internal and external sources and sinks of contaminants. Both concerns require a clear understanding of building ventilation processes and external exposure, especially of the ingress of external contaminants controlled by these processes.

There have been three previous reviews for ADMLC close to this topic; by Robins and Macdonald(2000), dealing with dispersion near groups of buildings, by Colville et al(1997), which partly dealt with external exposure of buildings, and by Milner et al(2004), which dealt more directly with the problem in hand, but in limited detail. There have also been some related reviews, of dispersion of accidental releases in urban areas by Hunt et al(2002), and for dealing with releases in the vicinity of buildings by Walsh and Jones(2002).

The present review adds to this earlier work, examining the relationship between external and internal exposure and methods of estimating it. These involve understanding the process of contaminant ingress as well as the nature of external exposure of buildings. The approach is essentially practical, noting the methods that can readily be used, their limitations and what sources of information are available.

Nearly all buildings operate with their internal atmospheres in some sort of dynamic equilibrium with the outside atmosphere. Air inside the building is usually exchanged with that outside, not only deliberately, controlled by various means in order to clear the internal air of internally generated pollutants or excess heat, but also adventitiously by infiltration, due to uncontrolled leakage paths in the building structure, through cracks, gaps and larger openings. The ventilation in most buildings is a mixture of these two processes. The relationship between internal and external levels of contaminants is a consequence of this equilibrium.

Contamination of the indoor environment is mainly governed by a combination of the pattern of contaminant concentration on the external surfaces and on the air exchange process described above. In principle, ingress of contaminants

occurs partially at air inlets in mechanically ventilated buildings and in areas where external pressure on the building surface is high in both mechanically and naturally ventilated systems. Similarly, contaminant egress occurs in areas where external pressure is low. In reality, this process is further complicated by the variability of wind speed and direction, temperature differences between the inside and outside of the building, and occupant activities, such as opening and closing of windows and doors.

Historically, exposure to pollutants internally and externally have been largely treated as separate activities. References to 'indoor pollution' in the external air pollution literature tend to discuss only internally generated pollutants (see, for example the current USEPA and WHO web sites on 'Indoor Air Quality' and 'Indoor Air Pollution' respectively). The concept of ingress of external pollutants was understood, but interest in their internal levels was limited at that time. Similarly, those concerned with ventilation and internally generated pollutants tended to regard the ventilation process as one of removing internally generated contaminants and replacing them with 'fresh' external air. Most dispersion measurements were (and to a large extent still are) concerned with concentrations at the ground rather than on building surfaces where infiltration might occur. The main internal interest in external pollutants was (and to an extent still is) with contamination of mechanical air inlets by local pollution sources.

Since around 2000, there has been a greater interest in both the indoor/outdoor exposure balance and in the nature of dispersion and exposure in urban areas, where most buildings are situated. Despite this, contaminant ingress remains an insufficiently investigated area and methods and models for predicting this behaviour are both few and uncertain; the disconnection between dispersion modelling and ventilation industry building ventilation practice is still largely apparent. Although there is a growing understanding of and published data on contaminant dispersion in urban areas, there is little understanding of the interactions between outdoor and indoor contaminant levels. The large amount of data on building ventilation does not generally consider this matter explicitly (except in particular cases) and there are fewer experiments dealing directly with the ingress of external contaminants.

This makes integrated calculations of building exposure and ingress particularly difficult. The previous ADMLC review (Milner(2004)) discussed some forms of external building exposure but provided only limited information on infiltration and the resultant internal exposure. However, more recent work has improved the state of knowledge in this area and provided simple methodologies for predicting ingress of external pollutants. There are also internal fire dispersion models which may be of interest, though these are not discussed here.

In view of the multidisciplinary nature of this problem and the probability that those with expertise on one aspect of it may not be well acquainted with another, brief reviews of the basic properties of both ventilation and infiltration and of the nature of external exposure are included here. Also, because a significant fraction of the work related to this problem is concerned with internal

exposure to conventional external pollutants, work in this area is described as well.

In the present review, we follow construction industry practice in referring to ventilation with regard to deliberate provision of ventilation air, and infiltration with regard to adventitious ventilation through cracks and gaps in the structure. The overall passage of air and contaminants into and out of buildings are referred to as ingress and egress respectively.

3 FUNDAMENTALS OF BUILDING VENTILATION AND INFILTRATION

This Section provides a brief introduction to building infiltration and ventilation, without which it may be difficult to follow other parts of this review. Sources of further information are given.

All buildings ventilate to some degree, ranging from carefully controlled systems to those with largely uncontrolled leakage and ventilation. The two main divisions are between 'mechanical' (forced air driven by fans) and 'natural' (driven by wind and buoyancy forces) ventilation. Irrespective of the intended method there is an additional ventilation process, of infiltration and exfiltration of air though adventitious openings, leakage paths, gaps and cracks in the structure, which nearly all except some specially designed structures experience.

A wide variety of ventilation and infiltration processes exist in practice. Some buildings (especially modern designs) are quite carefully designed for effective mechanical or natural ventilation, but many (especially older structures) are not. Others may have 'mixed mode' ventilation, a form of natural ventilation reinforced with some mechanical ventilation. It is also common for buildings to use different ventilation modes in different parts; using mechanical ventilation on some floors or only in workshops, a computer suite or a kitchen for example. Some sense of this variety of ventilation options can be found in CIBSE(2005a).

Thus some individual consideration usually needs to be given to the ventilation behaviour of different buildings. For the purposes of this present brief introduction the building is assumed to be empty internally.

Mechanically ventilated buildings usually have specific air inlets and exhausts and defined ventilation flow rates. This simplifies calculations of the ingestion and exhaust of contaminants due to this part of the ventilation process, as contaminant concentrations at the inlets are apparently all that is additionally required. However, this does not obviate the need for the additional calculation of infiltration and exfiltration though the structure, which can still occur. Some mechanically ventilated buildings balance the inlet and exhaust flows to try and provide a positive pressure through the structure, in which case only exfiltration through the structure can occur. However, this is not always successful as it depends both on a well balanced ventilation system and internal pressures high enough to overcome buoyancy and wind-driven pressure differences on the structure. This cannot always be guaranteed, especially in strong winds.

Natural ventilation and infiltration are driven by a combination of external pressures on the building envelope due to the wind and internal pressures from buoyancy forces due to internal/external temperature differences. Pressure differences due to buoyancy are sometimes called the 'stack effect' as they are due to the pressure difference caused by the density difference from the outside of the internal column of air. Some typical simplified diagrams of the process are shown in Figure 1. The diagrams assume that the internal temperature is

approximately constant and higher than outside, as is mostly (but not always) the case in temperate climates such as the UK. If the internal temperature is lower than outside, the buoyancy pressure differences are reversed and the infiltration and exfiltration patterns modified accordingly.

If the building is additionally mechanically ventilated, this may alter the internal/external pressure difference and thus the balance of the pressure differences across the building façade; the effect is the same as shifting the internal pressure line in the lower diagrams of Figure 1 along the horizontal axis. Since both the internal/external temperature differences and the wind speed may vary considerably, so does the relative balance between wind and temperature driven ventilation and infiltration. Figure 2, from Liddament(1996), is typical of diagrams showing this variation and shows the ventilation rate (as 'air changes per hour', ach) as a function of wind speed. The figures are typical of buildings of low to moderate height in the UK and show a number of interesting properties of building ventilation.

In the simple model, buoyancy driven ventilation rates depend only on the internal/external temperature difference and are thus independent of wind speed, as in Figure 2. Wind driven ventilation rates are approximately proportional to wind speed and thus produce the nearly straight lines on Figure 2. The variation due to the type of surface shown in Figure 2 is to account for the reduced wind speeds at higher levels of surface roughness. The ratio of surface roughness height between rural and urban surfaces is about 10:1, leading to a range of wind speeds (and subsequent ventilation rates) of around 2:1 at a fixed height, as in Figure 2.

Figure 2 also shows a critical wind speed above which the ventilation rate passes from buoyancy dominated to wind dominated, whose value depends on the internal/external temperature difference driving the buoyancy component of the ventilation and the varying wind speed due to differing surface roughness. There are two other important external variables controlling natural ventilation and infiltration rates. The first is building height. Increasing height increases both the buoyancy forces and the wind speed to which a building is exposed, generally increasing ventilation rates; in tall buildings the buoyancy forces can become quite large and can be a problem in controlling ventilation. The second is the effect of sheltering in urban areas, which further reduces the mean wind speed to which buildings are exposed, reducing the wind driven ventilation. This is discussed further later.

The plots in Figure 2 show a dip in the ventilation rate at the boundary between wind and buoyancy driven flows. The cause may be seen from inspection of the approximate ventilation patterns in Figure 1, which show that the two natural ventilation modes usually lead to different ventilation flow patterns. At the boundary the result can be a reduction in the overall ventilation rate, which is what is shown in Figure 2. This result is not inevitable and in some cases the two flows reinforce, producing a local enhancement in the ventilation rate around the boundary.

The boundary between buoyancy and wind driven ventilation in Figure 2 is shown to occur at wind speeds around 2-4 m s^{-1}, which is typical of UK behaviour in open terrain. Given that the median wind speed in Central England is about 3m s^{-1} at 10m height in open terrain, the implication is that most buildings in the UK commonly ventilate in both modes and probably for around half the time close to the boundary condition where both ventilation modes may be significant. The remarks above are mainly related to relatively isolated buildings. Besides the reduced mean wind speeds noted above, buildings in urban areas are also subject to additional sheltering from the wind by the other surrounding buildings. As a result critical wind speeds are further lowered and the frequency of buoyancy driven ventilation increased.

The building infiltration rates in Figure 2 are also typical of many UK buildings, in the range 0.25-1 ach, enhanced significantly in strong winds, for a 'sealed' building with doors, windows and ventilators closed. Once a number of doors and windows are opened the ventilation rate increases markedly, by up to an order of magnitude, and the difference between internal and external exposure starts to disappear. Traditionally, UK buildings have not been particularly well sealed compared with other countries with cool climates, such as Scandinavia and North America. However, growing pressure for improved energy efficiency and reduction of CO_2 emissions (around 40-50% of UK energy consumption is building related) has resulted in higher standards for control of building infiltration and ventilation (Building Regulations(2010)). This is having significant effects on new construction, but the high average age of the national building stock (ca 50 years) means that on average the values in Figure 2 have not altered much.

4 PRESSURE PATTERNS ON BUILDING SURFACES

4.1 Background

There have been two main sources of interest in the construction industry over building surface pressure patterns, for natural ventilation and infiltration and for structural loading and damage in strong winds. The latter has been by far the greater interest. A related interest has been in wind flow patterns around buildings, partly for problems of human comfort in strong winds or gusts, though these have not usually involved building pressure measurements. Very large numbers of building pressure measurements have been made for wind loading purposes worldwide, mainly in small scale wind tunnel experiments. Unfortunately most of this data has been commercial work for design purposes on idiosyncratic large new developments and has not become publicly available. However, there is a substantial body of useful published data, though as with dispersion data it tends to be somewhat disparate, so that systematic information on building types and urban layouts is less common.

Since natural ventilation and infiltration are driven by both internal buoyancy and external wind pressures, the contributions of both components are needed to calculate the total pressure difference across a building surface. Sources of information and calculation methods for finding these pressures are discussed below.

4.2 Buoyancy Induced Pressure Patterns

Buoyancy induced pressures on building surfaces are normally found by calculation. There seems to be no formal standard method for doing this. Simple calculations can be carried out on the basis of the pressure due to the buoyant gas column (the 'stack') within the building, assuming that it is internally well connected. The vertical pressure gradient is then linear if the internal temperature is constant and the pressure change, Δp, over a height, h, within the building is given (in many sources) by the usual simple expression,

$$\Delta p_h = hg\rho\left(\frac{T_h - T_o}{T_o}\right). \qquad (1)$$

Where g is the gravitational acceleration,
ρ is the air density (assumed constant for small temperature changes) and
T_h is the temperature at height h and T_o that at the ground.

In practice the internal pressure equilibrates to that outside at a 'neutral pressure point' at some height on the building (as in Figure 1), so that there is a negative pressure with respect to the outside at heights below this, causing an inflow, and a positive pressure at heights above this, causing an outflow. The height of the 'neutral pressure point' clearly depends on the distribution of

porosity and other openings over the building surface and the presence of deliberate openings for ventilation, but typically sits around 30% to 70% of the building height for tall structures and is usually above the mid height for low structures and domestic housing (ASHRAE(2009)). It is not affected by the temperature difference.

The simple case described above is formally for internally open structures, but is at least partially valid in zoned buildings with a high level of interconnection via stairwells and lift shafts etc. ASHRAE(2009) notes that multiple floors in a building can lead to a stepped vertical pressure profile (following the floor levels), but the overall pressure difference will remain about the same. Multizone structures only become significant when the pressure drop of the flow through the zones approaches that of the stack pressure. It is readily possible to carry out buoyancy-driven ventilation calculations on a spreadsheet in simple cases, by calculating an area-balanced ventilation and infiltration flow across the building envelope, which must sum to zero. This can include varying infiltration levels over different parts of the structure, specific openings and varying internal temperature over the building height.

More complex highly zoned structures are more likely to require use of a zonal model of some kind. Multicell and zonal model theory is discussed in Etheridge and Sandberg(1996) and Etheridge(2012); some models are discussed in Section 9. There is also now a much wider use of CFD modelling in calculating buoyancy-driven flows in complex internal environments. This is partly due to the improvements in CFD models in handling buoyancy forces, which some earlier CFD models did not properly use in the calculation, and partly due to a lack of any plausible alternative; it is difficult to set up small scale physical models of buoyancy driven dispersion. However, there can be difficulties in using CFD models reliably in buoyancy driven flows which are inherently unsteady, as commonly occurs. An example of a CFD buoyancy and wind driven flow calculation in a complex naturally ventilated building layout, due to Gan(2010), is shown in Figure 3.

A feature of buoyancy driven ventilation and infiltration that is not always appreciated is that the flow pattern generated by a temperature difference across a building structure may not be determinate. For example, an opening above the neutral pressure level in a building warmer than the outside may quite readily allow an outward buoyant flow of warm internal air or an inward flow of cooler, denser external air. This is especially so if there are effective stacks within the structure; a stair well or lift shaft can suffice. The flow pattern set up by the starting conditions can then remain stable.

4.3 Wind Induced Pressure Patterns

4.3.1 Background

The wide ranging and long running interest in wind induced pressure patterns on buildings, previously noted, has resulted in a quite large information base becoming available. Despite this, the great variety of practical building shapes

and urban layouts results in many idiosyncratic building topographies for which the available data base is of limited assistance. Individual assessments of building surface pressures therefore remain a common activity, especially where the building form is complex and/or has a high value. The discussion here is mainly aimed at the basic principles controlling pressure patterns and the accessible systematic data that is available. It starts by examining pressure patterns on isolated structures and then considers the effects of surrounding structures in urban areas.

The wind driven pressure patterns around buildings derive from the flow patterns. In isolated buildings, these derive from two main sources. Firstly, from the displacement of the wind around the building, generating deceleration on the upwind faces (and resultant high pressures) and acceleration around the roof and sides of the building (with resultant low pressures). Secondly, from the secondary effects of the basic flow patterns around the building, these are the horseshoe vortex around the upwind face of the building, strong trailing vorticity shed from sharp edges skewed to the flow and large scale separations on the building surfaces, mainly on the sides and downwind region. The three secondary components are sketched in Figure 4 (originally from Hall et al(1996b), also reproduced by Colville et al(1997)).

Most buildings exhibit regions of separated flow on their downwind faces most of the time, within which the variation in surface pressure is often small. The smaller separations, as on the sidewalls of the building in Figure 4, are more ephemeral. The other two secondary components are also more ephemeral, though their effects when present can be profound. The horseshoe vortex mainly occurs when the upwind face is nearly normal to the wind, once this face is skewed more than about 15º off the normal the flow tends to split around the upwind corner and the horseshoe vortex disappears. When present it can be enhanced or diminished by upwind structures depending on their relative size to the building; as, for example, Cook's(1985) illustration of the work of Penwarden and Wise, shown in Figure 5. Strong trailing vorticity is shed from sharp upwind corners skewed to the wind and can generate very low surface pressures locally; it is a common cause of roof damage in strong winds. It also modifies the surrounding airflow and can affect the form of the separation regions. Some complex roof shapes can generate quite spectacular trailing vortices. Equally, any change in the structure that alters the sharp wall/roof corner, for example by rounding it or by rebating the corner of the roof, can largely eliminate the trailing vortex. The horseshoe vortex around wide structures often shows some instability in turbulent shear flows, with trailing vortices occasionally being shed from the main vortex and passing over the obstacle, carrying plume material with them.

It is the sensitivity of flow patterns around buildings to the controlling variables that make general descriptions of pressure patterns uncertain except for some relatively simple cases of, say, rectangular structures. They depend strongly on the combination of the shape of the building, its surroundings and on the direction of the wind over it and are sensitive to small changes in these variables.

4.3.2 Pressure Patterns on Isolated Buildings

Some examples of mean pressure patterns around simple rectangular shapes are shown in Figures 6 to 9, derived from small scale experiments in wind tunnels. The pressures are given in the usual form of a pressure coefficient, $C_{p,}$ defined as.

$$C_p = \frac{p - p_0}{p_{ref} - p_0} = \frac{p - p_0}{\frac{1}{2}\rho U^2}, \qquad (2)$$

where p is the pressure on the building surface,
p_{ref} is the total (dynamic) pressure of the undisturbed wind and
p_0 is the static pressure in the undisturbed flow and
U is the reference wind speed based on p_{ref}.

Since buildings are exposed to the non-uniform wind and turbulence of a rough-wall atmospheric boundary layer flow, both in practice and in the usual form of wind tunnel experiments, the height at which p_{ref} is obtained affects the measurement. There is no formal standard for this, but it is most often at the height of the building a little way upwind; this should be confirmed for individual data (see, for example, BRE(1990, Part 6)). Similarly, there is no formal standard for measurement of p_0, but it is approximately constant over height in the undisturbed upwind flow. In a uniform flow the maximum value of C_p is about 1, at the flow stagnation point, but may vary depending on the height of the reference pressure measurement and the degree of turbulence in the flow. The lowest value can be below -2 near strong local trailing vortices, a major cause of roof damage in strong winds.

All four figures, 6 to 9, show the same basic characteristics of pressures on the upwind face of the building. The highest pressure, at the stagnation point of the flow where the flow divides around the building, is in a region fairly high up on the building face, at around two thirds to three quarters the building height; this applies both in the low, wide structures of Figures 6, 7 and 8, and in the tall, narrow structure in Figure 9. This high pressure region moves around the building towards the upwind corner as the wind direction varies. Figure 6 shows the pressures on all four faces of the building. Pressures on the walls approximately side-on to the wind show relatively low pressures in their upwind regions, increasing in the downwind direction. The rear-facing walls, being mostly within a separated flow, have relatively uniform pressures. The lower part of Figure 8 shows pressures on a building roof in different wind directions. Pressures are usually low in the upwind area of the roof and rise towards the downwind area. The two diagrams showing the flow around an upwind corner have very low pressures in the upwind corner of the roof (values of C_p of order -2) due to the strong trailing vortex pair generated at this corner of the roof.

Pressures on buildings of complex planform are clearly more difficult to deal with and may require more careful individual attention, but may often be approximated to simple forms. Figure 10 shows examples from Cook(1990).

Apart from many documents containing data like that of Figures 6-9 (see, for example, ASHRAE(1997, 2009), Cook (1985, 1990), Melaragno(1982), Wiren(1983), Orme(1994)), there have been some efforts to provide systematic data on pressure patterns on varying building shapes. Bowen(1976) provided systematic pressure data on a range of rectangular building shapes of 2x3 planform with heights ranging between 0.3 and 2x the widest side. His report contains full tabulated details of the pressure data. ESDU(1992) provides standardized data on pressure forces on rectangular blocks. Melaragno(1982) also provides some systematic pressure data on different building shapes, as does Orme(1994). Building Research Establishment Digest 346 (BRE(1990)) deals with wind pressure loading on buildings; Section 6 provides standardized surface pressure data for typical building shapes, which can be used for both wind loading and ventilation purposes. Figure 11 shows an example of surface pressure data from this digest, as used originally in Hall et al(1995).

There is also a body of data on building pressures for wind loading purposes. These are mainly incorporated in the Eurocodes(EC(2003)), also defined for the UK in a British Standard (BS EN 1991-1-4:2005 and Annexe A1: 2010). These provide systematic surface pressure data on buildings. However, it is in a fixed form suitable mainly for wind loading applications as it supplies only a single pressure on each building face based on a maximum gust loading likely to be experienced on that face.

4.3.3 Pressure Patterns on Buildings in Urban Arrays

There are two separate effects on buildings in urban arrays of the surrounding buildings. The first is 'sheltering', a reduction in the mean wind speed over the building which in turn reduces the wind pressures on it. The second is modification of the building's own pressure pattern due to modification of the wind patterns around the surrounding buildings.

There has been some interest in 'sheltering' in both the ventilation and wind loading fields as a simple first order correction to the effects of urban surroundings. The simple description is of the effect of increasing surrounding building density steadily blocking the wind flow and reducing, overall, the pressure coefficients on the building. ASHRAE(2009) quotes the effect on a building passing from open terrain to dense urban surroundings as reducing the surface pressure coefficients by about an order of magnitude. Figure 12, taken from Cook(1990), shows the common description by wind engineers (from Hussain and Lee(1980)) of the behaviour of wind flows over urban arrays of similar height, as passing from isolated roughness behaviour to a wake interference flow as the buildings' separated wakes start to interfere with one another to a 'skimming' flow where the separated building wakes entirely fill the spaces between the buildings. A similar diagram appears in Oke(1992). The two lower plots of Figure 12 show BRE measurements, in a cubical building array of uniform height, of the change in the overall building pressure loading (roughly equivalent to an area weighted mean pressure coefficient over the surface) with the building area density and wind direction. The middle plot shows the building

loading falling by about an order of magnitude from open terrain to a high area density (consistent with the remarks in ASHRAE(2009)). The lower plot, of the additional effects of wind direction, shows its diminishing influence with increasing area density.

Though the bulk effect of 'sheltering' on building surfaces seems relatively well ordered if the building and it surroundings are of similar size, the individual pressure patterns are less so. There has been some interest in this area, though only a limited number of systematic studies have appeared. Walker's (1992) review described the factors (upstream flow, wakes, geometry, wind direction, building separation and shelter from several obstacles) that affect the pressure coefficients on sheltered buildings.

The largest single study is probably that due to Wiren(1983, 1985), who investigated pressure patterns on buildings in arrays of uniform height and varying size. Figure 13 shows the urban layouts used and Figure 14 some typical results. A more detailed discussion of Wiren's data and its use by other workers is given in Kukadia et al(1998). The left hand plots in Figure 14 show the effect of the size of the surrounding array (starting with a single building, case A00) on averaged surface pressures on the upwind and downwind building faces in varying wind directions. The substantial modification of the isolated building pressure pattern can be clearly seen. The right hand plots show averaged pressure distributions across all four building faces in two specific cases (of a different number of surrounding buildings) in two wind directions, normal and at 30° to the long side of the building. In this case doubling the number of surrounding building rows had only limited effect on the pressure pattern compared with the effect of the change in wind direction.

Figure 15 and 16 show other building pressure measurements in urban arrays from Hall et al(1999a), in what appears still to be the only systematic work in which pressure and concentration patterns were measured on building forms in arrays in the same experiment; the related concentration measurements are considered later. These show 'folded out' plan views of pressure patterns on the five building faces of cubical and 4x1x1 building forms arranged in arrays of 16% and 44% area density. The former is typical of suburban housing estates, the latter with the more crowded regions of urban centres. The pressure patterns are shaded in the regions where the pressures exceed 75% of the mean surface pressure, where air ingress is then most likely to occur, and hatched where the pressures are below the 25%ile of the mean surface pressure, where air egress is most likely to occur. It can be seen from the plots for the isolated building in Figure 16 that the pressure patterns are similar to others described here; the high pressure regions are largely on the upwind face(s) and the low pressure regions are on the upwind part of the building roof and the side walls. The pressure pattern for the isolated building is not greatly altered in the array of 16% area density, but markedly changed in the array of 44% area density, where it becomes more disorderly and in some cases the regions of high pressure are on the downwind face of the building.

Figure 17 shows plots of the pressure differences across the building faces for the data of Figures 15 and 16. As with the BRE data from Cook(1990) described earlier, the main effects of increasing Area Density on the measurements was to greatly reduce the overall pressure differences over the building faces and to reduce the effects of wind direction over the array; though there were some exceptions to this rule of thumb.

Most of this discussion has been concerned with buildings within arrays of similar, relatively uniform height. There has also been some interest in the effects of arrays on the common occurrence of buildings significantly taller or shorter than the nominal array height. Effectively the building pressure pattern alters from that due to a 'sheltered' flow when the building is at or below the heights of its surroundings to an 'isolated' flow as its height above its surroundings increases. Some of Bowen's(1976) measurements of mean surface pressures over a building surrounding of different heights, reanalysed by Orme et al(1994), are shown in Figure 18. The height ratio h/H is that of the surrounding roughness height, h, to the measured building, H. The effect of sheltering (h/H=1) on the pressure differences can be seen, also that the transition to the isolated building result (h/H = 1/6) is not particularly orderly.

A related matter is the extent of the surrounding urban area which directly affects the pressure pattern on a building. This 'Area of Influence' has been of some interest both for building aerodynamics and other matters, such as sites for meteorological instruments. Wiren's(1985) work partly covered this matter as it used arrays of varying extent surrounding the measured building. For air flows around buildings, the major region of interest is typically up to about five surround building rows, but varies with parameters such as area density. A result from Lee et al(1979), reproduced by Cook(1990), estimating the boundaries of extent producing changes of 5% and 10% in a building pressure measurement is shown in Figure 19.

5 CONCENTRATION PATTERNS ON BUILDINGS FROM EXTERNAL SOURCES

5.1 Background

Concentration patterns on building surfaces from external sources must in principle be more multifarious than pressure patterns. Allowing for normalising the effects of wind speed and treating internal buoyancy forces separately, a building exhibits one external surface pressure pattern in a given wind direction and surroundings, but as many surface concentration patterns in this condition as there are potential contaminant source positions.

Measurements of concentration patterns on buildings from external dispersing sources are relatively uncommon. In an earlier review of the information then available on dispersion on and around buildings, as a precursor to the development of the Urban Dispersion Model for DERA (now Dstl) (Hall et al(1996a)), Hall et al(1996b) found about 250 papers and reports on the subject. Most of these were concerned with the effects of buildings on dispersion of long term (plume) releases, particularly on plume downwash due to the building. Most measurements were at the ground rather than on the building. Only a few papers considered plume impacts and measurements on buildings. There were no papers on plume impacts, on buildings within urban arrays, and none on impacts of short term releases ('puffs') on buildings in any situation. There have been more publications on plume impacts on buildings since that time; the major change over the intervening period has been the enormous surge of interest in dispersion in urban areas. However, within that subject, plume impacts on buildings have remained a minority interest with attention mainly concentrated on exposure at the ground. There are few measurements within the public domain of puff release impacts on buildings. Unlike building pressure patterns, there seem in consequence to be no comparable systematic data bases on concentration patterns on building surfaces from external sources.

Nonetheless there is sufficient data available to describe the general nature of exposure of buildings to external sources; this is presented here in as orderly a way as is practicable. Most of the work described concerns long-term, 'plume', releases. The specific characteristics of short term, 'puff', releases are also described as the time scales of their impacts on building internal exposure are significant.

5.2 Upwind 'Influence' Areas for Source Plume or Puff Interaction with a Building

It is helpful to identify, in the first instance, the upwind area from within which contaminant sources will impact on a building, in a similar way to the 'areas of influence' of urban surroundings on wind pressure patterns on buildings

discussed in Section 4.3.3. This is related to the 'inverse' problem of predicting the source strength and position from one or more receptor measurements. This form of the 'inverse' problem is a complex matter in its own right with a growing literature in recent years (see, for example the session on inverse modelling at the HARMO 14(2011) Conference) and is not discussed here, where the interest is the simpler one of predicting potential source positions for building exposure. This is not much discussed in the conventional dispersion modelling literature but is relatively easy to determine in simple cases as it is the same as a downwind dispersion pattern but inverted with respect to the source and recipient building. Figure 20 shows an example of an upwind source 'influence area' derived from a conventional dispersion calculation using the ADMS model. The calculation used a line source as a more practical representation of the face width of a building and was nominally intended to represent the exposure over a building 50m wide and 10m high in open terrain (z_0 = 0.1m) from sources up to about 1km upwind. However the result has been non-dimensionalised so that it can be applied at any scales or emission rates. The upper plot shows the upwind area over which releases will impact on the 'building', with contours showing the mean values, K_{mean}, of dimensionless concentration, K, which will occur across the 'building' from releases within this area. The dimensionless concentration, K, is defined in the usual way as

$$K = \frac{CUL^2}{Q}, \qquad (3)$$

where C is the measured concentration,
U is the wind speed at some reference height, L, and
Q is the rate of emission of contaminant.

In the present case L is taken as 0.2 of the width of the line source, nominally representing the height of a building 50m wide by 10m tall.

In principle, this 'inverse assumption' is only directly valid for point recipients. However, the error in using a point source to represent exposure across a line appears to be quite small for sources away from the immediate area of the line. The lower plot in Figure 20 shows the concentrations calculated across the line of the 'building' from the point sources indicated in the upper plot. Despite their variation in the lower plot, the mean value of K across the 'building' line, K_{mean}, was within 5% (usually 2%) of the contour value in all cases except source I, very close to and to one side of the 'building' line.

In open terrain or for sources in urban areas at longer upwind distances, the potential source positions of upwind releases are similar to the diagrams from simple model calculations in Figure 20. However at shorter ranges in urban areas within urban arrays 'influence areas' are more complex due to the highly modified behaviour of plumes that can occur due to local interactions with the building array.

Mfula(2004) investigated this problem with small scale wind tunnel experiments looking at building exposure within urban arrays. Figure 21, from Hall et al(2002), shows a result from Mfula's work, giving the upwind areas of source

location for potential exposure of a building (the shaded rectangle) within building arrays of cubical planform and 16% and 44% area density. The diagrams show two of the most important features of dispersion within urban arrays at short distances; the greatly enhanced lateral spreading and upwind travel of dispersing material. The contours on the upper figures are the mean dimensionless concentration, K, over the building faces for sources within the contours. The lower figures give similar contours for the largest fractional concentration difference across the building faces. Figure 22 shows similar results, also from Mfula(2004), for winds in different directions over urban arrays of 4x1x1 buildings, where the disturbances to the dispersion patterns and thus the area of source locations for building exposure are greater. The asymmetry of the source exposure areas in winds skewed across the array is quite marked, as is the very large lateral spreading and the significant region where sources downwind of the building produce exposure on the building faces.

There are similar questions with regard to line sources (due to road traffic for example) and the relative contribution of different parts of the line source to the exposure of a particular building. There is a related problem with the present application in, for example, determining over what part of a road a release of a vehicle emission might impinge significantly on a building. This is not commonly available data as most experiments with line sources do not distinguish this proportionate contribution. However, the experiments of Hall et al(1999a) used discrete sources distributed along the spaces in the building arrays from which it was then possible to produce the equivalent of line sources (by simple summation of the respective concentration patterns) and for which it was thus also possible to attribute the proportional contribution of different parts of the source to the total. This was done in a reanalysis of the data in Hall et al(2000). Some results of the work are shown diagrammatically in Figure 23 for cubical and 4x1x1 building forms in two building area densities. The units on the bars are of their mean proportionate contribution of dimensionless concentration, K, on the building surfaces. It can be seen that the proportion of the line source contributing to the building exposure may be small or large and varies with the wind direction and the urban array type and density. Further, the largest contribution proportion to the total exposure from the line source does not precisely follow the nominal wind direction, which is modified by the form of the array.

The source exposure areas shown in Figure 20, for open terrain with low surface roughness, show a relatively narrow width of the area over which a building will be significantly exposed to a source, as is typical in conventional dispersion calculations. This implies a high sensitivity of building exposure to a single source at any distance from the building over periods longer than about an hour (the nominal averaging time for the calculations) due to small variations in the wind direction, so that some intermittency in longer term exposure from single sources can be expected. For releases at shorter distances in urban arrays, the wider spread of the exposure areas, as in Figures 21 and 22, reduces this sensitivity to the wind direction and implies a more persistent longer term exposure. In practice, the dispersion patterns in the near field in urban arrays

can also show large shorter term variations in the temporal exposure, irrespective of variations in the longer term wind speed, as it is not uncommon for near field urban dispersion to show intermittent switching between different quasi-stable dispersion patterns.

5.3 Concentration Patterns on Buildings in Open Terrain

The most important parameter affecting the nature of building exposure is the distance of the contaminant source from the building and most of the discussion here will be on this basis. The main effect of source distance on exposure of the building of interest, apart from a reduction in concentrations of a release on the building surfaces, as the lower plot in Figure 20 shows, is an increasing uniformity of exposure over the building surfaces with increasing distance as the plume cross section becomes proportionately larger compared with the building dimensions.

Some sense of this behaviour can also be seen in Figure 24, which shows some experimental data from wind tunnel experiments by Hall et al(1996c) of concentration patterns on and around a building normal to the wind from a ground-based plume at three different upwind distances. The flow visualisation images of the plume on the left of the figure show the relative size of the plume (at upwind source distances of 6, 20 and 65 building heights) to the building, which at the shortest distance is comparable in size to the building and at the greatest distance is significantly larger than the building. The concentration patterns on the building surfaces are shown in the centre plots, where it can be seen that the variation in concentration over the building surfaces increases markedly as the plume source approaches the building. The right hand plots in Figure 24 show the plume concentration at the ground upwind and downwind of the building (which sits in the shaded space on the plot). The data are for a variety of building orientations to the wind (all results are not shown here, the bottom plot of this set is for an elevated source); the upper curves in each plot are for the building set with its long face normal to the wind, as with the rest of the data in Figure 24. There are two main points of interest in the right hand set of plots. The first is that the building set normal to the wind appears to have only limited effect on concentrations within the plume at the longer source distances. The second is that at the shorter distances and with the building faces skewed to the wind, concentrations in the plume around the building are more markedly affected. This is due to changes in the secondary flow components around the building, shown in Figure 4. The case for 60° wind direction (with the long face of the building skewed at 60° to the wind) showed the greatest change in local plume concentrations, due to the generation of a strong trailing vortex from the long edge of the building roof.

As a plausible first order approximation for sources further than about 10 building heights or 4-5 building widths upwind, it would be reasonable to assume that concentration patterns over the upwind face, roof and side faces of the building are similar to those in the same positions in the approaching plume,

perhaps a little reduced. Concentrations over the downwind faces of the building tend to be approximately uniform (due to efficient mixing in the separated flow that usually, but not always, occupies the downwind faces) at the mean concentration of the concentration over the roof and sidewalls.

The dispersion of sources closer to buildings is significantly more difficult to predict, both because of the more marked effects of the secondary flow components around the building and of the sensitivity of the dispersion pattern to quite small changes in the source position. This leads to a large spatial and temporal variability of building concentration patterns from nearby sources. Plumes or puffs are relatively small compared with the building size and may pass over or around either side of the building, or partition variably between the three directions depending on quite small variations in the source position compared with the stagnation point on the upwind faces of the building, which also controls the way in which the flow subdivides around the building. Figure 25 shows some examples, using flow visualisation (from Hall et al(1996b)), of these complex flows that result from small changes in building orientation and source position. Figure 26 shows some similar diagrams from Robins and Fackrell(1983) as reproduced by Hall et al(1996b).

Most work of this sort does not, however, say much about exposure patterns on the building itself and is concerned mainly with the effects of the building on the subsequent dispersion, especially on concentrations in the building's wake. Practical interest in concentrations on the buildings themselves has been limited and there are few systematic data bases of this behaviour, as there are for building surface pressures. This is despite some of the first measurements of dispersion associated with buildings, by Halitsky(1963), being of this sort. There are effectively two forms of exposure of the building surface. Firstly, direct impact of the plume or puff on the building and its displacement around the building following the flow pattern; these dispersion patterns may be quite unsteady. Secondly, that of a diffused exposure over a relatively large area when plume or puffs are entrained in the regions of separated flow around the building, usually on its downwind faces.

These two types of exposure can occur together in some circumstances. Figure 27 shows time dependent measurements of concentrations in a building wake from releases in and around its separated wake. The data are from Hall et al (1996b,c) and were part of the work shown in Figure 24 (of upstream plume impacts on a building), which shows relatively uniform distributions of the plume concentration over the downwind building faces within the separated flow region. In the case in Figure 27 the releases were all downstream of the building but were either in or became entrained in the separated wake and carried upwind to the downwind face of the building. The measurement point in the data of Figure 27 was on the ground a little way downwind of the building, but a measurement on the downwind face of the building would have produced a similar result. In this case the measurements show both types of plume exposure at the measurement point at the same time, of diffuse exposure in the separated wake and occasional direct impact of the plume as it meandered within the separated wake. The resultant exposure pattern is of a relatively uniform concentration

over time from the diffused plume material, overlaid with occasional large excursions in concentration as the meandering plume passed over the measurement point. This type of double exposure is common in releases in or near to separated flows on buildings.

Wilson has taken a consistent interest in impacts of nearby sources on buildings. His main interest has been in impacts on ventilation air inlets from sources on or near the building of concern; a particular interest was in finding simple rules for predicting this type of behaviour, especially the more extreme levels of resultant exposure. This has produced one of the few systematic bodies of work in this area. The bulk of it has been summarised for practical application in ASHRAE(1997, 2009, 2011) and in CIBSE(1999). Figure 28 shows, on the left, some results from Wilson(1976) of concentration patterns on different building shapes from a flush source on the roof. On the right is some related work by Wilson and Winkel(1982) using a wide variety of building shapes and both flush and elevated sources.

There is little information on direct impacts of nearby plumes on buildings. Figure 24, already discussed, shows some plume impaction measurements from Hall et al(1996c). Figure 29 shows some results from Wilson and Britter(1982) (originally from Wilson and Netterville(1978)) of the surface concentration patterns from an upwind plume directly impacting on a building, on the left of the figure. The plot on the right of the figure is of the maximum concentration on the building, compared with that in the undisturbed plume at the same distance. The main point of interest is that at source distances beyond about six obstacle dimensions (the figure uses upwind distance as x/a on this axis, where a = (frontal area)$^{0.5}$) maximum concentrations at the impact region are similar to the maximum values in the free plume; at shorter distances the maximum concentration is reduced.

One feature of concentration patterns around buildings needing more consideration is that of releases in courtyards and enclosed spaces, which are ubiquitous in building construction, as observation of any aerial photograph of an urban area will show. These areas are generally poorly ventilated and contaminant releases within them can result in high concentrations. This type of dispersion has received little attention, so direct measurements are uncommon. The shape of the courtyard, especially its ratio of depth to width, alters the dispersion behaviour significantly. Figure 30 shows measurements from Hall et al(1999b) of flow patterns and concentrations at the ground within a 'courtyard' (an enclosed space in the centre of a building) from a release at its base. It can be seen that the concentration within the courtyard varies considerably with its depth, showing a minimum at depth/width ratios of about unity. This is due to the recirculating flow in the courtyard having its greatest effectiveness in ventilating the cavity when its depth and width are about equal. An important feature of the measurements in Figure 30 are the values of the dimensionless concentration, K, at the base of the courtyard; K is defined using Equation (3) but with the width, W, of the courtyard used as the characteristic dimension L. The value of K is generally large, rising to levels in excess of 100 for the deeper courtyards. In comparison, the typical equivalent value of K just downwind of

the building, for the same internal or a similar local external release, would be around 1 or less. For releases external to the courtyard the internal concentration becomes similar to that over the opening with increasing time. However, the ventilation rate of these spaces is quite low (essentially the cause of the high internal concentrations), so that both the rise of concentration to the external value and the decay rate of short term internal releases will be slow.

5.4 Concentration Patterns on Buildings in Urban Areas

The detailed characteristics of urban dispersion are not considered here, only some relevant examples are given and attention is concentrated on building exposure. There are good and still relevant reviews on the general nature of short range dispersion in urban areas by Robins and Macdonald(2000) for ADMLC, and by Hanna and Britter(2002). There has also been a surge of interest in urban meteorology and dispersion within urban areas over the last fifteen years. This has included major field experiments, for example in the UK in London (the DAPPLE project, Arnold et al(2004), Wood et al(2009)), by UMIST (Macdonald et al(1998a, b)) and in the US in Salt Lake City (Allwine et al(2002)), Oklahoma City (Clawson et al(2005)) and with container arrays (Biltoft(2001, 2002)), and a substantial number of small scale physical modelling exercises, mainly in wind tunnels. Regretfully for the present purpose, the great bulk of this work has been concerned with exposure of the external environment with little attention to exposure of building surfaces and there is only limited information on building exposure specifically.

As with pressure patterns, a building closely surrounded by others experiences modified concentration patterns from dispersing sources. There are two factors modifying and enhancing dispersion in urban areas. The first is due to increased atmospheric turbulence from the higher surface roughness, which is accounted for in conventional dispersion models in the usual way via the increased surface roughness length, z_0. The second, which is important mainly at shorter ranges below about 1km, is due to lateral and vertical displacement of the plume around the building array and enhanced mixing in a succession of separated building wakes. This secondary dispersion can significantly modify (and usually enhance) dispersion rates at short distances, including the generation of upwind dispersion. Some urban array layouts and wind directions can also significantly displace the plume or puff path from that of the nominal wind direction. The plots in Figures 21 and 22, which are effectively inverted dispersion patterns, show the sort of dispersion behaviour that can occur. At longer distances these secondary effects become less dominant as the plume becomes large compared with the scale of the building array and the dispersion reverts to that associated with the surface roughness and atmospheric turbulence in the normal way. At the shorter ranges, both dispersion processes give rise to Gaussian distributions of concentration and there is additionally a constant interchange of dispersing material between them across the building flow canopy. As a result the two components are generally indistinguishable except for their combined effect on the overall dispersion. Further secondary effects on dispersion at shorter ranges

can be caused by larger buildings protruding significantly above the overall canopy height, which add an individual contribution to the overall flow and dispersion patterns.

Some flow visualisation images of short range dispersion over urban arrays are shown in Figures 31 and 32, from the Dstl UDM archive (some appeared in Hall et al(1997)), which illustrate some of the basic properties of plumes dispersing in urban arrays. The upper photographs of Figure 31 are plan views of a dispersing plume in open terrain with two densities of urban cubical building arrays, showing the enhanced lateral dispersion in the array. The lower plots are of plan views of dispersion through arrays of wide buildings (of 4x1x1 shape) in different wind directions, showing how the dispersion can be enhanced (with the buildings across the wind) or diminished (with the buildings along the wind) by the form of the building array. The lower photograph, with the building long sides at 45° to the wind, shows the deflection of the plume (downwards in the photograph) away from the wind direction (left to right in the photograph). Figure 32 shows, in the upper photographs, the effect of source height on the dispersion. The dispersion in the centre photograph, with the source at building height, is difficult to distinguish from that on the left with the source at the ground due to the rapid vertical mixing that occurs within the array. Only with sources well above building height, as in the right hand photograph, is a different initial dispersion pattern distinguishable. The lower photographs show the effect of a tall structure on dispersion within a lower height array; dispersion around the taller structure is partially independent of dispersion over the lower array and also produces rapid vertical mixing of the plume in the wake of the taller structure.

As in open terrain, the nature of building exposure in urban areas depends strongly on the distance of the source from the building. In a review of building exposure to air pollution, Hall et al(1996b) defined the nature of the exposure in terms of the scale of the urban regime, following definitions originally laid out by Munn(1981) in a monograph on urban monitoring networks, which suggested a division of:

microscale (0-100m)
neighbourhood scale (100-2000m)
urban scale (5-50km)
regional scale (100-1000km)
continental, hemispheric and global scales.

In a similar way, Munn defined a number of characteristic time scales associated with pollutants:

minute to minute variations
the daily (diurnal) cycle
large scale weather fluctuations (3-5 days)
weekly emission cycles
annual emission and weather cycles.

The nature of the exposure was represented diagrammatically as in Figure 33, which was intended to show the relative variability of exposure from sources at different distances. As the source moves nearer the building, the level of variability in the exposure pattern increases. In the present application it is only the first three temporal and spatial regimes that are likely to be of interest.

As with buildings in open terrain, sources within urban areas at sufficient upwind distances effectively generate a relatively uniform concentration pattern over a building's surface and at intermediate distances the distribution in concentration across the building roughly follows the Gaussian distribution, but with an averaged distribution over areas of the building surface within separated flow regions. This therefore remains a plausible first order presumption for building exposure patterns at these ranges. However, it is also necessary to account for the modification of rates of dispersion within the urban building array (they are usually enhanced) and sometimes of the plume path at short and intermediate ranges. There may also be upwind travel of releases, so that sources downwind may be significant to the exposure of a building. The extent of these shorter ranges is probably best defined by the number of rows of buildings rather than distance per se, so that the intermediate range of source distances might be defined as those at less than ten rows of buildings upwind. It is a helpful feature (from the point of view of prediction methods) that despite the 'digitisation' of the flow about a building array of size comparable to the plume, measurements show that concentration distributions in the plume remain close to the Gaussian form for sources down to about two rows of buildings upwind. In some cases of high array area density, the concentration distributions remain closely Gaussian even up to releases in the immediately upwind street.

Thus as with buildings in open terrain, it is again the building surface concentration patterns from releases adjacent to, or within one or two building rows (in any direction within an urban array), that are the most difficult to predict. The sensitivity of building concentration patterns to small changes in source position and wind direction noted for buildings in open terrain is, if anything, exacerbated for buildings in urban arrays. As noted previously, there is only limited experimental data on concentration patterns on urban buildings from which to derive useful data. Figures 34, 35 and 36, respectively from Cermak(1974), Dabbert and Hoydysh(1991) and Pavageau et al(1996), show examples of wind tunnel measurements of concentration patterns on the faces of urban buildings from ground level line sources. Line sources were used in all cases, representing traffic flows, but despite this probably making the building concentration patterns more uniform than from a point source the adjacent building faces show complex and quite variable concentration patterns. Part of the difficulty in predicting building concentration patterns from local sources is illustrated in Figure 37, from Scaperdas(2000), showing the high sensitivity of flows around a street junction to small changes in the building layout and wind direction. The variation of building surface concentration patterns with urban area density and upwind source direction is shown by some further concentration measurements on a building within a cubical array by Hall et al(1999a) in Figure 38, which match the pressure measurements for similar

conditions shown in Figure 16, made in the same experiments. The figure shows, from left to right, the effects of increasing array density over open terrain and, from top to bottom, the effects of increasing upwind source distance. It is clear from the spacing of the contours that the variation in concentration over the building becomes more uniform with increasing upwind source distance and increasing area density of the surrounding array. An example of the effect of lateral displacement of sources in the near field is shown in Figure 39, from Hall et al(2000), using the data from Hall et al(1999a), for cubical buildings in an array of 16% area density. The upper plot shows how the concentration distribution varies with the lateral displacement of the source. Note how the region of high concentration on the building surface is on the upwind face of the building (immediately adjacent to the source) with the source located immediately upwind, but on the downwind building face with the source displaced laterally by two building spacings. The lower plot shows the variation of the mean concentration over the building surfaces with a laterally displaced source, where it can be seen that the overall building exposure falls rapidly with increasing lateral displacement of the source.

Because of this high variability in building exposure to sources at short ranges, it is difficult to estimate exposure patterns in a formalised way. Though wind tunnel experiments or (possibly) CFD calculations can provide detailed information in specific cases, the costs and elapsed time associated with such studies mitigate against a large number of such cases being investigated. There remains a need for rapid and efficient simple methods of identifying the more severe cases and their probability of occurrence both for direct practical application and guiding more complex time consuming studies. There are several practical approaches for handling this type of problem in a simplified way, three examples are shown here. The first is to carry out a large number of individual calculations or experimental measurements and to examine these statistically in order to estimate the probable range and upper bound of the probable exposure. The second is to use simple methods of estimating the probable range of the exposure levels with a limited amount of calculation. The third is to assign bulk probabilities of exposure to different areas of a building surface derived from more complex surface concentration patterns of the sort shown here.

An example of the first approach is shown in Figure 40, using wind tunnel data from a model of the Marylebone Road area collected during the DAPPLE programme by Robins and Cheng(2005). This plot shows a definable upper bound for the variation of concentration with distance; it also shows a very large variation in the range of concentrations measured at distances mostly within 500m, of around three orders of magnitude.

An example of the second approach is the simple methodology proposed for very short range exposure (within a few rows of buildings) by Kukadia and Hall(2011a), intended mainly for building design purposes but with direct application to the present problem. This operates on the basis described previously of the two most common forms of building exposure being direct exposure of a small area of the building to a directly impinging plume or of diffuse exposure to the plume dispersed within a separated wake. It is also

possible, as the discussed example of Figure 27 shows, for both types of exposure to occur together. The model is based partly on the STREET model of Dabbert et al(1973), which was proposed for estimating the concentration in urban streets due to traffic emissions. It used similar assumptions of the two types of exposure, but applied them separately to the upwind and downwind faces of a canyon street. It is now appreciated that urban street wind flows are more complex and variable than this, so that either form of exposure can occur arbitrarily on local building surfaces and possibly in combination. The basic rules used by Kukadia and Hall for estimating the two forms of exposure from near sources, shown diagrammatically in Figure 41, include:

a Sources likely to impact on the building are initially identified.
b Direct exposure to the plume from a source can occur if the plume path to contact the building is in line of sight or does not pass around more than two corners of surrounding buildings, beyond which diffuse exposure will occur. This is similar to Wilson's 'stretched string' approach to account for impact concentration from nearby sources (summarised in ASHRAE(2011)).
c Diffuse exposure will additionally occur around or downwind of a building for impacting plumes and those in the immediate region downwind of the building.

There are further rules for elevated sources and a structure for applying the methodology is laid out. It is not intended to produce precise estimates of exposure but to identify and roughly scale the most critical sources for exposure of the building, so that these can either be avoided by design modifications or examined more carefully otherwise.

An example of the third approach is shown in Figure 42 from Hall et al(2000) based on the experiments partly illustrated in Figure 38 from Hall et al(1999a). This shows the level of probability of exposure of different parts of buildings in an urban array from a source in the immediately upwind street, shown on the surfaces of the folded-out building plans in the figure. Details of the analysis, which is applied to both natural and mechanical ventilation, can be found in the original report.

6 BUILDING INFILTRATION AND VENTILATION RATES

6.1 Background

Building infiltration and ventilation are of direct interest in construction practice and have been subject to both calculation and direct measurement over many years. In buildings with no forced (mechanical) ventilation, infiltration and ventilation of external air into buildings may be driven by the wind or buoyancy forces through gaps and small cracks in the structure, ventilation louvres and other deliberate openings, and through open doors and windows; usually through a combination of these processes. Mechanically ventilated buildings have designated air inlets and outlets and usually a system for distributing air though the building. However, in most mechanically ventilated buildings some element of wind and buoyancy driven ventilation still prevails. Some buildings operate using both mechanical and natural ventilation; the combination of these ventilation processes and the usually sub-divided internal structures of most buildings make calculation of real building ventilation rates a complex matter in many cases. In consequence, direct measurement of ventilation in real buildings retains its appeal, both in research and practical application.

The examples of building ventilation calculation given here are relatively straightforward, mainly to show the principles involved, and are mainly based on empty internal structures. Discussion of the more complex aspects of building ventilation can be found in ASHRAE(2009), Liddament(1996), Cook(1990), Etheridge and Sandberg(1996) and Etheridge(2012). CIBSE(2005a) also provides practical details of the design of naturally ventilated non-domestic buildings and BSI(1991) gives details of both principles and design methods for natural ventilation.

6.2 Calculating Infiltration and Ventilation

The basic equation for estimating the transfer of material across openings in a building envelope is, for a transfer volume flow rate, V,

$$V = kA(C_p - C_{pi})^{1/n}, \qquad (4)$$

where C_p and C_{pi} are respectively the local external surface pressure and internal pressure on the building,
k is a constant related to the nature of the opening and
A is the surface area of the opening.

k for a large opening is equivalent to the discharge coefficient of an orifice, with values of about 0.5 and 0.6 respectively for sharp edged square and circular openings, but may otherwise vary considerably with the shape of the opening. The exponent, n, in Equation (4) varies between 1 and 2, depending on the

nature of the opening. For large openings n→2; for small openings, cracks, crevices and porous media n→1. A broad rule of thumb is that openings of centimeter size and above have values of n approaching 2 and openings at millimeter size and below have values of n approaching 1. There is a discussion on methods of finding n for different openings in Walker et al(1997) and a discussion of the characteristics of flows through envelope openings in Etheridge and Sandberg(1996) and in Etheridge(2012).

The value of n is important in building air ingress since, if n=2 Equation (4) becomes that for a conventional orifice and the wind-driven air ingress and egress rates are directly proportional to the wind speed. If n=1 the airflows through the openings are laminar and the ingress and egress rates are proportional to the square of the wind speed. Close inspection of the upper plot of Figure 2 will show that the lines for the wind-driven part of the ventilation rate are in fact slightly curved, implying values of n below 2.

The total air ingress rate of the building, V_b, is then given by the positive part of Equation (4) integrated over the building surface, that is the positive part of,

$$V_b = \int_A k \cdot \mathrm{sgn}\left\{C_p - C_{pi}\right\}\left(\left|C_p - C_{pi}\right|\right)^{1/n} dA\,, \qquad (5)$$

where sgn is the 'signum' function for the sign of a number or function.

The practical difficulties of defining volume flow rates across openings in the building envelope (unless they are, for example, large and clearly delineated ventilation openings) have led to estimates of effective building surface porosity in bulk terms in the form of the ratio 'opening area/total area' (A/A_{Total}). Thus, for example, Cook(1990) quotes from BRE(1974) typical effective porosities (as opening ratios A/A_{Total}) in the range $4x10^{-4}$ to 10^{-3}, with a value of n close to 2. This estimate also appeared to be correct for UK measurements over the succeeding period 1976-86, the approximate mean age of the UK building stock. Cook also quotes other data, including US, Canadian and Swedish data where buildings tended to be better built and less porous, as given in Table 1. Orme et al(1994) also provide detailed information on building surface porosity.

More recently built UK buildings are less porous, approaching and currently improving on values similar to those in the other countries quoted above (See Building Regulations(2010) part F).

The difficulty in using data of this sort is that it is bulk data for the building and does not distinguish the porosities of different parts of the building surface, roof and walls for example, which may matter in infiltration calculations, discussed later here, which are variable across the surface.

Table 1. Typical Building Porosity Characteristics from Measurements. From Cook(1990).

	Porosity (A/A_{Total})	n
Office Buildings		
Canada	$3.6\times10^{-4} \pm 0.46\times10^{-4}$	1.5 – 1.6
USA	$3.9\times10^{-4} \pm 1.64\times10^{-4}$	1.6 – 1.8
Housing		
UK	10.4×10^{-4}	
Canada	3.8×10^{-4}	
Sweden	2.07×10^{-4}	
Partition Walls		
Netherlands	$6.7\times10^{-4} \pm 1.5\times10^{-4}$	1.3 – 2
Single Leaf Door		
	Gap when closed 1.5 mm/m run	1.7

Equation (4) also requires an internal pressure, C_{pi}, for the interior of the building and building 'internal pressures' are a matter of significant practical interest for this reason. They are discussed specifically by Cook(1990), Etheridge and Sandberg(1996) and Etheridge(2012). This is not a parameter normally measured and its value is usually inferred by calculating the internal pressure that results in a net zero flow balance across the building envelope, so that if the porosity is assumed to be uniform across the building envelope, then,

$$\int_A (C_p - C_{pi})^{1/n} dA = 0 . \qquad (6)$$

From analysis of Hall et al's(1999a) surface pressure data on cubical structures (examples are shown in Figure 16), Cheng et al(2012) noted that the internal pressure from the net pressure balance using Equation (6) corresponded closely to the area weighted 60%ile of the external surface pressures. Methods of estimating internal pressures are given by Cook(1990) and BRE Digest 346 part8 (BRE(1990)). BRE digest 346 also notes that relatively large openings in building surfaces of the order of a few percent of the surface area tend to bring the internal pressure close to the external pressure near the opening. There is also a review of suitable calculation models in Orme(1999).

The internal pressure is nominally constant from wind driven ventilation in well connected buildings. However where buoyancy forces are significant there is clearly a vertical internal pressure distribution in addition. The internal pressure may also vary in multizone internally compartmented structures where there is a significant resistance to internal air movements. Interpreting this in relation to the external pressure pattern usually requires more complex modelling techniques. Mechanically ventilated buildings can also modify the base level of the internal pressure, relative to which the wind and buoyancy driven pressures

additionally act. In some cases, in clean rooms or buildings requiring isolation for other reasons, it is common to raise the internal pressure so that all ventilation through the building envelope is outwards. However, this may require high pressures to resist the effects of strong winds and there is a cost penalty in additional energy consumption. The effects of mechanical ventilation on the overall building ventilation pattern are not always understood or may alter over time if the ventilation system deteriorates. Some buildings have quite complex ventilation systems, part mechanical, part natural in combination or in different parts of the structure.

Despite these inherent complexities, useful basic building ventilation calculations can be made quite simply on a spreadsheet, given an external pressure pattern and some assumptions about the porosity of the structure. It is possible in such calculations to include both wind and buoyancy driven pressure, variable surface porosity, values of n in Equation (4) and any large openings in their own right. There is also some external assistance available, for example the VEETECH(2012) web site has a simple ventilation rate calculator based on standardized building ventilation data.

6.3 Measurements of Infiltration and Ventilation

It will be appreciated from the previous section that determining building infiltration and ventilation rates purely by calculation can be both complex and uncertain. In view of its practical importance, direct measurements of ventilation are common, both for research and commercial reasons. There are two basic methods, either using passive tracer gas methods or by pressurising the building.

Passive tracer gas measurements involve releasing a suitable gas and either measuring its decay over time, following a short release, or by releasing gas continuously and determining its equilibrium concentration in the building. Either method will give the characteristic time constant of the ventilation rate. Measurements can be either short term, over hours, or long term, over days or weeks. Short term measurements have the advantage of being identified with specific meteorological conditions, of wind speed, direction and external temperature, all of which may affect the ventilation rate. Long term measurements are easier to implement and provide a better indication of the overall average building ventilation properties; however, they cannot indicate the variation in ventilation with different external conditions. Passive trace gas methods have recently been revised and standardised, details can be found in Upton and Kukadia(2011).

Pressurisation methods usually involve fitting a large fan to a suitable opening in a building (typically a doorway) and using it to pressurise the closed building to a fixed value. Knowing the fan characteristic it is possible to estimate the ventilation flow rate for this level of internal pressure. Liddament(1996) and Cook(1990) discuss the methodology. Pressurisation levels have varied, but in the UK the standard pressure rise normally used is 50 Pa. The building

regulations (2010, Part L) require sample airtightness testing of new domestic builds and large refurbishments; the methods are based on BS En 13829:2001 (Thermal Performance of Buildings - Determination of Air Permeability) and detailed in ATTMA(2010). This procedure is formally known as an 'airtightness' test, which is not the same as a building infiltration rate; its main use is for satisfying building acceptance requirements for both regulatory and commercial reasons. However, there is a relationship between airtightness pressure test data and infiltration (other vents are normally sealed for this type of test). ATTMA(2010), Cook(1990), Etheridge(2012), ASHRAE(2009, Chapter 16) and Sherman(1998) discuss how ventilation data may be obtained from pressurisation tests. ATTMA(2010) quote a simple expression for determining approximately the total area of openings on the building,

$$A = \frac{V_{50}}{5.57}, \tag{7}$$

based on the assumption that any openings in the structure behave as sharp edged orifi (when n=2 in Equation (4)),
where A is the equivalent total leakage area of the openings and
V_{50} is the flow rate through the pressurising fan at a pressure rise of 50 Pa.

Sherman(1998) quotes a similar formula for US domestic buildings,

$$NL = \frac{ACH_{50}}{20}, \tag{8}$$

where ACH_{50} is the number of air changes per hour in the building when pressurised to 50 Pa.

NL is the 'Normalised leakage', a standardised form of the leakage area accounting for the building shape, defined in ASHRAE(1988) as,

$$NL = 1000\frac{ELA}{A_f}\left(\frac{H}{2.5m}\right)^{0.3}, \tag{9}$$

from which the 'effective leakage area', ELA, similar but not identical to 'A' in Equation (7), can be found.
Here, A_f is the building floor area and
H is the building height in m.

There is also a 'pulse pressurisation' method, described by Sherman and Modera(1988), which uses a pressure pulse instead of a continuous pressure from a fan and the pressure decay pattern is measured, from which building ventilation rates are derived.

Regretfully, despite the large number of building pressurisation measurements made regularly in the UK, there is no cumulative data base of measurements which would provide valuable statistical properties of infiltration in the UK building stock. However, at the time of writing there do seem to be moves to

start one. There is a review containing an international comparison of building airtightness by Limb(1994).

A number of investigators, Piggins (1991), Walker (1992) and Liddament (1996) have reviewed the literature on wind driven building infiltration rates and summarised the information on building infiltration in a number of publications. Piggins(1991) compared infiltration rates calculated using six different pressure coefficient data sets (BRE, Wiren, Balazs, Akins et al, Gandemer and Bowen), initially for an isolated building and then with surrounding buildings of different area densities (from BRE and Wiren). The surrounding buildings in urban arrays were assumed to be of the same height as the building being modelled.

Piggins' combined plots from these data are shown in Figure 43. The left plot is of common data from seven sources; despite variations in the building shapes and test conditions, the variation between them is of the order of ±12%. The right hand plot is of the effect of surrounding building density (as area density, the fraction of the plan area occupied by buildings). The marked effect of the area density on the infiltration rate, via the surface pressure pattern, is clear; the infiltration rate falls by over a factor of two from open terrain to 20% area density. At higher area densities the wind driven infiltration rate falls further and buoyancy-driven ventilation then tends to become dominant. Note also the large variation in infiltration rates with both wind speed and area density, which cover a range of around 30:1 in Figure 43. Thus the use of nominal building infiltration estimates may be unreliable in specific cases.

Piggins' data was based essentially on 1970's and 80's practice, where ventilation rates were higher than current standards require. However, in view of the average age of the UK building stock of around 50 years, Figure 43 is still representative of typical UK values. There seem to have been few changes in the succeeding ten or so years. Some additional data from pressure test measurements of the 1980's and 90's are shown in Figure 44. A feature of the data is the wide range of infiltration rates occurring between similar buildings, both in the UK and in different countries, showing relatively high UK infiltration rates. Current ventilation requirements are lower, mainly due to the emphasis on energy saving. The current Building Regulations (2010, Part F) use a different lower limit, of 13-30 l s^{-1} for dwellings with 1-5 bedrooms, equivalent to an air change rate of the order of 0.2 air changes per hour in a light wind. The minimum requirement for offices is around 15 l s^{-1} per person. Upton and Kukadia(2011) list typical current standards and guidance values for different building types and usage.

7 INGRESS OF EXTERNAL CONTAMINANTS

7.1 Calculating External Contaminant Ingress

Given building pressure and concentration patterns, together with some infiltration data, calculating the rate of ingress of external contaminants is relatively straightforward, but the method depends on the form of the ventilation process.

For mechanically ventilated buildings the contaminant ingress rate is apparently given simply by the inlet flow rate and contaminant concentration at the system air inlet. There remains a significant interest in avoiding ventilation air inlet contamination. In practice this may be a more complicated matter in larger ventilation systems, which may have multiple inlets (sometimes for pressure balancing purposes) or may be compartmented for different regions of the same building. In addition, as noted earlier, there usually remains a wind and buoyancy driven infiltration component to the ventilation which should be considered.

For natural (wind and buoyancy induced) infiltration and ventilation, the rate of contaminant ingress is given (from Equation (5)) by the positive part of the integral,

$$M = \int_A C_e k \mathrm{Sgn}(C_p - C_{pi}) \left(\left| C_p - C_{pi} \right| \right)^{1/n} dA , \qquad (10)$$

over the building surface, where
C_e is the local external concentration on the building surface and
M is the total rate of contaminant ingress.

Similarly, the negative part of the integral,

$$M = \int_A C_i k \mathrm{Sgn}(C_p - C_{pi}) \left(\left| C_p - C_{pi} \right| \right)^{1/n} dA , \qquad (11)$$

where C_i is the internal concentration, gives the rate of egress of internal contaminants. If there are no internal losses of contaminant, at equilibrium the rates of contaminant ingress and egress should balance.

If a building is exposed to a source at some distance and its plume cross section is large compared with the building, C_e is approximately constant over the building surface and Equation (10) then becomes equivalent to the product of the building ventilation rate, V_b (from Equation (5)) and the external concentration, C_e. It will be appreciated that this calculation can then be made using approximate bulk building ventilation rate data of the sort discussed in Sections 6.2 and 6.3, which is readily accessible from various sources.

The greatest difficulty lies in estimating contaminant ingress rates from sources closer to a building, where the local variations of both pressure and

concentration across the building surface directly affect the local rate of contaminant ingress on the surface, and must be known at least approximately in order to obtain a plausible estimate of the rate of contaminant ingress.

In these circumstances, in attempting to define the areas of major contaminant ingress, the concept of a 'risk of ingress' was developed at BRE (Cheng et al(2012a,b)), partly intended to indicate the critical areas of ingress for dealing with ventilation design to avoided excessive ingress. The 'risk of ingress', I_R, locally on the building surface is defined as the positive part of,

$$I_R = (C_p - C_{pi})^{0.5} K , \qquad (12)$$

where K is the dimensionless concentration of the contaminant on the building surface.

It is clear that Equation (12) is a version of Equation (11) with n=2 , though the value of n may be altered to taste. It is applicable to both wind and buoyancy driven ingress. Cheng analysed Hall et al's(1999a) data for cubical obstacles, shown in Figures 16 and 38, to determine the distribution of I_R over their surfaces for wind-driven ingress, this data remaining one of the few systematic data sets of pressure and concentration patterns from the same experiment. Results of two of the calculations are shown in Figure 45 and 46; Figure 45 shows results for a single cubical building in open terrain and Figure 46 shows results for a cubical building in a building array of area density 16%. The related visualised plume images are the top left image in Figure 25 for Figure 45 and the upper centre image in Figure 31 for Figure 46, though in this latter case the source is just outside, rather than inside the array

In both cases the contaminant source is on the ground a little way upwind of the building (at two and one building heights distance respectively). Both figures show in order:

At the top left the plan layout of the buildings and the source position.
At the lower left the external pressure distribution, as C_p,
At the lower centre the pressure difference across the building faces, as C_p-C_i, assuming an internal pressure derived using Equation (6),
At the upper centre the concentration pattern on the building surfaces as dimensionless concentration, K.
At the right, the risk index, I_R, calculated from the adjacent pressure and concentration patterns.

Both plots of I_R in the figures show coloured contours in areas where there is contaminant ingress and blank areas where there is contaminant egress.

Figure 45, for the cubical building in open terrain shows high concentrations of contaminant around the lower parts of the upwind and side face of the building, with little exposure on the roof and a lower, but even, distribution of material across the downwind face. The related pressure difference pattern shows high positive pressure differences on the front face, low pressure differences at the sides and roof, mainly near the upwind edges and a nearly neutral pressure on

the downwind face. The resultant Risk Index pattern shows high levels of contaminant ingress on the upwind face, especially near the ground, almost no contaminant ingress on the side faces and the roof, but a second area of lesser levels of ingress across the whole downwind face.

Figure 46, for nearly the same source arrangement in a 16% area density array, shows again high concentrations of contaminant near the ground on the upwind and side faces of the building, but there is also a lower but significant level of concentration across the building roof, with a similar uniform distribution of contaminant concentration across the rear face of the building. The associated pressure difference pattern shows lower pressure differences over much of the building surface, but with higher pressure differences as before on the upwind face, negative pressures over most of the sidewalls and roof and low but varied pressure differences across the downwind face. The resultant Risk Index pattern shows again high values on the upwind face, smaller (asymmetric) areas of ingress risk on the sidewalls and an area of ingress risk in the centre of the downwind face. Thus the presence of the surrounding building array has both modified the risk ingress pattern and reduced the overall levels of risk of ingress.

7.2 Temporal response to Variable External Exposure

An important feature of contaminant ingress is the internal response to external changes in concentration. For a reasonably well sealed building with a ventilation rate of order 0.5 ACH, the characteristic (exponential) response time of a building with a well-mixed interior to external changes is then about two hours. Many incidents may involve time scales of this order or less, even for incidents of longer time scales small variations in the shorter term wind direction can significantly alter the exposure of a building to a relatively slender plume.

This subject has been of some previous interest, not only for response to releases during incidents, but also to short term changes in local air pollution levels, due to traffic flows for example. It was discussed by Hall et al(1996b) with regard to local air pollutants, but has been of longer interest with regard to handling exposure of the populace to toxic releases from industrial accidents. Here, the importance of the use of buildings as shelters from external exposure was a major consideration, as was the opposite requirement, of estimating the rate of release to the outside from contaminants released inside buildings. Wilson(1988) discussed the sheltering effectiveness of buildings with regard to the rate of internal penetration of external contaminants and the probable internal transfer paths in simply compartmented buildings. Wilson and Morrison(2000) further discussed the effectiveness of buildings as shelters from external exposure and provided a standardised decision control chart for the Canadian Association of Fire Chiefs. There is also a discussion by Fletcher(1997), who considered building internal environment response to external exposure.

Wilson(1990) went on from his earlier work to devise two simple numerical models for calculating both external and internal exposure, called EXPOSURE

and SHELTER. Wilson's equation (with a correction for an original misprint) for the mean internal concentration C_i for a well-mixed internal space (for both natural and mechanical ventilation), at time t is,

$$C_i(t) = e^{\frac{-t}{\tau}}\left[C_{i,s} + \int_{t_s}^{t} \frac{C_o(t')}{\tau} e^{\frac{t'}{\tau}} dt'\right] . \qquad (13)$$

for the exposure to a time variant uniform external exposure, C_o, after some arbitrary start time t_s, where,
$C_{i,s}$ is the initial internal concentration and
τ is the characteristic time response of the building ventilation (essentially 1/ACH).

Equivalents to Equation (13) occur in various parts of the literature. It can be integrated numerically fairly readily and Figure 47 shows some example calculations of building internal concentrations resulting from various external exposure patterns. This infiltration model is an integral part of Dstl's Urban Dispersion Model (Hall et al(2001)) and the figure is taken from an example using it. In all the plots the solid line is the external concentration and the broken line the internal concentration in response to the external value. The maximum external concentration, C_o is set arbitrarily at a value of 10. In cases (a) to (e) the initial indoor concentration is zero, in case (f) it is 10. In case (a), the external concentration is initially set at a constant value, at which it remains. In response the internal concentration rises exponentially, following the classic exponential response to a stimulus; the internal concentration increases by a factor of 1/e (63%) of the external/internal concentration difference (C_o-C_i) for each characteristic time interval, τ. In case (b) the initial external concentration is set to zero, but is later increased to its maximum over one time step. The internal concentration then rises exponentially to this value, as in case (a). In case (c), the external concentration falls linearly from an initially set maximum of 10. The internal concentration initially rises exponentially to match the external value then also follows this external fall linearly, but remains higher than the external concentration due to the lagging time response of the internal concentration to the falling external value. In case (d), the initial external concentration is set to 10, but is reduced to zero later over one time step. The internal concentration initially rises exponentially towards the external value and then falls exponentially to zero after the external concentration falls. Due to the lagging time response of the building ventilation, the internal concentration never reaches the maximum external value. In case (e), the external concentration follows the Gaussian distribution over time that would be expected of a large passing puff of contaminant (though the external Gaussian form in this case is normally skewed). The internal concentration follows the same pattern, but with a time delay and with a maximum lower than the external value. In case (f) there is an initial internal concentration (as might result from an earlier event) and the external concentration initially falls to zero, but is increased later to its maximum value over one time step. The internal concentration initially falls as clean external air ventilates the building and then rises again after the external air is contaminated again.

The internal response of mechanically ventilated buildings to external contaminants is largely similar to that described above, except that concentration levels at the ventilation inlets are the main (but not sole) point of contaminant entry. For simple calculations Equation (13) can be modified to deal with these cases without difficulty. Compartmented buildings, whether naturally or mechanically ventilated pose more difficulties, as individual compartments within the structure may show individual response patterns depending on the ventilation patterns within the structure; see, for example, the experiments of Santos et al(2011) on the infiltration by a trace gas of a compartmented building. Wilson(1988) describes some of the internal ventilation patterns that can occur in simply compartmented buildings. Large buildings with mechanical ventilation systems and complex multipartitioning require individual attention as it is doubtful whether there is a 'typical' building in this respect. Additionally, the VEETECH web site provides a simple tutorial on the response of building interiors to external exposure. The way in which spaces in a building actually ventilate may also be significant. All the discussion in this review essentially assumes a 'well mixed' interior in which the contents are uniformly mixed in a short time. Often this is not true and the actual interior ventilation rate may be well below that of the 'well mixed' assumption due to the lack of mixing within the space. This is a matter of some interest in building design and there is significant literature on it; see for example Bolster and Linden(2007), and the contents of the International Journal of Ventilation.

Some examples of external and internal measurements of time varying conventional pollutants are shown in Figure 48, taken from internal and external pollution measurements in and around a building in central Birmingham by Kukadia and Palmer(1998). The building in question was mostly naturally ventilated, but had a single floor mechanically ventilated, so that both types of ventilation could be investigated together. The upper plot is of carbon monoxide (CO) concentration, a largely externally produced and relatively unreactive pollutant. The lower plot is of carbon dioxide (CO_2) concentrations, also unreactive, where there was a significant level of internal production (mainly due to the occupants) and a lower relatively constant external concentration. The CO was mainly traffic generated, with major sources close to the building. The upper plot shows both high level and rapid fluctuations of external CO, mainly during the day when traffic levels were high. Internal CO concentrations in the mechanically ventilated part of the building were not identical to the naturally ventilated part, partly due to the different gas inlet conditions, mainly at a specific inlet in the mechanically ventilated part but more broadly distributed across the building faces in the naturally ventilated part. The lower plot shows a uniform base concentration of external CO_2, replicated internally when the building was uninhabited, and relatively high additional concentrations of internally generated CO_2 during the working day. At night, the internal CO_2 concentrations fell to close to the external values over some hours, the delay being due to the relatively slow building ventilation rate. The single large peak in internal CO_2 concentrations in the mechanically ventilated part of the building is thought to have been due to contamination of the air inlet by flue discharge of the gas-fired heating plant on the building roof.

8 INTERNAL LOSSES OF CONTAMINANTS

It is usual for there to be internal losses of infiltrating contaminants, both of gases and of particles. The losses may be by deliberate filtration of the incoming air, losses on transfer through the building fabric and losses due to deposition on to internal surfaces. These are dealt with in turn here. Gases and particles behave differently in all these removal processes. Gases may react internally. Particles may agglomerate, reducing the particle number count and size distribution but not the mass concentration. There is some information on this subject in a previous ADMLC review by Milner et al(2004).

It is common, but not universal, for mechanically ventilated systems to treat the inlet air, adjusting the temperature and humidity and possibly removing extraneous gases and particles. Since this is a mainstream activity of the construction and ventilation industries, it will only be discussed in general terms here. There are excellent reviews of ventilation air treatment in both the ASHRAE Handbook (ASHRAE(2011)) and in a number of CIBSE guides (see CIBSE(2005b) for example).

Gaseous and particle abatement systems have relatively high installation and maintenance costs, so that their use tends to be on the basis of perceived need rather than being an automatic component of standard installations. Some sort of chemical absorbent would be required for acid gases, active carbon filtering for organic vapours and a mechanical filter for particles. It would be unusual to find a complete suite of gas and particle control systems in an installation unless for some special purpose; abatement systems tend more to be chosen to suit local needs.

Particle filters are probably the most commonly used abatement devices, but operate to respectable (perhaps 75% plus) rather than absolute removal efficiencies and with a variable efficiency with particle size; it would be unusual to find HEPA particle filtering standards except in special purpose buildings like biological laboratories or some manufacturing plant (for semiconductors for example). Similar constraints apply to gas removal systems. Absorbents for acid gases are relatively specialised and a range of absorbent materials might be used depending on the contaminant(s) of interest. Joffe(1996) examined the application of chemical filtration to contaminated indoor air. He noted that 'while simple conceptually, efficient chemical filtration of indoor air is, in fact, a complex task comprising detailed planning, an efficient technology, and careful implementation'.

Carbon filtering is more commonly used for removing organic vapours, especially for odours (the removal of kerosene odours from airport buildings for example) or for controlling internal environments where odours or other organic vapours are generated internally and a high proportion of internal air recirculation is used (90% ventilation air recirculation is typical). Carbon filters also have an ability to remove some acid gases and particles, partly to the detriment of the filter's efficiency. It is also common for acid gases and particles to be removed in

mechanical system ventilation ducting, though it is at the expense of corrosion, for acid gases, and accumulated dust, for particles.

The apparent existence of gas or particle abatement in a ventilation system does not guarantee effective control. All of these abatement methods require regular maintenance. Particle, carbon and acid gas filters all have a limited life and require replacement on a fixed schedule if they are to remain effective. This is often neglected and in addition mechanical deterioration over time can result in leakage gas flow paths developing around the abatement equipment.

The loss of gases and particles in passing through the building envelope and then internally is understood and has been the subject of significant but intermittent attention in the ventilation and air pollution literature, in some cases as a possible deliberate design feature in naturally ventilated buildings. It has become of greater interest in more recent years in air pollution with a growing understanding of indoor exposure as a significant but poorly understood contributor to the overall exposure of the populace to air pollutants.

Where not deliberately abated, internal loses of infiltrating contaminants can only be (with a few exceptions) by deposition on to interior surfaces, whether internally or by filtration through the external building fabric. Gases can only be removed at surfaces by reaction or absorption. Particles are normally permanently removed on contact with a surface. The nature of this deposition is not fundamentally different from dry deposition in the external atmosphere, a well studied subject, and the same general rules apply. These are briefly described below as an aid to further discussion. There is a longer discussion of atmospheric deposition modelling in Jones(1983) and in Hall et al(2005).

The deposition rate, D, to a unit area of surface is usually defined as,

$$D = Cv_d, \qquad (14)$$

where C is the local ambient concentration and v_d is the deposition velocity. This basic principle applies to both external and internal deposition and to gases and particles. Note that this is a rate of removal of material, a dynamic function, not a fixed fraction of the internal mass of contaminant, which seems to be a commonly used description of internal losses. In a building with an infiltrated contaminant, C may be known but not v_d. Further, in atmospheric flows there is a single surface, the ground, but in a building there are multiple surfaces, the building floor, walls and ceiling plus the surface of any artefacts (furniture or other equipment) in the building. In a building with multiple compartments, the internal surface area of the building itself may be large, which increases the overall rate of deposition.

Deposition velocities are best estimated using resistance models, which attach 'resistances' to the three stages of the deposition process, for the transfer of material to the surface laminar sublayer by turbulent diffusion, R_a, its following transfer through the laminar sublayer by molecular diffusion, R_b, and its removal at the surface by chemical reaction, absorption, dissolution or (in the case of particles) contact with the surface, R_s. This is standard practice for atmospheric

deposition calculations. The three resistances are then summed and the inverse of the resistance gives the deposition velocity, so that for gases,

$$v_d = \frac{1}{R(\text{total})} = \frac{1}{R_a + R_b + R_s}. \quad (15)$$

The two aerodynamic resistances, R_a and R_b, are given in atmospheric flows approximately by

$$R_a = \frac{5.76}{u_*}, \text{ and (for gases) } R_b = \frac{7}{u_*}, \text{ so that,} \quad (16)$$

$$R_a + R_b \approx \frac{13}{u_*}, \quad (17)$$

where u_* is the aerodynamic friction velocity (proportional to the local air speed over the surface).

For highly reactive or very soluble gases over liquid surfaces the surface resistance, R_s, is approximately zero, so that the deposition velocity is then directly proportional to the airspeed close to the surface. Thus acidic or reactive gases on bare plaster or concrete surfaces may show nearly zero surface resistance. Moderately reactive, soluble or acid gases in the same circumstances may have surface resistances comparable to or more than the aerodynamic resistances, so that the deposition velocity is significantly reduced along with some of the dependence on local airspeeds. Similarly, acidic or reactive gases over painted plaster or concrete surfaces may have a significantly increased surface resistance due to the need for the gas to diffuse though the coating before any reaction with the base material can occur. Organic vapours may be soluble on wet surfaces or can be absorbed into many plastic surfaces (for example, PVC or PVC coatings, soft furnishings, painted or varnished surfaces). In these cases there is not normally a surface reaction and the gas diffuses into the surface, developing an equilibrium between the external and internal surface concentrations. The process is normally reversible, so removal of the external concentration will then result in a diffusion of the gas out of the surface and a continuation of contamination of the building. The nature and proportion of different surface types in buildings, which are critical to deposition and absorption processes, is a complex matter in its own right and has been subject to specific attention. For example Hodgson et al(2004) produced inventories of building contents in US houses by type and by fraction, as the surface area to volume ratio, which varied by up to factor of three between different rooms. They also noted that painted surfaces dominated surface areas in all rooms and that the furniture and fittings had surface areas comparable to or exceeding those of the empty rooms; they also discussed the significance of surface types to VOC absorption/desorption.

For particles above sub-micron size, transfer though the laminar sublayer by molecular diffusion (essentially the Brownian motion) is very slow, so R_b is large, and may be enhanced or diminished by a number of other processes. These are gravitational deposition, impaction due to particle inertia in moving airstreams,

thermophoresis (deposition driven by surface temperature gradients) and electrophoresis (deposition driven by charge gradients). Though particles can be resuspended, this is difficult to do to a particle which has been in contact with the surface for more than a brief period. Small particles especially can be subject to quite powerful molecular forces at the surface and resuspension usually requires some energetic action, high velocity air flows or mechanical abrasion for example.

The resistance equation for particle deposition including gravitational deposition is slightly modified from Equation (15) (see Hicks et al(1987), Seinfeld and Pandis(1998)), to,

$$v_d = \frac{1}{R_a + R_b + R_a R_b v_s} + v_s \ , \qquad (18)$$

where v_s is the gravitational settling velocity only. It will be noted that the surface resistance, R_s, does not appear in Equation (18) as its value is taken to be zero.

There is some variation of this equation between authors, but it does show clearly the effect of the additional deposition component for particles due to gravitational settling. Other particle deposition processes can be added into the equation as desired. Some sense of the different processes affecting deposition of particles of different sizes and their relative importance can be seen in Figure 49, which shows calculations, for deposition velocities of different particle sizes in the atmosphere. Figures of this type are common in the literature, there is a version of it in Jones(1983). Note the minimum in the deposition velocity for particle sizes around 1μm; above this deposition is dominated by gravitational settling, below it by molecular diffusion.

In a building, deposition of gases on to surfaces is independent of their alignment. For particles the aerodynamic components of the deposition are also independent of surface alignment but, clearly, gravitational settling of particles is only positive on floors and upward facing surfaces, on walls it has no effect and on ceilings and downward facing surfaces its contribution to the deposition is negative. However, the other factors affecting particle deposition noted above act on all surfaces. The effects of electrophoresis especially on small particle deposition may be underestimated. Virtually all particles in the atmosphere carry a charge and their contribution to deposition is not commonly discussed, except when applied to electrostatic precipitators.

It will be appreciated from the discussion above that internal contaminant deposition depends on a deposition velocity affected by the local airspeed over the surface, the material (gas or particle, reactivity or solubility) and, in the case of particles, the aerodynamic diameter and the presence of other depositing forces besides gravitational settling. Under these circumstances the use of blanket values of deposition velocity in calculations of internal losses needs to be treated with caution. There has been a significant interest in this subject, mainly in relation to indoor particle deposition. Karlsson(1994) reviewed and developed indoor infiltration deposition models and infiltration gas loss models, also

providing some experimental data on gas and particle deposition. He quoted nominal gas deposition velocities, mainly in domestic buildings, as summarised in Table 2.

Table 2. Estimates of Internal Surface Deposition Velocities of Different Gases.
From Karlsson(1994)

Gas	Range of surface deposition velocities (m s^{-1})
NO_2 (moderately reactive)	$0.1 - 8x10^{-4}$
SO_2 (very reactive)	$1.4x10^{-4}$
O_3 (highly reactive)	$3\text{-}6x10^{-4}$
HNO_3, NO_3 (highly reactive)	$7x10^{-4}$
NO, CO (low reactivity)	0
Cl_2, (very reactive)	$1x10^{-4}$
NH_3, (moderately reactive, very soluble)	$3\text{-}5x10^{-5}$
Trialkylphosphonoacetate	$1.6\text{-}2.6x10^{-4}$

These deposition velocities are, as noted by Karlsson, all significantly lower than would be expected on the ground in the atmosphere. Karlsson also noted the critical effect of the room ventilation rate, so that a relatively well sealed room could attain an indoor/outdoor concentration ratio approaching 0.1, while a more conventional ventilation rate (around 0.5 ACH) resulted in a ratio nearer 0.4.

There is a limited literature on indoor particle deposition. Lange(1995) reviewed modelling methods and deposition data (on particles) from a number of sources; Kildeso et al(1999) measured dust build up (equivalent to a deposition rate) on indoor surfaces (mainly in offices) and there is a more general review identifying research needs by Thatcher et al(2001). This was followed in Thatcher et al(2002) by an analysis of their own and other particle deposition measurements in measurements. Figure 50 shows some of their results of the reduction in particle concentration loss for different particle sizes. Note the minimum of the particle loss rate for sizes around 1μm, where the deposition velocity is at a minimum, as shown in Figure 49. Significantly raised internal ventilation airspeeds enhanced the deposition rate in this case, consistent with Equation (17).

Losses in contaminant ingress through building façades does not differ in principle from that internally, but the nature of the surface exposure is different in that the flow is either infiltration though small gaps in the structure, where the air flow is mostly laminar, or ventilation though large inlets or open doors or windows. In the latter case losses are unlikely to be very large, but in the former case may be significant. For gases, small gaps allow more rapid diffusion to the walls, so that effective removal can occur on the right types of surface. Removal of particles in small gaps is more complex. In the laminar flows likely to exist here particle diffusion to the walls will be slow, but deposition due to gravity or other particle forces maybe easier due to the short travel distances over which the force needs to act. Larger particles, above micrometre size, can

be more readily lost in convoluted gaps with sharp turns due to particle inertia. For example, a 1mm gap in a door frame with an airflow of 1 m s^{-1} through it and a right angle bend on its inside corner will not pass particles larger than about 20μm aerodynamic diameter.

There has been some specific interest in the filtering properties of the building fabric, mainly in relation to particle abatement, and some measurements and calculations of the relationship between indoor and outdoor exposure have been reported. Taylor et al(1999) described the principle of deliberately using the building as an air filter, with air-permeable walls ('Dynamic Insulation'), though this has yet to be taken up as a general design principle in construction. There are a number of specific models for particle penetration through small gaps in the building shell by Tung et al(1999) and by Liu and Nazaroff(2001), while Thatcher et al(2003) use a 'concentration rebound' method for the same purpose. Liu and Nazaroff(2002) produced an analysis for particle penetration through windows and Liu and Nazaroff(2003) went on to calculate and measure particle penetration through deliberately made cracks in different materials. Some of their results from this latter work are shown in Figure 51. The material used seemed to make a limited difference to the overall result, which again showed maximum penetration for particle sizes around 1μm, where the deposition velocity passes through a minimum. Their model calculations proved a reasonable approximation to the data.

Internal/external concentrations of atmospheric pollutants also provide information on internal deposition rates. Figure 52 shows internal and external measurements of a reactive gaseous pollutant (NO_2) from the same building and measurement series as in Figure 48, from Kukadia(1999) with a mechanically ventilated floor in an otherwise naturally ventilated building. The measurements show the same damping and delayed response to external concentration fluctuations as for the unreactive pollutants in Figure 48. However, they also show an overall lower level of internal concentration than externally in both the naturally and mechanically ventilated parts of the building due to internal losses.

Internal/external pollutant measurement from another, naturally ventilated, building from Kukadia et al(2000), are shown in Figure 53, for paired measurements of air pollutants inside and outside a naturally ventilated laboratory building in Manchester. The six plots are of matched internal /external average concentrations from a number of sampling sites both inside and outside the building. The straight line on each plot is the 1:1 line of similar internal and external concentrations. The measurements were made over a period of about six months covering a range of wind and weather conditions. The plots show fairly consistent indoor attenuation increasing with reactivity, except for CO_2, which had high levels of internal generation. Average ratios of internal to external concentration are given in Table 3.

Table 3. Measurements of Internal Losses of External Gaseous Pollutants From Kukadia et al(2000).

Air Pollutant	Mean Internal/External Concentration Ratio
CO_2 (unreactive but internally generated)	>1
CO (unreactive)	1
NO (low reactivity)	0.85
NO_2 (moderately reactive)	0.6
SO_2 (very reactive)	0.65
O_3 (highly reactive)	0.45

The effect of gas reactivity on the internal losses is clear, especially for the more highly reactive gases. The degree to which these losses are due to the infiltration process or internally is not known.

Figure 54 shows similar types of measurement for particles made in a naturally ventilated commercial office building in London (Kukadia et al(2011b)). The upper plots are of internal against external PM_{10} concentrations and the lower plots are of the particle size distribution within the PM_{10} size range. The three pairs of plots are for winter, spring and summer conditions, between which the, ventilation rate varied due to the inhabitants actions. The office in which the measurements were made was empty in winter and spring, with windows and door closed, but inhabited in the summer. This change in use shows in the PM_{10} concentrations, which were attenuated inside when the office was empty, but higher inside than outside when it was occupied. This was thought to be partly due to the greater level of internal particle generation internally in the occupied office, allied to more opening of windows in summer. Differences in the particle size distributions for the three periods were less clear; particle numbers at all sizes were significantly attenuated on average (typically by a factor of five) and particle counts of the larger sizes covered a range of almost two orders of magnitude.

Figure 55 shows averaged indoor/outdoor concentrations of gaseous pollutants and PM_{10}, and of particle number by size for different periods in the same experiment described in Figure 54. The gaseous pollutant concentrations show no internal attenuation for unreactive CO, little attenuation of NO but significant levels of attenuation for the more reactive NO_2. The PM_{10} particle mass concentrations showed attenuation over most of the year but were higher internally than externally during the summer period when the office was occupied. This plot also shows the mean ventilation rate of the building, which was significantly higher in summer than in winter, and attenuation of the more reactive gases roughly followed the ventilation rate, increasing as the ventilation rate reduced. The particle size distributions also showed variable attenuation with the season and the larger particle sizes especially were more highly attenuated in the winter when the building ventilation rate was lower.

It is clear from this discussion that internal attenuation of both reactive and soluble gases and of particles infiltrated from outside can generally be expected,

but that the manner in which this attenuation occurs is more problematic. It is individualistic between different gases and particle sizes and depends on a variety of factors including the building ventilation rate and type, the infiltration process and the availability of the type and areas of internal surface on which surface deposition or absorption can occur.

9 BUILDING VENTILATION MODELS

Numerical models of building ventilation and infiltration are an important feature of ventilation practice. They are only discussed briefly here as the earlier ADMLC review (Milner et al(2004)) has covered this to some degree and they are too complex a matter to discuss as a small part of the present review.

Models vary from those that use simple calculation methods for obtaining approximate bulk estimates of building exposure and ventilation or infiltration rates into buildings to complex CFD calculations. Building exposure patterns from sources at longer distances can be found from conventional dispersion modelling techniques, though (as noted previously) these tend to fail at distances blow about 1km in urban areas, where the form of the urban array as well as its overall aerodynamic roughness (the single surface parameter usually used in dispersion modelling) starts to affect the dispersion patterns around buildings.

Many of the simpler types of calculation, as noted earlier in this report can be carried out at spreadsheet level. They require a minimum of basic data on the building and its exposure and pressure patterns, much of which can be found in data on bulk building properties of the sort described here. For example the VEETECH website will provide building ventilation and other data from a limited input. Similarly, Kukadia and Hall(2011a) provide a simplified procedure for calculating exposure of buildings to multiple sources of pollutants in urban areas, from which building pollutant infiltration rates can be estimated. More detailed infiltration calculations can also be carried out at spreadsheet level provided that adequate data on building pressure patterns, external exposure patterns and the building envelope infiltration properties are supplied. Wilson's(1990) SHELTER and EXPOSURE models are good examples of simple exposure and ingress calculations which can also be used on spreadsheets.

More complex models of internal ventilation flows are common in the construction industry, especially for calculating airflows through multi-compartmented mechanically ventilated buildings for design purposes. There are thus numerous building ventilation models that attempt to calculate airflows through buildings. They require inputs of external conditions at the assumed points of air ingress, which has to be supplied by other means. There are discussions of the principles involved in such models in Etheridge and Sandberg(1996) and, Etheridge(2012) and in the ASHRAE handbook (ASHRAE(2009)). The COMIS model (Feustel(1998)), developed at the Lawrence Berkeley National Laboratory (available as free download), is an example of a model that calculates the airflow and contaminant distributions in buildings. Various elements including ducts, fans, doors, windows etc can be simulated and schedules of their operation or use can be included in the model.

More sophisticated models have also become available which include more variable external contaminant infiltration. The US National Institute of Standards and Technology have developed the CONTAM model (Dols(2001), Walton & Dols

(2005), Wang et al(2010)) which is a multizone airflow and contaminant transport model and available as a free download. It can be used to determine the infiltration and exfiltration of air in and between rooms in buildings with mechanically driven ventilation systems. Wind pressures on the outside of the building and buoyancy effects resulting from the difference in temperature inside and outside the building are used to predict building internal airflow and ventilation rates. Contaminant concentrations are determined from these airflows and can be used to estimate internal personal exposure. The latest version of this model contains many features, including the ability to model spatially varying external contaminants, wind pressures and deposition. Internal deposition can also be modelled within CONTAM, either with a user-defined deposition surface area for each zone with a constant assumed deposition velocity, or using the volume of the zone with a concentration dependent fixed depletion rate. In the former case an additional re-suspension model can also be added. There is an additional option to model the deposition of particles inside ducts by defining the contaminant filtering properties of duct segments. CONTAM also has the option to simulate one internal zone using CFD so that this zone can have a variable temperature and contaminant concentration. There is a need for independent validation studies of such models. Both COMIS and CONTAM were reviewed by Lorenzetti(2002).

Dimitroulopoulou et al(2006, 2008) have developed a tool to predict the impact of external contaminant releases on indoor office environments and the associated individual human exposure. The tool uses output from models such as CONTAM as input to their INDAIRC++/EXPAIRC++ modelling framework which has been developed to cover the larger number of zones that are typically found in office buildings. The tool can be used to calculate frequency distributions of contaminant concentrations in these zones and also to determine frequency distributions of exposure, and inhaled dose, of individuals taking different evacuation routes from the building.

In their ADMLC review of 2004, Milner et al remarked that the use of conventional CFD modelling (using a Reynolds averaged 'RANS' type of turbulence model) for building ventilation was not widespread and remained something of a research activity. In the intervening time the considerable improvements in desktop operating speeds and capacity, together with improvements in model solution procedures, has made its use more commonplace as a working design tool (see Liddament(2003), ASHRAE(2009, Ch15)). It appears to be useful for calculating internal flows, especially in natural ventilation, as in the example by Gan(2010) in Figure 3. However this type of CFD model experiences more problems in dealing reliably with external building flows and dispersion. The difficulty lies in the RANS turbulence model, which is essentially a small scale diffusive model. This can be satisfactory for flows where the turbulence is essentially small scale or not a dominant feature of the flow. However, in both dispersion and flows around buildings, the flow field is one with a dominant large scale turbulence component associated with the atmospheric boundary layer. This directly affects flows and dispersion around buildings, which additionally produce large scale fluctuating and eddying motions

of their own in their flow field. The flows are thus both time-dependent and driven to a significant extent by large turbulent eddy behaviour, which RANS models cannot simulate reliably. Similarly it affects calculations of external dispersion as turbulence is the primary driver of the dispersion. More recent CFD model developments, which use large eddy scale (LES) or detached eddy scale (DES) models to directly model the structure of the large scale turbulence, show much greater promise in calculating these complex, time dependent flows. Unfortunately, at present their development is roughly at the equivalent stage of RANS CFD modelling as described by Milner et al in 2004. They are substantially more computer intensive, requiring advanced multiple processing computers and large memory capacity to obtain plausible run times. They are also presently in what might be called 'development' mode as they are time consuming to set up and operate and are still subject to development of their modelling methods. Thus they do not presently class as workplace tools for building pressure, ventilation and exposure calculations. There is an interesting discussion by Cochran and Derickson(2010) on the use of CFD models in wind engineering, in which they remarked at the time of writing that the cost of LES model calculations on a building airflow for 36 wind directions far exceeded the cost of the same wind tunnel measurements on a model with 600 pressure taps. There is also a general problem in providing adequate experimental data sets for CFD model validation. Those involving building flows and dispersion require adequate information about the turbulent structure of the approach flow. This process is ongoing, but some sense of the difficulties in making reliable validation comparisons is given in earlier work of Leitl(2000) and by Schatzman and Leitl(2002).

There is a general principle in the use of building ventilation and exposure models from spreadsheets upwards, as described here, which is that the amount of information required about a building and its exposure tends to increase exponentially with the complexity of the model. More sophisticated models usually require more sophisticated input data. This is also an individualistic process to some degree as most buildings are, or eventually become, unique, due to both their own structural properties and their surroundings. Only a limited number of buildings, for example relatively small and low value structures such as domestic housing tend to be built to standard designs. Large, high value structures are more likely to be individual designs. Determining the detailed properties of a building for infiltration calculations can not only be a time consuming process but, also, the essential information may not always be available. Thus the cost and escalating effort required to set up and run more sophisticated calculations makes this a less likely option except for designing new buildings of high value, specific examples of multiple low value structures or in dealing with buildings which, because of their usage, are unusually sensitive to the ingress of contaminants. ASHRAE(1997, p25.7) noted 'To determine the pressure difference across the building envelope and the corresponding air exchange rates, building specific information about the exterior pressure distribution due to wind and the location of and airflow rate/pressure distribution relationship for every opening in the building are needed. These inputs are difficult to obtain for any given building, which makes such a determination

unrealistic.’ To this must be added the additional uncertainties associated with predicting the contaminant exposure pattern on the surface of the building, described in Section 5.

10 DISCUSSION AND CONCLUSIONS

This review has dealt in order with the chain of events during which buildings are internally exposed to external contaminants. It has involved:

The probability and nature of the external exposure.
The process of building ventilation and the forces that drive it.
The nature of external contaminant ingress and the risk of it occurring.
The internal consequences of short term external exposure.
Contaminant losses internally and during the infiltration process.
Methods of calculating ventilation, infiltration and internal exposure.

All of these matters are major or minor specialisms in their own right and it has only been possible here to cover the individual subjects briefly, noting their essential characteristics for the present application. They are reviewed briefly below. We have tried to provide sources for obtaining further information where possible. However, it will be clear from the discussion in the main text that there are a number of substantial deficiencies in the information data base in this chain of processes.

The probability and nature of building external exposure can be estimated plausibly for sources at longer distances, around 1km and beyond, using conventional dispersion calculations. Inside this distance, especially in urban areas, estimating exposure on building surfaces becomes progressively more difficult and uncertain as the source approaches the building. There is little systematic data on building exposure at short ranges in different conditions for both plume and (especially) puff releases, which exacerbates the prediction problem. The time dependence of external building exposure, even from nominally constant releases, has received little attention. Modelling the probability of exposure at shorter ranges is similarly difficult, especially in urban areas, as dispersion patterns are modified by the details of the release interaction with the building itself, with the surrounding building array pattern and with the wind direction, all of which should be taken into account. Simple prediction methods for external exposure, such as that of Kukadia and Hall(2012), can be helpful in this respect, but would benefit from further development and calibration.

Building ventilation, air ingress and the forces that drive it are well understood matters in the construction industry. In comparison with the position in predicting external contaminant patterns on buildings, the construction industry is about a generation ahead in its efforts to predict building pressure patterns and ventilation in systematic ways. There is a large research data base and attention has been given to systematic studies and the development of standard prediction methods for both building surface pressure patterns and ventilation rates for buildings of conventional form. However, buildings of unusual shape, complex structures and those with complex internal partitioning are still the subject of detailed individual attention and experimentation, whether naturally or mechanically ventilated. For example, modern buildings designed for

effective natural ventilation often have complex, carefully designed internal flows which account for all ventilation conditions. There appears to be no recent systematic data base of UK building ventilation properties; no attempt being made to use for this purpose results of the large number of building pressure tests regularly made on a commercial basis.

The process of contaminant ingress is a complex mixture of pressure driving forces and exposure patterns on the building surface. For sources at longer distances, where exposure patterns on buildings become more evenly distributed, ingress is easier to calculate as it is dominated by the external ventilation pattern. At shorter ranges both pressure and concentration patterns may vary considerably, and the resultant potential ingress patterns with them. The concept of 'risk of ingress' described here is a helpful way of examining probable areas of significant ingress over the building surface, from which (given the surface porosity or details of openings) rates of ingress can be calculated. So far, partly due to lack of suitable compatible pressure and concentration data, it has not been possible to explore this methodology more fully.

Internal temporal response to external variations of exposure is particularly important when considering buildings as shelters, but is in any case a characteristic of the internal exposure. It is likely to occur not only in response to exposure to short term releases, but also to longer term releases. Exposure to plumes is normally intermittent in both the short term (due to turbulence) and the longer term (due to plume meandering and variations in the mean wind direction). There are additional effects at shorter ranges within urban building arrays as wind flow patterns within the urban array (and the associated dispersion) can switch intermittently between different quasi-stable patterns, triggered by the larger turbulent eddies and by small changes in the mean wind direction. The examples of internal exposure given here are for simple, well connected, internal structures. However, for buildings with multiple internal compartments and complex internal flows, more complex conditions can prevail and different parts of a building may show different responses to external exposure.

Contaminant losses both internally and during infiltration through the fabric or in the ventilation system can be a significant contribution to internal attenuation of contaminants. The process of loss (by deposition) to internal surfaces is similar to that at the ground in the atmosphere, but subject to different internal conditions of air speed, surface type and roughness. It is highly variable and different for particles (depending on particle aerodynamic diameter and other properties) and gases (depending on reactivity, solubility and surface resistance). Removal of gases may be permanent or temporary. From the few examples given here for experiments on particles in narrow cavities, it seems that high initial losses of contaminants through infiltration and the ventilation system are quite possible, before considering further losses internally. Internal attenuation of external contaminants is also a dynamic process, arising from the balance between the rate of ingress and rate of internal removal. Thus the ratio of internal/external contaminant concentration is the product of a complex process and not a reliable guide per se for predicting internal conditions.

Though models and methods exist for dealing with parts of this dynamic process of external exposure to contaminants, their ingress though the building fabric by infiltration and ventilation and their losses internally, integrated models for predicting this whole process are limited. The freely available CONTAM model is one of the few, but addresses some parts of this problem in a limited and probably unreliable way. Spreadsheet models, partly using empirical approximations, can be used for the whole process and are readily adaptable, but no integrated model of this sort seems to exist in the public domain. There is a practical difficulty in using more sophisticated models for this sort of calculation, in that they require exponentially increasing amounts of basic data on the parameters driving the exposure, ingress and internal loss of external contaminant and on the building's properties. Apart from the cost and complexity of such sophisticated calculations, all the information required to operate them may (in many cases) simply not be available.

It should be clear from this review that in the practical application of ingress and internal exposure calculations there are significant uncertainties that arise naturally in every part of this complex calculation chain. In consequence the estimation of internal exposure to external pollutants is in most cases never likely to be very precise. This also suggests a law of diminishing returns in attempting more sophisticated calculations.

11 ACKNOWLEDGEMENTS

We are grateful to a number of individuals for discussions on the state of the art and availability of base data in their specialist fields. These especially include Vina Kukadia, Paul Blackmore, Stuart Upton and Chris Scivyer at BRE and Martin Liddament of VEETECH.

12 REFERENCES

Allwine KJ, Shinn JH, Streit GE, Clawson KL, Brown M.(2000) Overview of Urban 2000. Bull. Am. Meteorol. Soc., Vol. 83, pp 521-536.

ASHRAE(1988) Air Leakage Performance for Detached Single-Family Residential Buildings. American Society of Heating, Refrigeration and Air Conditioning Engineers (ASHRAE), Standard 119.

ASHRAE(1997) AHSRAE Handbook. Fundamentals, Chapter 15, Ventilation and Infiltration. ASHRAE, 1997.

ASHRAE(2009) AHSRAE Handbook. Fundamentals, Chapter 16, Ventilation and Infiltration. ASHRAE, 2009.

ASHRAE(2011) ASHRAE Handbook. HVAC Applications, Chapter 45, Building Air Intake and Exhaust Design. ASHRAE 2011.

Arnold SJ. et al(2004) Introduction to the DAPPLE Air Pollution Project. Science of the Total Environment, Vol. 332, Pp. 139-153.

ATTMA(2010) Measuring Air Permeability of Building Envelopes. Technical Standard L1 (Dwellings), Technical Standard L2 (Non-Dwellings). The Air Tightness Testing and Measurement Association, Northampton, UK. October 2010.

Biltoft CA. (2001) Customer Report for Mock Urban Setting Test. Dugway Proving Ground, USA. DPG Document Number 8-CO-160-000-052. Prepared for the Defense Threat Reduction Agency.

Bolster DT, Linden PF.(2007). Contaminants in Ventilated Filling Boxes. Journal of Fluid Mechanics, Vol. 591, Pp. 97-116.

Bowen AJ.(1976). A Wind Tunnel Investigation Using Simple Building Models to Obtain Mean Surface Wind Pressure Coefficients for Air Infiltration Estimates. Report No. LTR-LA-209, National Research Council of Canada, National Aeronautical Establishment. December 1976.

Building Regulations(2010): Part F – Ventilation: Part L, Conservation of Fuel and Power. RIBA Bookshops. ISBN 978-1-85946-370-3. Also as web downloads.

BRE(1974) The Wind Loading Handbook. Building Research Establishment, 1974.

BRE(1990) BRE Digest 346: The Assessment of Wind Loads: Part 6: Loading Coefficients for Typical Buildings. Part 8: Internal Pressures. Building Research Establishment, 1990.

BSI(1991) Code of Practice for Ventilation Principles and Designing for Natural Ventilation. British Standards Institution, BS 5925:1991.

Cermak JE, Lombardi DJ, Thomson RS. (1974). Application of Physical Modelling to the Investigations of Air Pollution Problems in Urban Areas. 67th Annual Meeting of the Air Pollution Control Association. Denver USA, June 9-13. Paper No. 74-160.

Cheng H, Kukadia V, Hall DJ, Upton SL. (2012a). A New Methodology for Identifying Areas of Buildings at Risk of Pollutant Ingress. Building Research Establishment, Client report number 269-512, June 2012.

Cheng H, Hall DJ, Kukadia V, Upton SL. (2012b). Identifying Areas at Risk of Pollutant Ingress on Buildings. Paper present4ed at 2012 Annual UK review Meeting on Outdoor and Indoor Air Pollution Research, 3-4th May, Cranfield University.

CIBSE(1999). Minimising Pollution at Air Intakes. CIBSE Technical Memorandum, No TM21: 1999, February 1999. ISBN 0-900953-91-8.

CIBSE(2005a) Natural Ventilation in Non-Domestic Buildings. CIBSE Applications Manual AM10:2005. ISBN 978-1903287-569.

CIBSE(2005b) Guide B. Heating, Ventilating, Air Conditioning and Refrigeration. Chartered Institute of Building Services Engineers, ISBN 978-1903287-3.

Clawson KL, Carter RG, Lacroix DJ, Biltoft CA, Hukari NF, Johnson RC, Rich JD, Beard SA, Strong T.(2005) Joint Urban 2003 (JU03) SF_6 Atmospheric Tracer Field Tests. NOAA Technical Memorandum OAR ARL-254, May 2005.

Colville RN, Scaperdas AS, Hill JH, Smith FB. (1997). Review of Models for Calculating Air Concentrations when Plumes Impinge on Buildings or the Ground. National Radiological Protection Board. NRPB Report No. R302, 1997.

Cook NJ.(1985). The Designers Guide to Wind Loading of Building Structures. Part 1. Building Research Establishment/Butterworths. ISBN 0 408 00870 9.

Cook NJ. (1990). The Designers Guide to Wind Loading of Building Structures. Part 2 - Static Structures. Building Research Establishment/Butterworths. ISBN 0 408 00871 7.

Dabbert WK, Ludwig FL, Johnson WB. (1973). Application to an Urban Diffusion Model for Vehicular Applications. Atmospheric Environment, 1973, Issue 7, Pp.603-618.

Dabbert WF, Hoydysh WG.(1991). Street Canyon Dispersion: Sensitivity to Block Shape and Entrainment. Atmospheric Environment. Vol. 25A, No. 7, pp1143-1153.

Dimitroulopoulou C, Ashmore MR, Hill MTR, Byrne MA, Kinnersley R. (2006). INDAIR: A probabilistic model of indoor air pollution in the U.K. Atmospheric Environment, Vol 40, 33, pp. 6362-6379.

Dimitroulopoulou C, Kukadia V, Upton S, Ashmore MR, Terry A, Spanton AM, Hall DJ, Jaggs M. (2008). Development and validation of a probabilistic model for IAQ and human exposure in offices: Project Overview. Paper presented at the Indoor Air Conference, Copenhagen, 17-22 August 2008.

Dols WS. (2001). A Tool for Modeling Airflow and Contaminant Transport. ASHRAE Journal, March 2001, Pp. 35-41.

EC(2003) prEN 1991-1 4.6 June2003. Eurocode 1: Actions on Structures – Parts 1-4: General Actions – Wind Actions. Defined for the UK in British Standard BS EN 1991-1-4:2005 and Annexe A1: 2010. See also BS6399-2: 1997 Incorporating Amendment 1, Loading for Buildings – Part 2: Code of Practice for Wind Loads. ISBN 0 580 27447 0.

ESDU(1992). Fluid Forces, Pressures and Moments on Rectangular Blocks. Engineering Sciences Data Unit (ESDU). Fluid Mechanics External Flow Sub Series, Volume 2, 71016.

Etheridge D, Sandberg M. (1996). Building Ventilation: Theory and Measurement. Wiley. ISBN 0 471 96087 X.

Etheridge D. (2012). Natural Ventilation of Buildings: Theory, Measurement and Design. Wiley. ISBN 979 0 470 66035 5.

Feustel HF. (1998) COMIS – An International Multizone Air-Flow and Contaminant Transport Model. Lawrence Berkeley National Laboratory, LBNL-42182. Available at http://epb.lbl.gov/publications/pdf/lbnl-42182.pdf

Fletcher J. (1997). Ventilation Control as a Function of Indoor and Outdoor Air Quality. CIBSE/ASHRAE National Conference, 1997. Paper No. AIVC11130 Proceedings, Pp120-128.

Gan G. (2010) Interaction Between Wind and Buoyancy Effects in Natural Ventilation of Buildings. The Open Construction and Building Technology journal, Vol 4, Pp 134-145.

Hall DJ, Kukadia V, Walker S, Marsland GW. (1995). Plume Dispersion from Chemical Warehouse Fires. BRE Report No. CR 56/95. September 1995.

Hall DJ, Spanton AM, Macdonald R, Walker S. (1996a). A Review of Requirements for a Simple Urban Dispersion Model. Building Research Establishment, Report No. CR 77/96, April 1996.

Hall DJ, Spanton AM, Kukadia V, Walker S. (1996b). Exposure of Buildings to Pollutants in Urban Areas - A Review of the Contributions from Different Sources. Building Research Establishment, Report No CR 209/96. December 1996. Published as Chapter 12 in 'Effects of Air Pollution in the Built Environment '(Ed P Brimblecombe) World Scientific Publishing Co. 2003. ISBN 1-86094-291-1. Also in short form in the Proceedings of the 'International Conference on Energy and the Environment.' Brunel University 1997.

Hall DJ, Kukadia V, Spanton AM, Walker S, Marsland GW. (1996c). Concentration Fluctuations in Plumes Dispersing Around A Building - A Wind Tunnel Model Study. Building Research Establishment, Report No. CR16/96, January 1996

Hall DJ, Macdonald R, Walker S, Mavroidis I, Higson H, Griffiths RF. (1997). Visualisation Studies of Flows in Simulated Urban Arrays. Building Research Establishment Ltd, Report No. CR 39/97, February 1997.

Hall DJ, Walker S, Spanton AM, Kukadia V. (1999a). Pressure and Concentration Patterns on Building Forms in Urban Arrays. Building Research Establishment, Report No CR125/99, April 1999.

Hall DJ, Walker S, Spanton AM. (1999b) Dispersion from Courtyards and Other Enclosed Spaces. Atmospheric Environment, Vol 33, pp1187-1203, 1999.

Hall DJ, Sharples H, Walker S, Kukadia V. (2000) Attribution of Pollutant Concentrations on Buildings from Local Traffic – Effects on Ventilation Requirements. Building Research Establishment. Report No 81461, May 2000. Also in International Journal of Ventilation. Vol. 2, No. 2, pp. 169-182. September 2003.

Hall DJ, Spanton AM, Griffiths IH, Hargrave M, Walker S, John C. (2001). The UDM. A Model for Estimating Dispersion in Urban Areas. Paper Presented at the Seventh International Conference on Harmonisation Within Atmospheric Dispersion Modelling for Regulatory Purposes. Belgirate, Italy, 28-31 May 2001.

Hall DJ, Walker S, Mfula A, Spanton AM, Kukadia V. (2002). Pressure and Concentration Patterns on Buildings in Urban Arrays and the Ingestion of Contaminants. Paper presented at the Sixth George Mason University Transport and Dispersion Modelling Workshop. George Mason University, Fairfax, Virginia, USA. 10-11 July 2002.

Hall DJ, Spanton AM. (2004). A Wet and Dry Deposition model for the UDM. Envirobods Ltd, Technical Report No. 04/04, February 2004.

Hall DJ, Spanton AM. (2005) Review of Models for Dispersion Following Fires. Atmospheric Dispersion Liaison Committee. Report ADMLC/2003/1. April 2005.

Hall DJ, Spanton AM, Powlesland, CB. (2005). Review of Modelling Methods of Near-Field Acid Deposition. Environment Agency, R&D Technical Report P4-083/3/TR. May 2005. Available from the Environment Agency web site or the authors.

Halitsky J. (1963). Gas Diffusion Near Buildings. ASHRAE Transactions, Paper No.1855, Vol. 69: Pp 464-485.

Hanna SR, Britter RE. (2002). Wind Flow and Vapour Cloud Dispersion at Industrial and Urban Sites. American Institute of Chemical Engineers, Center for Process Safety, ISBN 0-8169-0863-X.

HARMO14(2011) 14th Conference on Harmonisation within Atmospheric Dispersion Modelling for Regulatory Purposes. Kos, Greece, October 2-6 2011. Session on 'Inverse Dispersion Modelling and Source Identification'. Available at www.harmo.org/harmo14.

Hicks BB, Baldocchi DD, Meyers TP, Hosker RP Jr, Matt DR.(1987) A Preliminary Multiple Resistance Routine for Deriving Dry Deposition Velocities from Measured Quantities. Water, Air and Soil Pollution. Vol 36, pp311-330.

Holmes JD. (1986). Wind Loads on Low Rise Buildings: Chapter 12. The Structural and Environmental Effects of Wind on Buildings and Structures. Faculty of Engineering, Monash University, Melbourne, Australia.

Hodgson AT, Ming KY, Singer BC. (2004). Quantifying Object and Material Surface Areas in Residences. Indoor Environment and Atmospheric Sciences Department, Berkeley National Laboratory, USA, December 2004.

Hongo T, Yoshida M, Sanada S, Nakamura O. (1979). Experimental Study of Wind Forces on Tall Buildings. (part 1)) Aerostatic Forces. Annual Report of the Kajima Institute of Construction Technology, 1979. Vol. 27 Pp. 209-216.

Hoydysh WD, Dabbert WF. (1994). Concentration Fields at Urban Intersections: Fluid Modelling Studies. Atmospheric Environment. Vol. 28, No. 11, pp. 1849-1860.

Hunt JCR, Carruthers DJ, Britter RE, Daish NC. (2002). Dispersion from Accidental Releases in Urban Areas. Atmospheric Dispersion Liaison Committee. Report No. ADMLC/2002/3.

Hussain M, Lee BE. (1980) An Investigation of Wind Forces on Three-Dimensional Roughness Elements in a Simulated Atmospheric Boundary Layer Flow, Part II: Flow Over Large Arrays of Identical Roughness Elements and the Effects of Frontal and Side Aspect Ration Variations. Sheffield University, Department of Building Science, Report BS56.

Joffe MA. (1996). Chemical Filtration of Indoor Air: An Application Primer. ASHRAE Journal, February 1996, Pp 42-49.

Jones JA. (1983). Models to Allow for the Effects of Coastal Sites, Plume Rise and Buildings on Dispersion of Radionuclides and Guidance on the Value of the Deposition Velocity and Washout Coefficients. National Radiological Protection Board, Report No. NRPB-R157, December 1983.

Karlsson E. (1994). Indoor Deposition Reducing the Effect of Toxic gas Clouds in Ordinary Buildings. Journal of Hazardous Materials, Vol. 38, Pp. 313-327.

Kildeso J, Vallarine J, Spengler JD, Brightman HS, Schneider T. (1999). Dust Build-up on Surfaces in the Indoor Environment. Atmospheric Environment, 33

Kukadia V, Palmer J. (1998) The Effect of External Atmospheric Pollution on Indoor Air Quality: A Pilot Study. Energy and Buildings 27 (1998) pp223-230

Kukadia V, Hall DJ, Walker S. (1998). Building Ventilation and Indoor Air Quality: The Impact of Urban Air Pollution - A Review BRE Report No CR 135/98. July 1998.

Kukadia V. (1999) The Effect of External Pollution on IAQ: Some Case Studies. Paper presented at the Environmental Health Congress, September 1999, Bournemouth.

Kukadia V, Hall DJ, Walker S, Sharples H. (2000). The Effect of External Pollution in the Context of Low Energy Architecture. Presented at the World Renewable Energy Congress – VI 2000. July 2000, Brighton UK.

Kukadia V, Hall DJ. (2011a). Ventilation for Healthy Buildings – Reducing the Impact of Urban Air Pollution. Produced for the BRE Trust by BRE Press, ISBN 978-1-84806-147-7.

Kukadia V, Upton SL, Hall DJ, Spanton AM. (2011b). The impact of outdoor pollution on IAQ. 2011 Annual UK Review Meeting On Outdoor & Indoor Air Pollution Research. 10th/11th May 2011, Cranfield, Bedfordshire MK43 0HG

Lange C. (1995) Indoor Deposition and the Protective Effects of Houses Against Airborne Pollution. Riso National Laboratory, Denmark. Report No. Riso-R-780(EN), May 1995.

Lee BE, Hussain M, Soloman B. (1979). A method for the assessment of the wind induced natural ventilation forces acting on low rise building arrays'. Department of Building Science, University of Sheffield, Report no. BS 50.

Leitl B. (2000) Validation Data for Microscale Dispersion Modelling. EUROTRAC Newsletter 22/2000.

Liddament MW. (1996) A Guide to Energy Efficient Ventilation. Air Infiltration and Ventilation Centre, March 1996.

Liddament MW. (2003) CFD Grows Up. CIBSE/ASHRAE national Conference, 10th December 2003.

Limb MJ. (1994). Ventilation and Building Airtightness: An International Comparison of Standards, Codes of Practice and Regulations. Air Infiltration and Ventilation Centre. Technical Note No. AIVC 43, February 1994.

Liu DL, Nazaroff WW. (2001). Modeling Pollutant Penetration Across Building Envelopes. Atmospheric Environment, Vol 35 Pp 4451-4462, 2001.

Liu DL, Nazaroff WW. (2002). Particle Penetration Through Windows. Proceedings of the 9th International Conference on Indoor Air. Monterey, USA, 30th June-5th July, 2002, Pp 862-867.

Liu DL, Nazaroff WW. (2003). Particle Penetration Through Building Cracks. Aerosol Science and Technology, Vol 37, Pp. 565-573, 2003.

Lorenzetti DM. (2002). Assessing Multizone Airflow Simulation Software. Lawrence Berkeley National Laboratory, Report No. LBNL-49578, January 2002.

Macdonald RW, Griffiths RF, Hall DJ. (1998a). A Comparison of Results from Scaled Field and Wind tunnel Modelling of Dispersion in Arrays of Obstacles. Atmospheric Environment, Vol. 32, No. 22, pp3845-3862,1998.

Macdonald RW, Griffiths RF, Hall DJ. (1998b). Scale Model Study of Building Effects on Dispersion in the Urban Canopy at Intermediate Source distances. Proceedings of the 5th International Conference on Harmonisation within Atmospheric Dispersion Modelling for Regulatory Purposes. 18-21 May, 1998, Rhodes, Greece. To appear in Int J. Environm. Poll.

Melaragno MB. (1982). Wind in Architectural and Environmental Design. Van Nostrand Reinhold, ISBN 0-442-25130-0

Mfula AM. (2004). Physical Modelling of Urban Building Exposure to Outdoor Pollution: A Wind Tunnel Study. PhD Thesis, University of Manchester Institute of Science and Technology, October 2004.

Milner JT, Dimitrilopoulou C, Apsimon HM. (2004). Indoor Concentrations in Buildings from Sources Outdoors. Atmospheric Dispersion Liaison Committee. Report No. ADMLC/2004/2.

Munn RE. (1981). The Design of Air Quality Monitoring Networks. Macmillan. 'Air Pollution Problems' Series. ISBN 0 333 30460 8.

Oke TR. (1992). Boundary Layer Climates. Routledge. ISBN 0-415-04319-0.

Orme MS, Liddament MW, Wilson A. (1994). Numerical Data for Air Infiltration and Natural Ventilation Calculations. Air Infiltration and Ventilation Centre. AIVC Document No. AIC-TN-44_1994,

Orme MS. (1999). Applicable Models for Air Infiltration and Ventilation Calculations. Technical Note 51, Air Infiltration and Ventilation Centre. ISBN 1-902177-09-6.

Pavageau M, Rafailidis S, Schatzmann M. (1996). Physical Modelling of Wind Driven Car Pollution Dispersion. Conference on Traffic Induced Air Pollution, Emissions, Impact and Air Quality. Graz 29-30 April.

Perera MDAES, Parkins LM. (1992). Airtightness of UK Buildings: Status and Future Possibilities. Environmental Policy and Practice, Vol. 2 (2) pp143-160.

Piggins J. (1991). A Preliminary Comparison of Calculated Building Ventilation Rates Using Six Different Pressure Coefficient Datasets. Air Infiltration Review, Vol 12, No 3.

Robins AG, Fackrell JE. (1983). Mean Concentration Levels Around Buildings Due to Nearby Low Level Emissions. CEGB Report No. TPRD/M/1261/N82.

Robins AG, Macdonald RW. (2000). A Review of Flow and Dispersion in the Vicinity of Groups of Buildings. Atmospheric Dispersion Liaison Committee (ADMLC), Annual Report 1998/1999 (Published 2000), Annexe B.

Robins AG, Savory E, Scaperdas A, Grigoriadis D (2002). Spatial variability and source-receptor relations at a street intersection. J. of Water, Air and Soil Pollution: Focus, 2, 381-393.

Robins AG, Cheng H. (2005). Wind Tunnel Investigation of Pollutant Dispersion in Urban Area. Paper Presented at Physmod 2005, International workshop on physical modelling of flow and dispersion phenomena. August 24-26, 2005. The University of Western Ontario, London, Ontario. Canada.

Santos JM, Mavroidis I, Reis NC, Pagel EC. (2011). Experimental Investigation of Outdoor and Indoor Mean Concentrations and Concentration Fluctuations of Pollutants. Atmospheric Environment, Vol. 45, Pp. 6534-6545.

Scaperdas A. (2000). Modelling Air Flow and Pollutant Dispersion at Urban Canyon Intersections. PhD Thesis, Imperial College, University of London, June 2000.

Schatzmann M, Leitl B. (2002). Validation and Application of Obstacle Resolving Urban Dispersion Models. Atmospheric Environment, Vol 36, Pp4811-4821.

Seinfeld JH, Pandis SN. (1998). Atmospheric Chemistry and Physics. Wiley. ISBN 0-471-17816-0.

Sherman M, Modera MP (1988). Signal Attenuation Due to Cavity Leakage. J. Acoustical Society of America, Vol 84(6), pp2163-2169.

Sherman M. (1998). The Use of Blower Door Data. Lawrence Berkeley Nuclear Laboratory, Report LBL35173, March 13th 1998.

Taylor BJ, Webster R, Imbabi MS. (1999). The Building Envelope as an Air Filter. Building and Environment, 34, Pp. 353-361,1999.

Thatcher TL, McKone TE, Fisk WJ, Sohn MD, Delp WW, Riley WJ, Sextro RG. (2001). Factors Affecting the Concentration of Outdoor Particles Indoors (COPI): Identification of Data Needs and Existing Data. Ernest Orlando Lawrence Berkeley National Laboratory, Environmental Energy Technologies Division. Report No LBNL-49321, December 2001.

Thatcher TL, Lai ACK, Moreno-Jackson R, Sextro RG, Nazaroff WW. (2002). Effects of Room Furnishings and Air Speed on Particle Deposition Rates Indoors. Atmospheric Environment, Vol 36, Pp. 1811-1819.

Thatcher TL, Lunden MS, Rezvan KL, Sextro RG, Brown NJ. (2003). A Concentration rebound Method for Measuring particle Penetration and Deposition in the Indoor Environment. Aerosol Science and Technology, Vol. 37, Pp 847-864, 2003.

Tung TCW, Chao CYH, Burnett J. (1999). A Methodology to Investigate the Particle Penetration Coefficient Though Building Shell. Atmospheric Environment, Vol. 33, Pp. 881-893.

Upton SL, Kukadia V. (2011). Ventilation Rate Measurement – New tracer Gases and Techniques for Healthy Indoor Environments. Building Research Establishment, Publication IP 13/11.

VEETECH(2012). VEETECH Web Site, www.veetech.co.uk

Walker IS. (1992), 'Pressure Coefficients on Sheltered Buildings', Air Infiltration Review, Vol 13, No 4, 1992.

Walker IS, Wilson DJ, Sherman MH. (1997). A Comparison of the Power Law to Quadratic Formulations for Air Infiltration Calculations. Energy and Buildings, Vol 27, No3, June 1997.

Walsh C, Jones JA. (2002). Atmospheric Dispersion from Releases in the Vicinity of Buildings. National Radiological Protection Board. NRPB Report No. W16, June 2002.

Walton GN, Dols WS. (2005). CONTAM User Guide and Program Documentation. National Institute of Standards and Technology , US Department of Commerce, NISTIR 7251, October 2005, Revised December 2010. Available at http://www.bfrl.nist.gov/IAQanalysis/docs/CWHelp30.pdf

Wang L, Dols WS, Chen Q. (2010). Using CFD Capabilities of CONTAM 3.0 for Simulating Airflow and Contaminant Transport In and Around Buildings. ASHRAE, HVAC&R Research, 16(6), 749-763.

Wilson DJ, Netterville DDJ. (1978). Interaction of Roof Level Plume with a Downwind Building. Atmospheric Environment, Vol. 12, pp.1051-1059.

Wilson DJ. (1976). Contamination of Air Intakes from Roof Exhaust Vents. ASHRAE Transactions Vol 82, Part 1, pp1024-1038.

Wilson DJ, Winkel G. (1982). The Effect of Varying Exhaust Stack Height on Contaminant Concentration at Roof Level. ASHRAE Transactions Vol. 88, Part 1, Paper No 2696.

Wilson DJ, Britter RE. (1982). Estimates of Building Surface Concentrations from Nearby Point Sources. Atmospheric Environment. Vol. 16, No. 11, pp2631-2646.

Wilson DJ. (1988). Variation of Indoor Shelter Effectiveness Caused by Air Leakage Variability of Houses in Canada and the USA. USEPA/FEMA Conference on the Effective Use of In-Place Sheltering as a Potential Option to Evacuation During Chemical Release Emergencies, Emmitsburg, Maryland, Nov. 30/Dec. 1, 1988.

Wilson DJ. (1990). Exposure-1, Shelter-1. Models for Predicting Outdoor and Indoor Exposure Hazards from Toxic Gas Releases. Department of Mechanical Engineering, University of Alberta, Technical Reports, 72, 73, 74. March 1990.

Wilson DJ, Morrison B. (2000). Ordering Shelter or Evacuation During an Outdoor Toxic Gas release Incident: The C.A.F.C. Decision Flow Chart. Paper presented at Fire-Rescue Canada 2000, Annual Meeting of the Canadian Association of Fire Chiefs, Montreal, August 13-18th, 2000.

Wiren BG. (1983). Effects of Surrounding Buildings on Wind Pressure Distributions and Ventilative Heat Losses for a Single Family House. Journal of Wind Engineering and Industrial Aerodynamics, 15, 15-26.

Wiren BG. (1985). Effects of Surrounding Buildings on Wind Pressure Distributions and Ventilation Losses for Single-Family Houses -Parts 1 and 2. National Institute for Building Research Bulletin M85:19 Part 1: 1.5 - Storey Detached Houses. Part 2: 2-storey terrace houses.

Wood CR et al. (2009). Dispersion Experiments in Central London – the 2007 DAPPLE Project. Bulletin of the American Meteorological Society July 2009, Pp955-969.

13 FIGURES

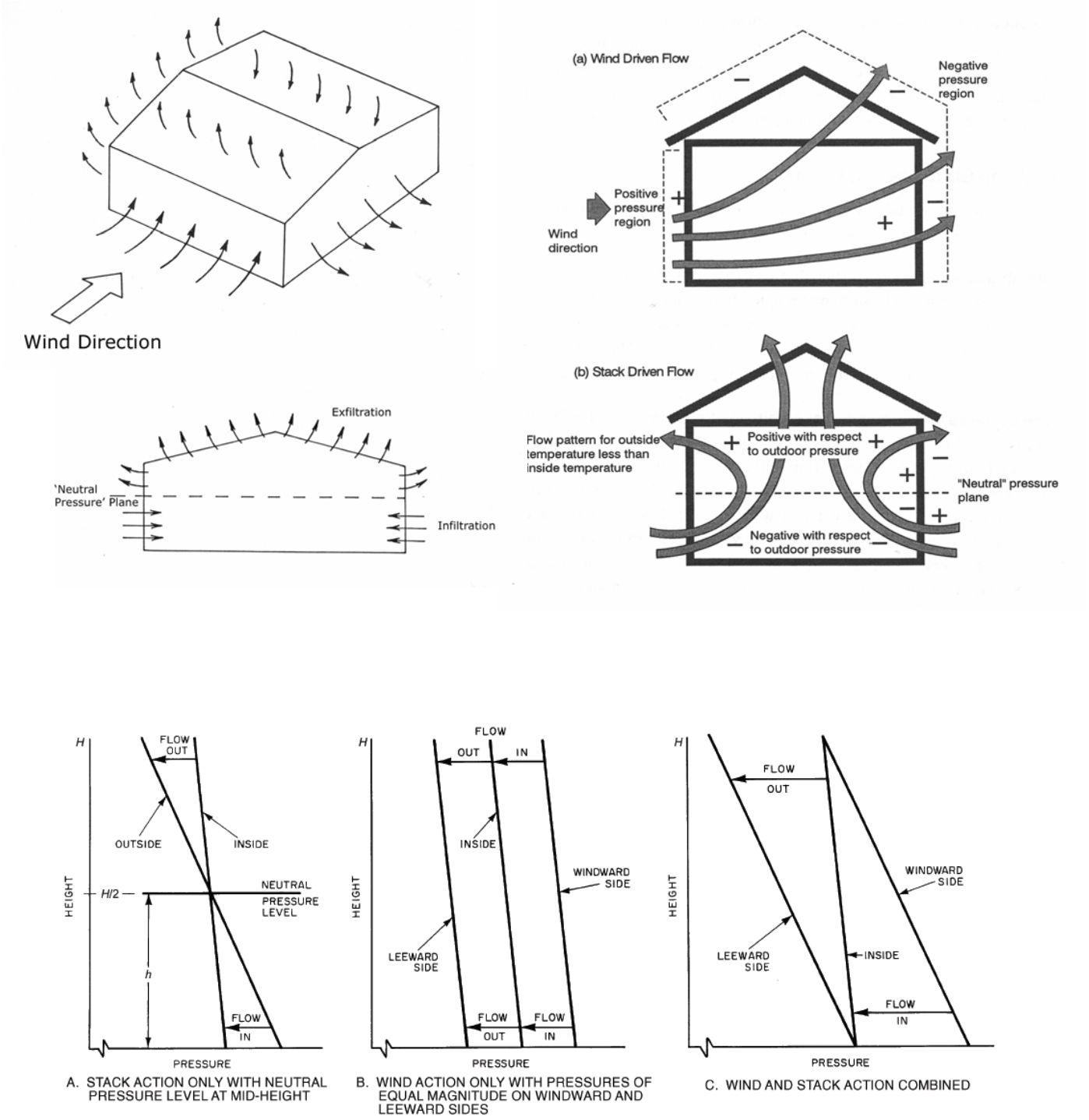

Figure 1. Natural Ventilation Driven by Buoyancy and Wind Pressures on a Building.
Upper Left : From Hall and Spanton (2005).
Upper Right: From Liddament (1996).
Bottom: From ASHRAE (1997), showing the effect of the combination of Buoyancy and Wind Pressures on the Infiltration Flow.

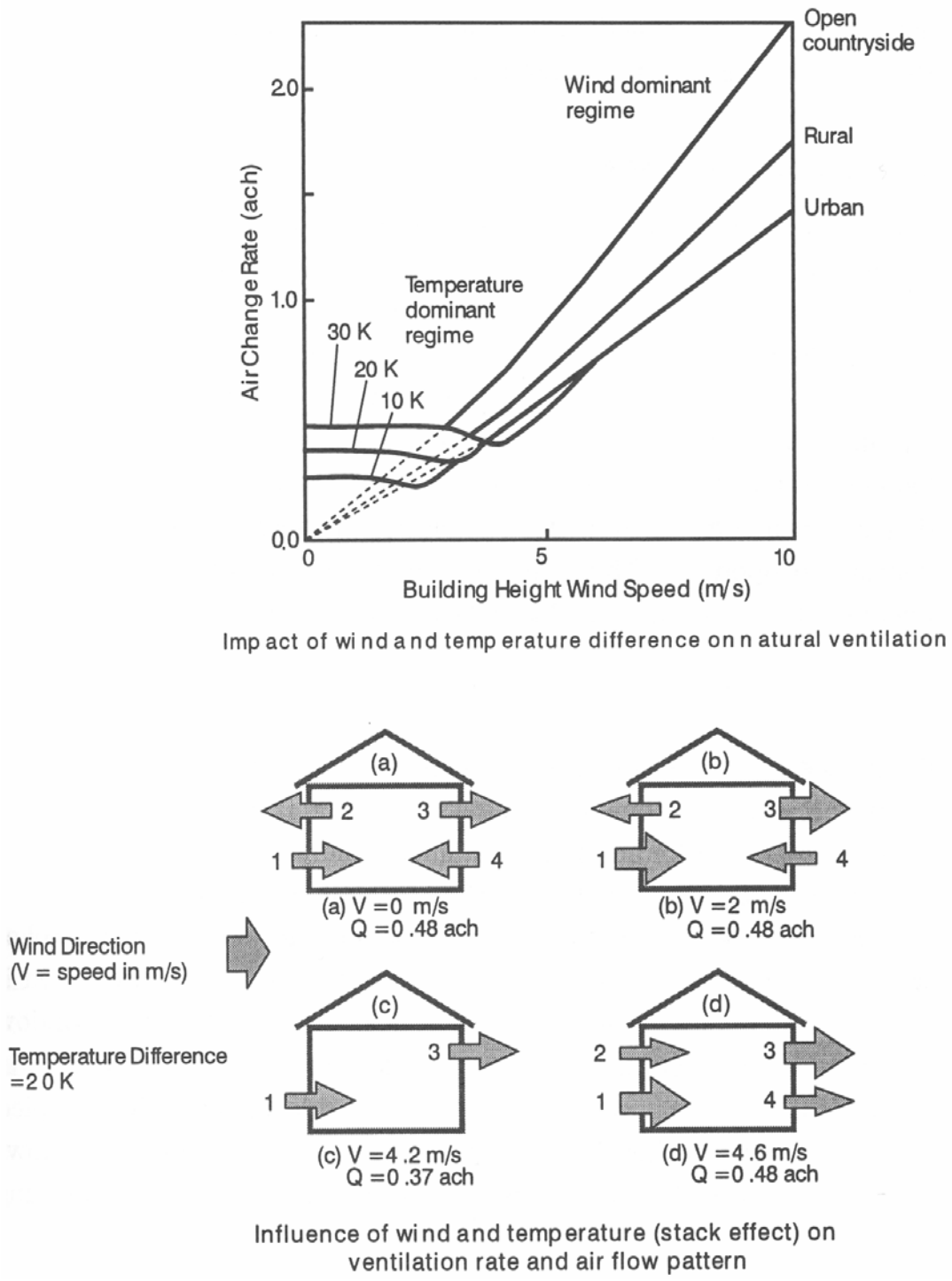

Figure 2. Typical Effects of Wind speed and Internal/External Temperature Difference on Natural Ventilation and infiltration. (ach = air changes per hour).
From Liddament (1996).

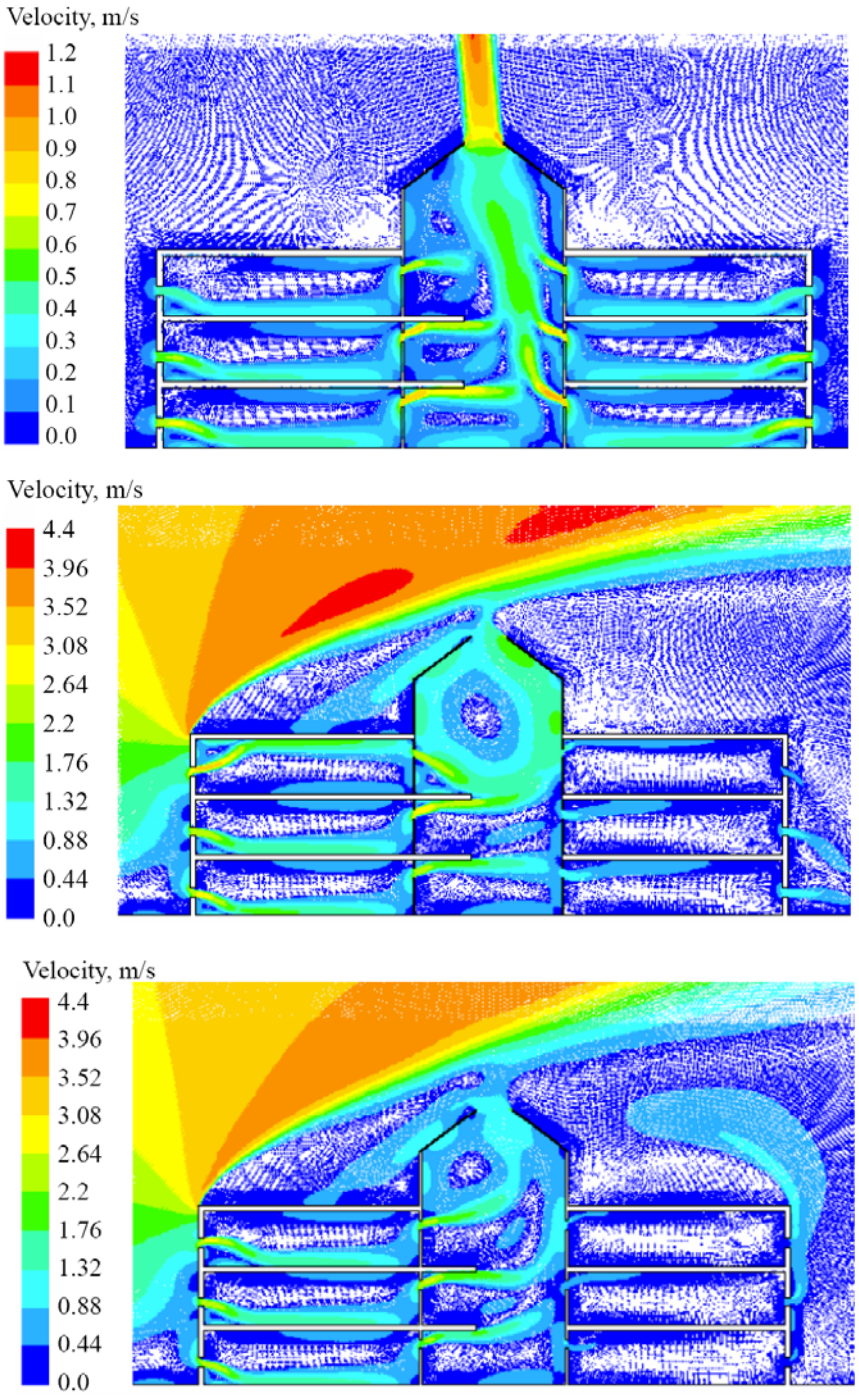

Figure 3. Example of a CFD Calculation of Ventilation Process in a Complex Naturally Ventilated Building with an Atrium.
Upper: Buoyancy Driven Only.
Middle: Wind Driven Only.
Lower: Combined Buoyancy and Wind Driven.
From Gan(2010).

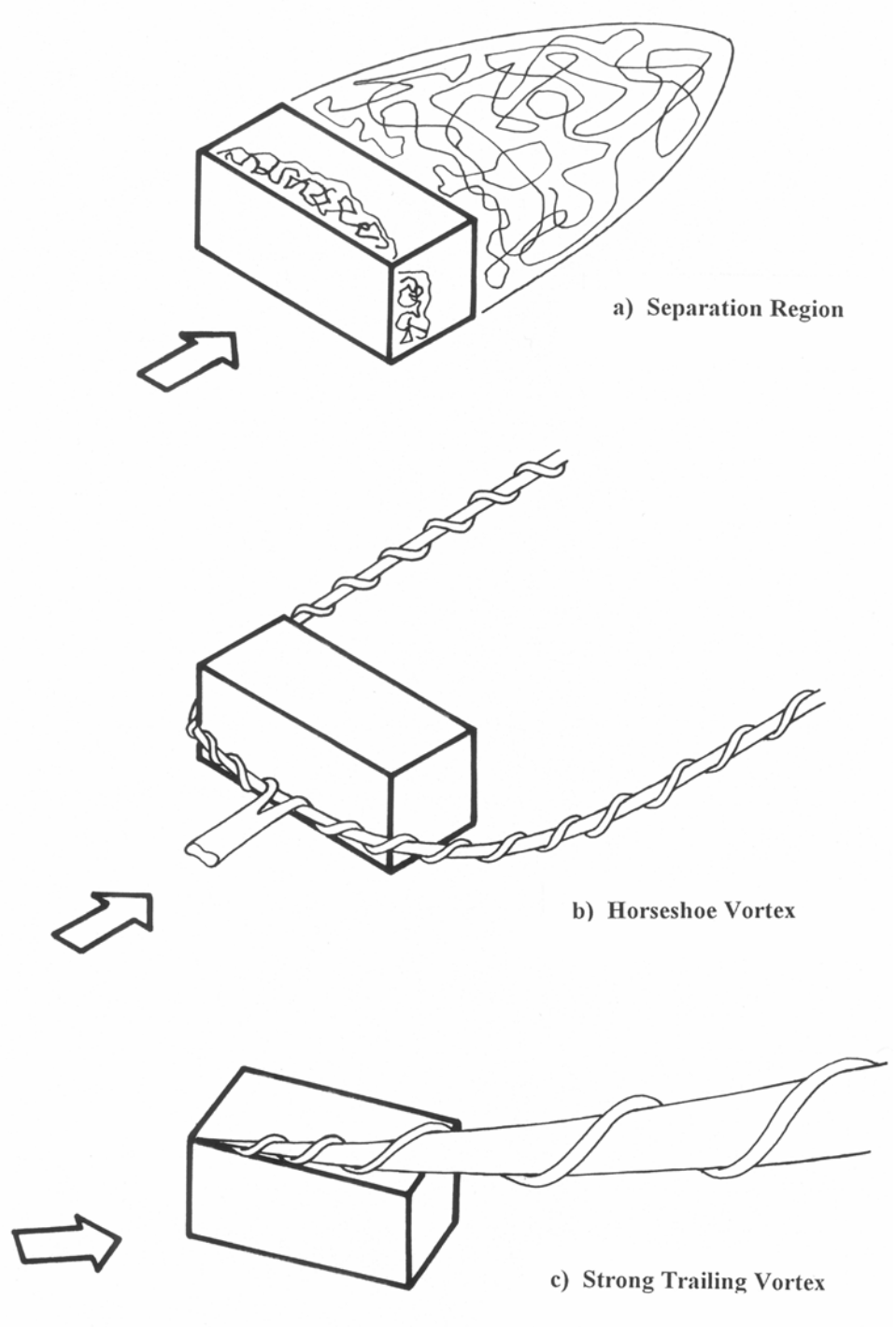

Figure 4. The Main Secondary Components of the Flow Pattern around a Single Rectangular Obstacle.
From Hall et al(1996a), also reproduced by Colville et al(1997).

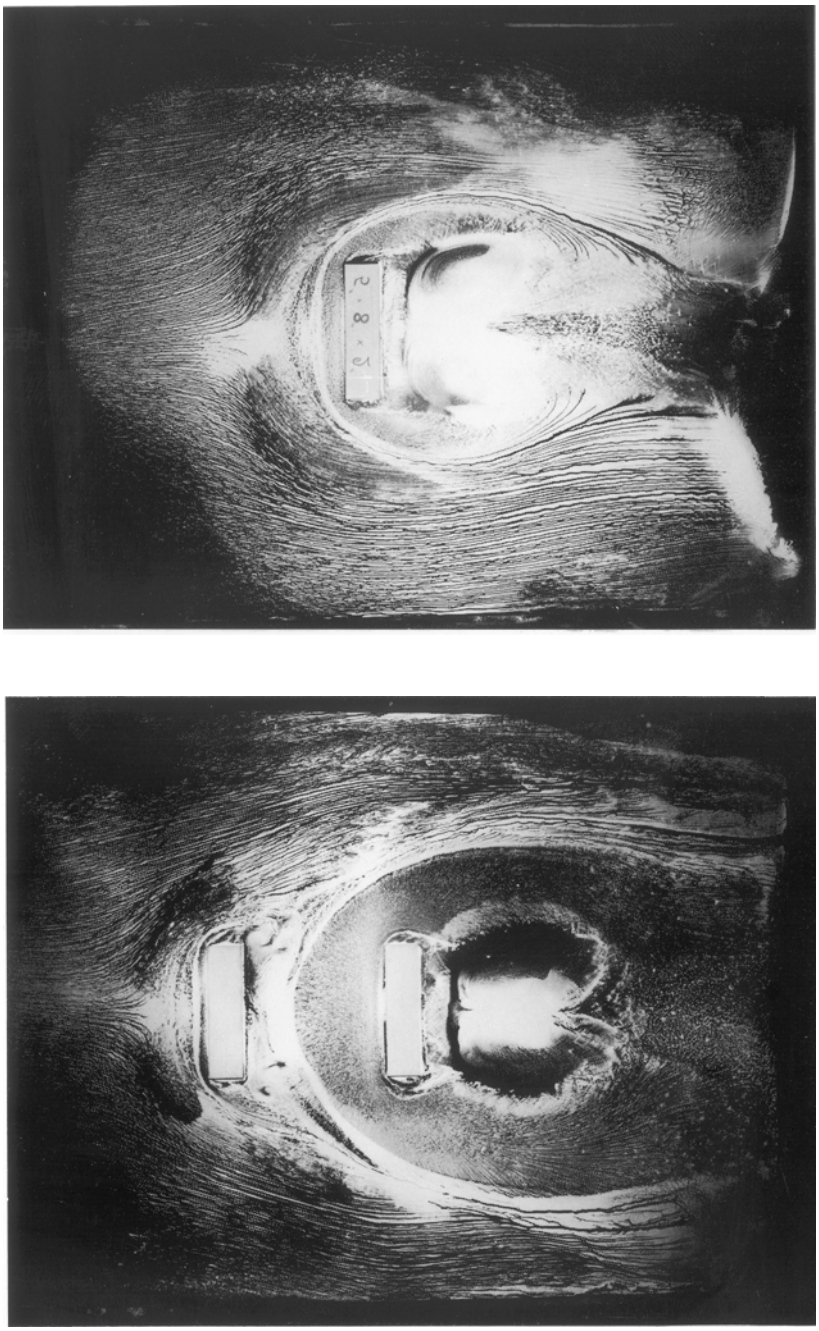

Figure 5. **Surface Flow Visualisation of Horseshoe Vortices around a Single Obstacle.**
Upper: In isolation.
Lower: With a Smaller Obstacle Upwind(Right).
From Penwarden and Wise, as Reproduced by Cook(1985, p170).

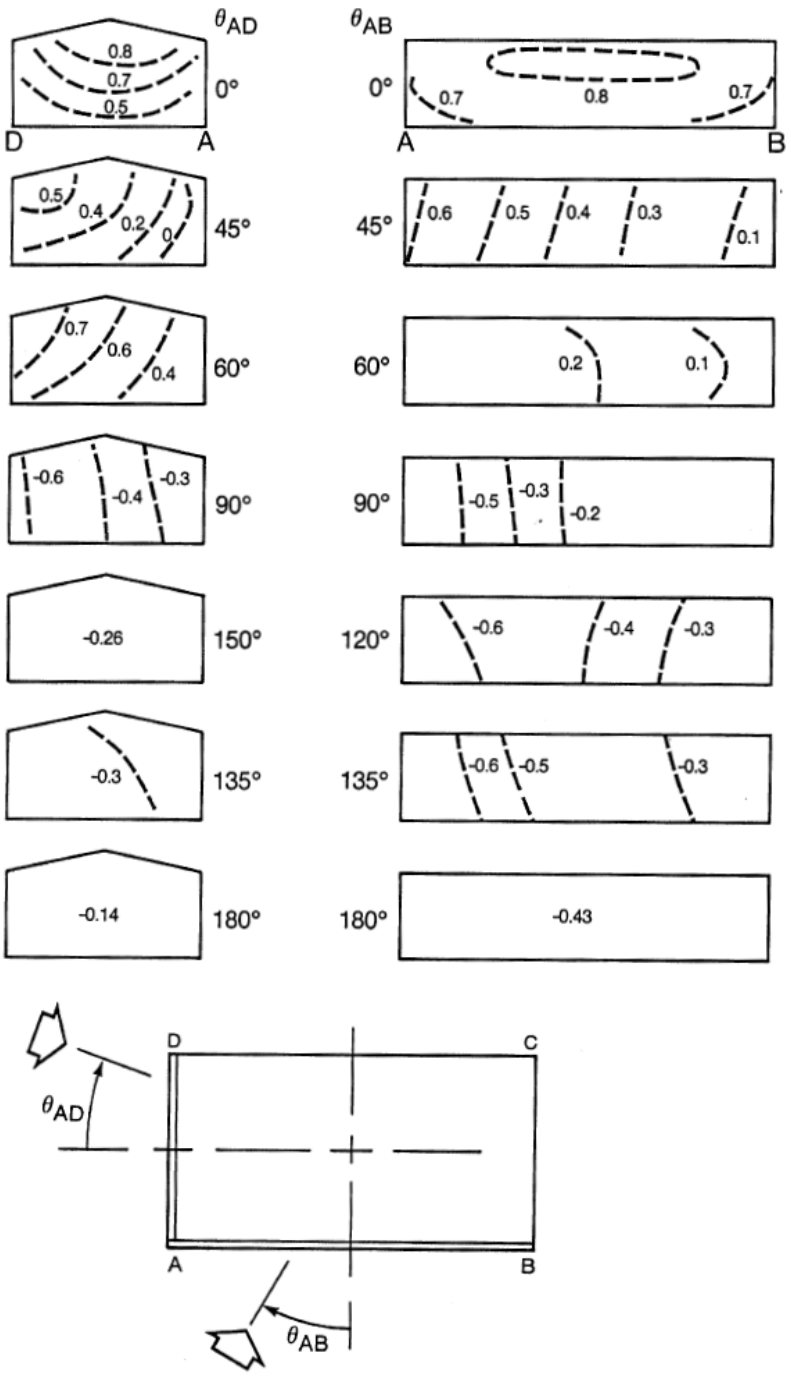

Figure 6. Pressure Patterns (as Cp) on a Low, Wide Rectangular Obstacle at Different Directions to the Wind.
From ASHRAE Handbook (1997), Chapter 15. Originally Due to Holmes(1986).

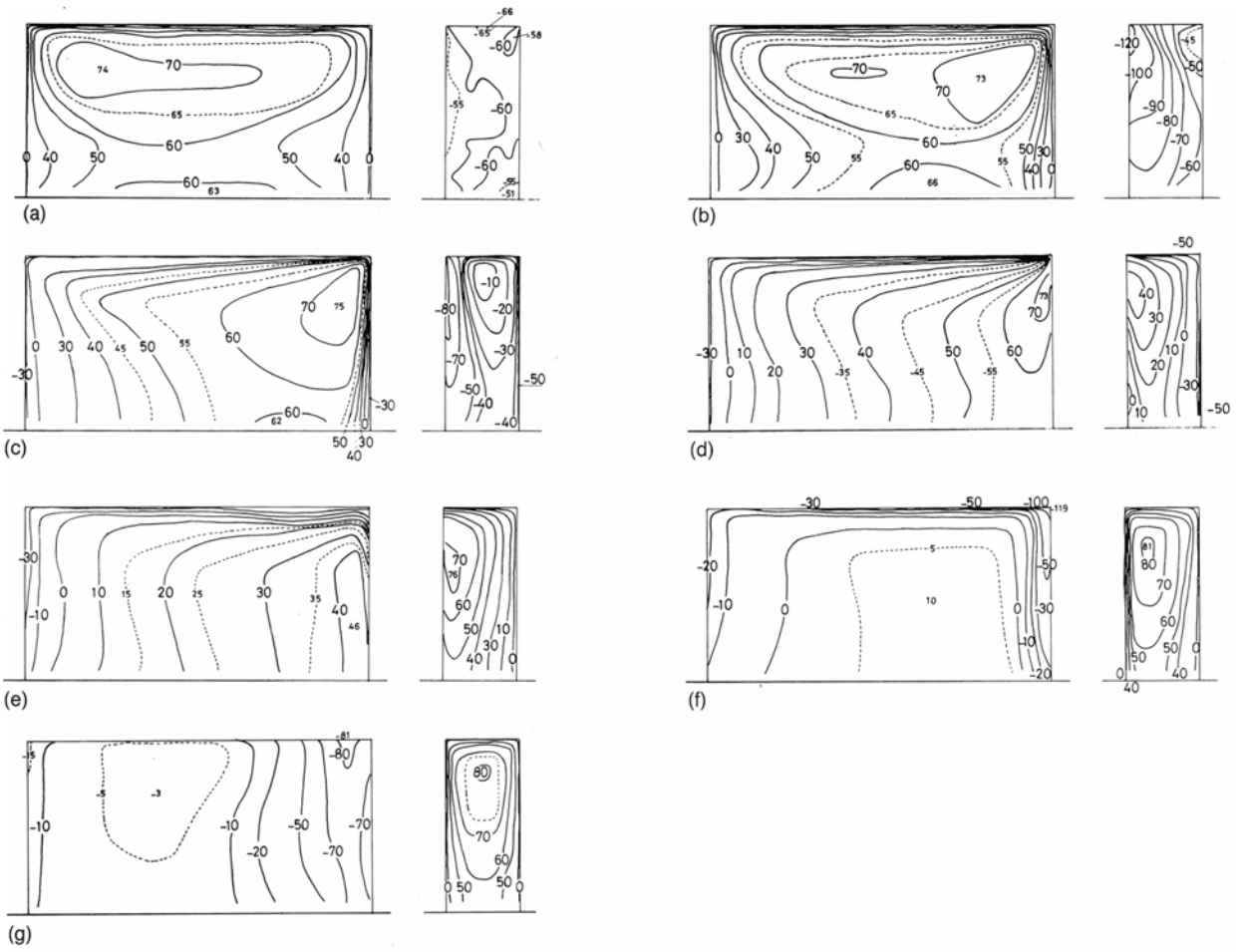

Figure 7. Pressure Patterns (of C_p x 100) on the Upwind and Side Faces of a Low, Wide Rectangular Obstacle at Different Directions to the Wind.
a) 0°, Wide Face Normal to the Wind
b) Rotated 15°, c) 30°, d) 45°, e) 60°, f) 75°
g) 90°, Narrow Face Normal to the Wind
From Cook (1990), Originally Due to Hongo et al(1979).

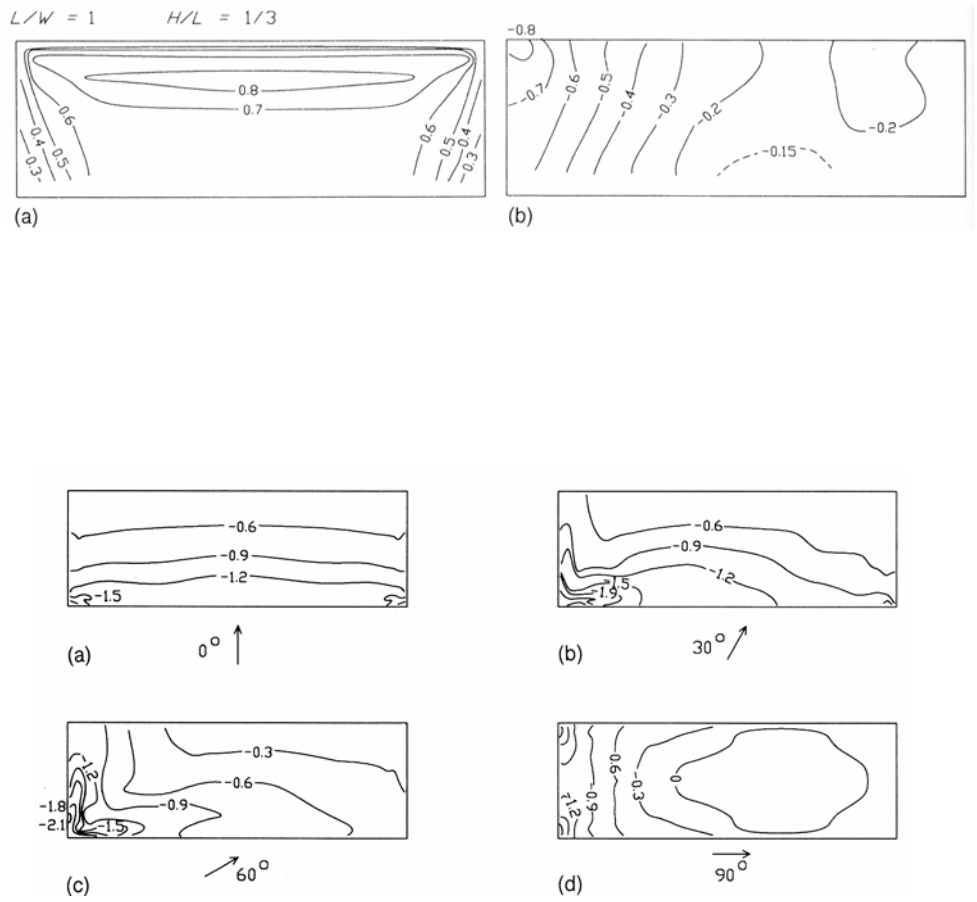

Figure 8. Pressure Patterns (as C_p) on Low, Wide Building Surfaces.
Upper : On the Front (a) and Sidewalls (b) of a Low Building with Square Planform.
Lower: On the Roof of a Building of 3:1 Planform and low height over a Range of Wind Directions.
From Cook(1990), Data from BRE Wind Tunnel Experiments.

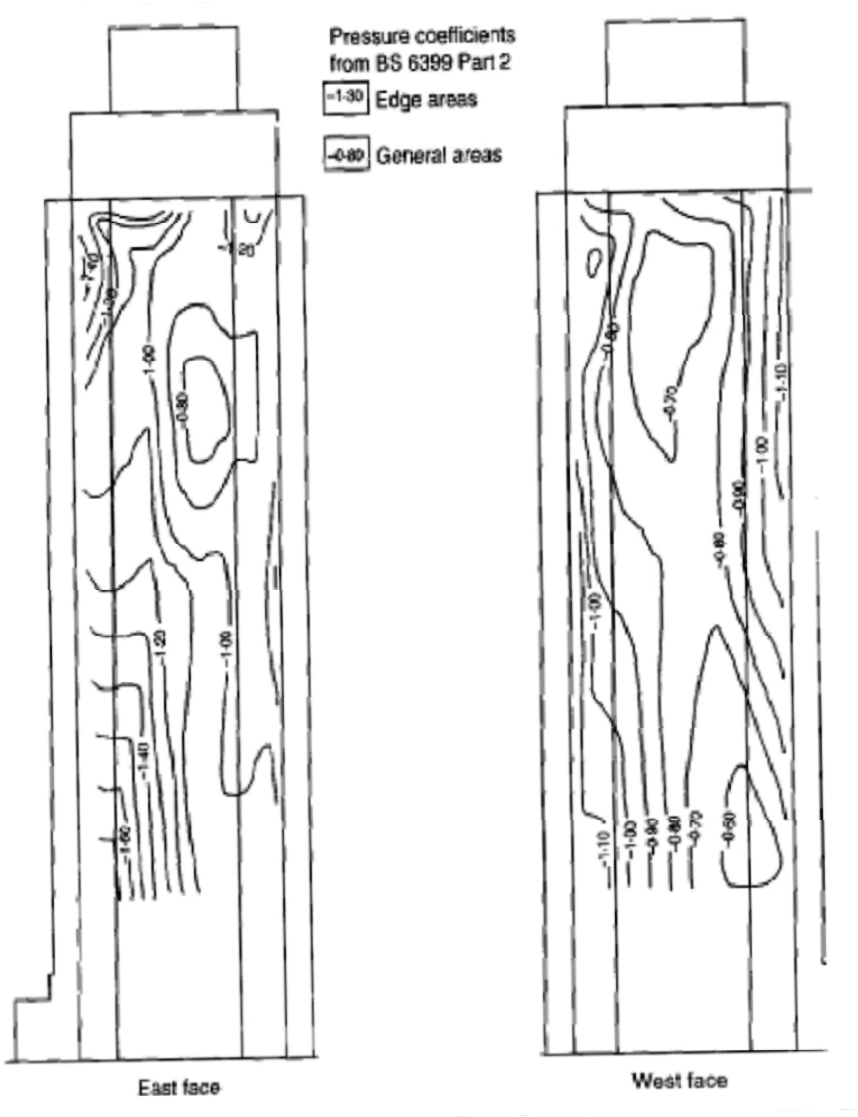

Figure 9. Pressure Patterns on the Upwind Face of a Tall Slender Obstacle (Height/Width ≈ 4).
'East Face' Following Surrounding Tall Buildings.
'West Face' Following Unobstructed Urban Fetch.
From Blackmore(1997), from BRE Wind Tunnel Experiments.

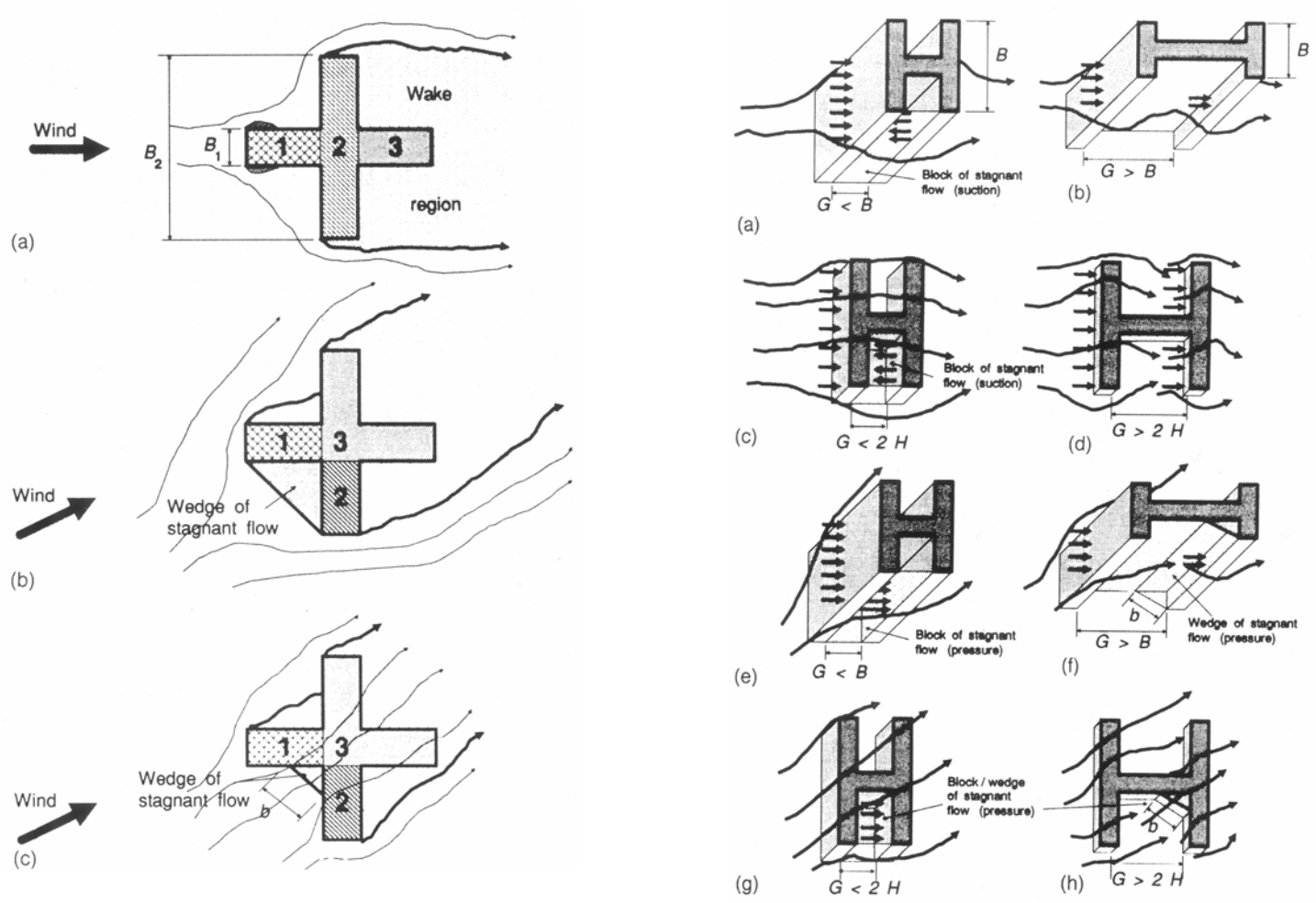

Figure 10. **Wind Flows and Pressure Patterns around Buildings of Complex Planform. From Cook (1990).**

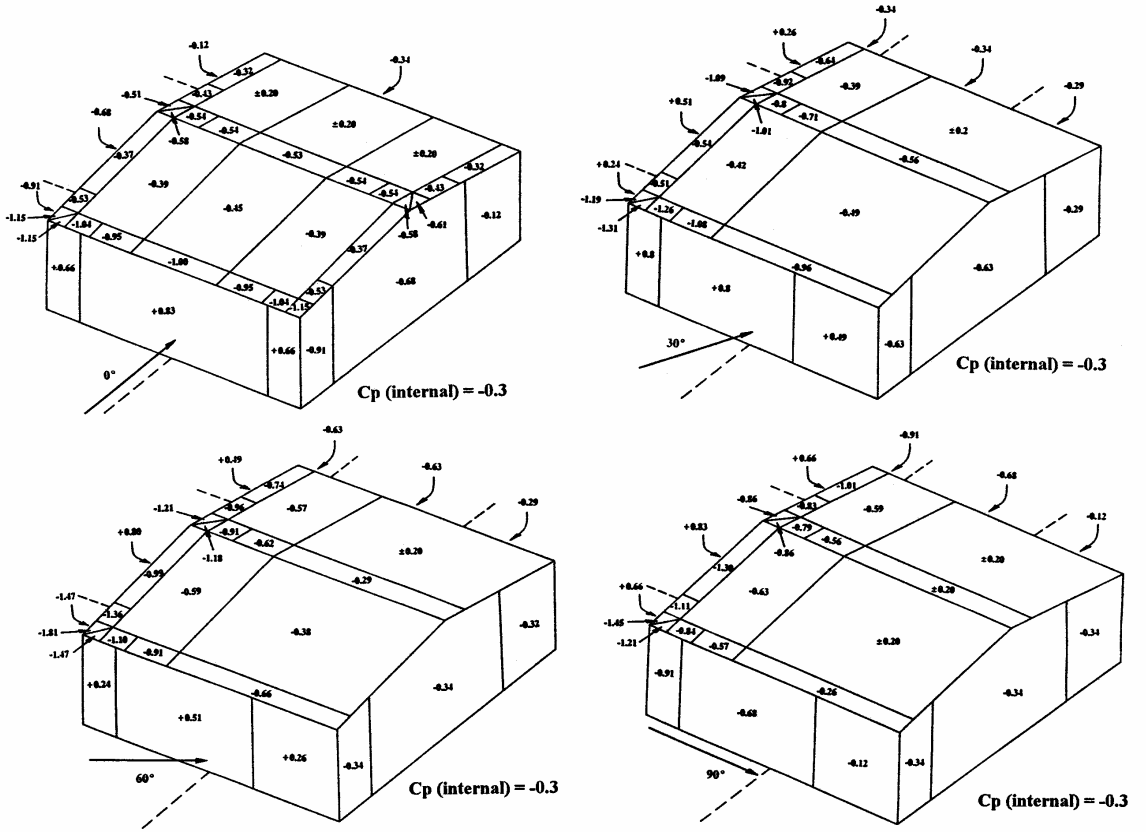

Figure 11. Example Surface Pressure Patterns on a Building, as C_p, in Different Wind Directions From Hall et al(1995), using Data from BRE Digest 346 (BRE(1990)).

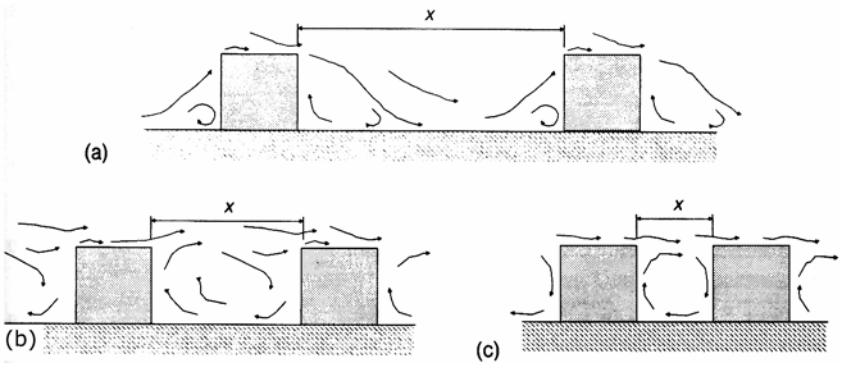

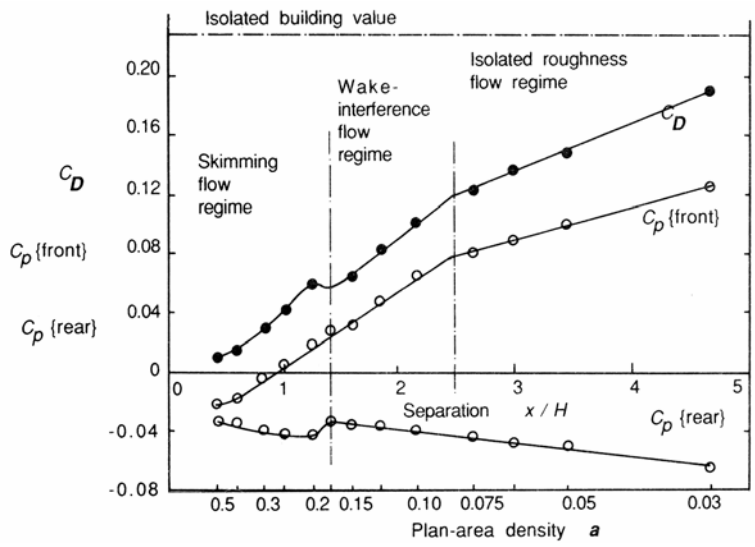

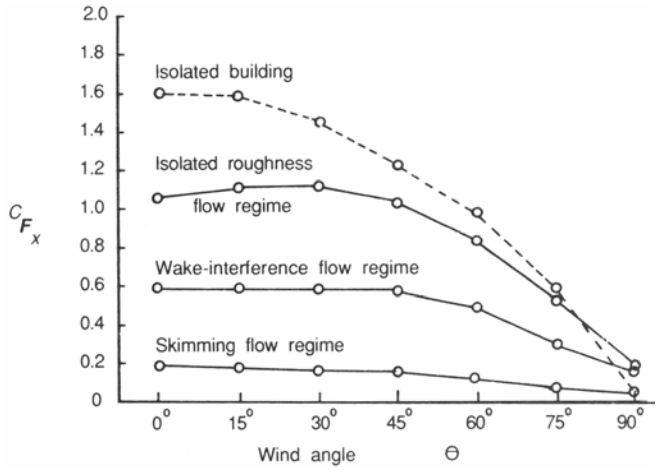

Figure 12. **Effect of Surrounding Structures on Building Surface Pressures.**
Upper: Different Flow Regimes:
a) Low Urban Density (ca 5%) Isolated Roughness Flow.
b) Moderate Urban Density (ca 10%) Wake Interference Flow.
c) High Urban Density (>20%) Skimming Flow.
Middle: Effect of Urban Array Density on Overall Loading.
Lower: Effect of Wind Direction and Array Density on Overall Loading.
From Cook (1990), BRE Measurements.

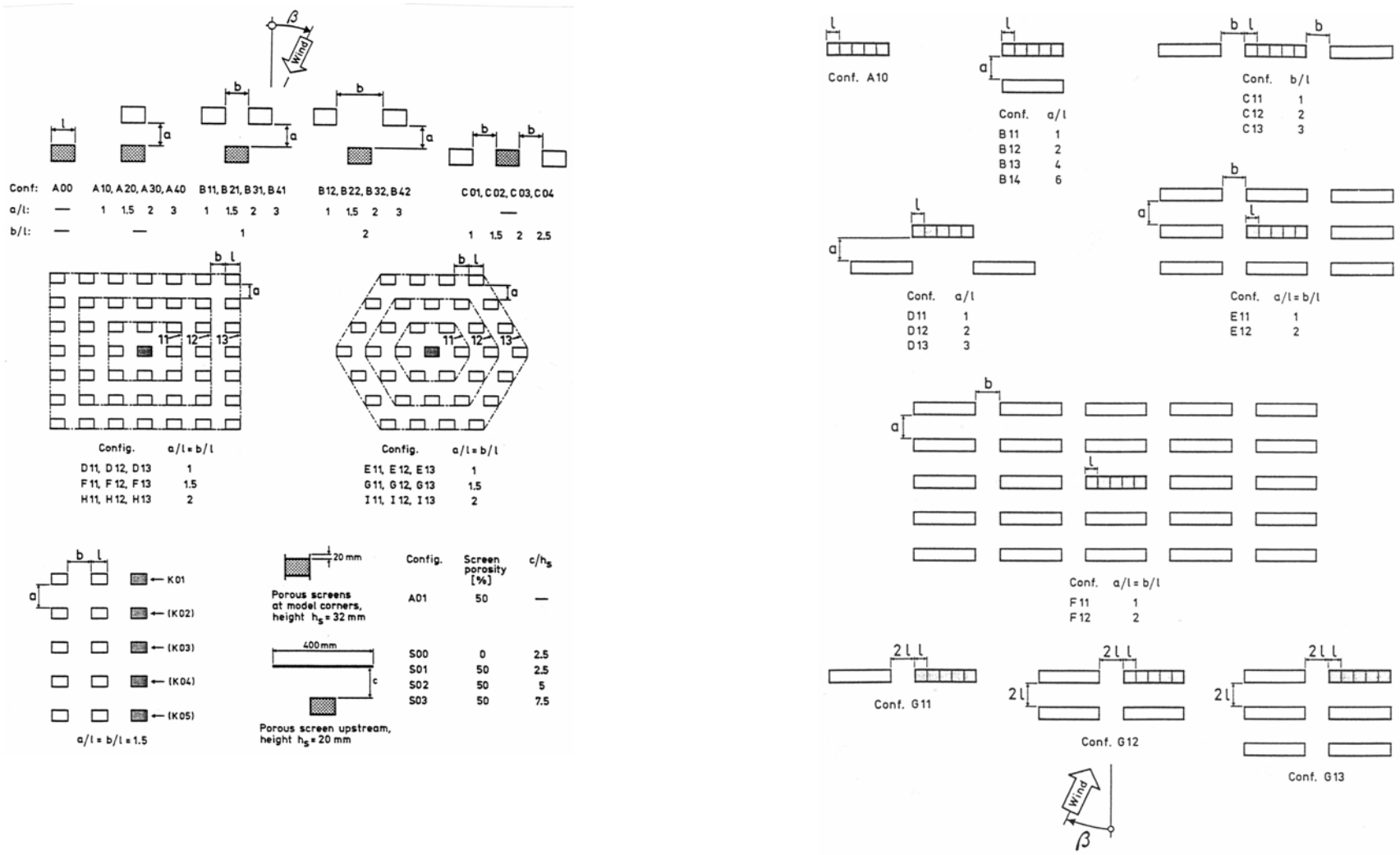

Figure 13. Range of Wiren's(1985) Experiments on Pressures on Buildings in Urban Arrays.

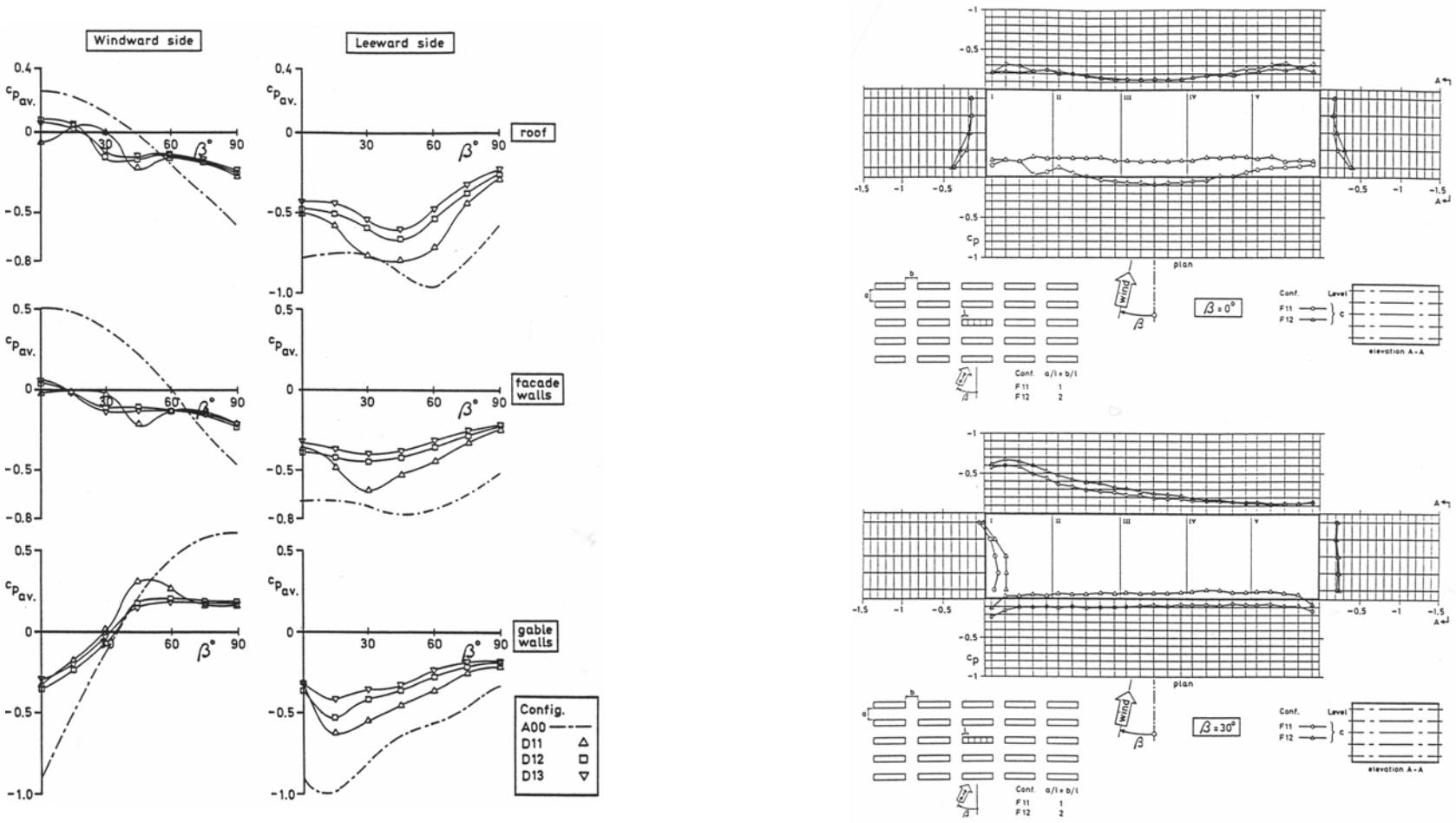

Figure 14. Some Typical Results of Wiren's(1985) Building Pressure Measurements on Buildings in Similar Sized Urban Arrays.

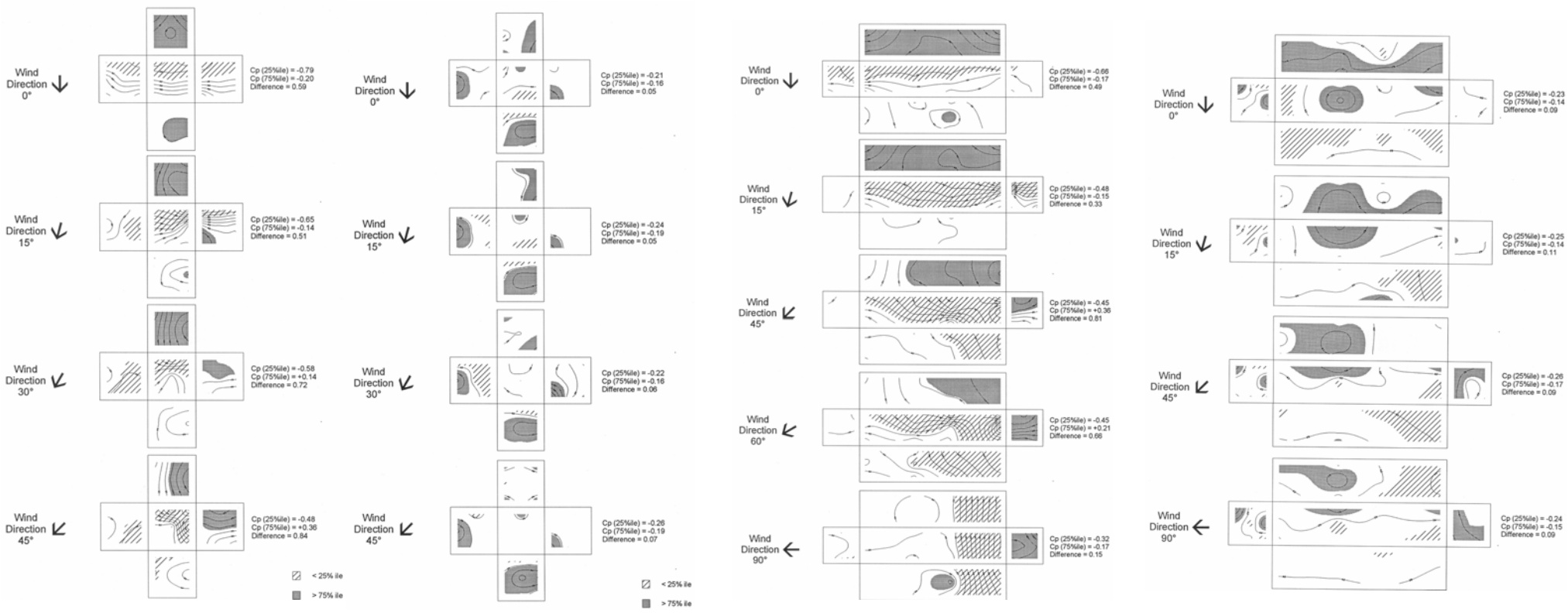

Figure 15. Pressure Patterns on Cubical and 4x1 Building Forms in Unobstructed Flow and 44% Array Area Densities with Varying Wind Directions. The Building Walls Are Folded Outwards in the Plan Views.
LHS of each pair, unobstructed flow, RHS in 44% area density.
Shaded areas show pressures above 75%ile of area weighted mean on surfaces.
Hatched areas show pressures below 25%ile of area weighted mean on surfaces.
From Hall et al(1999a), the matching concentration patterns are in Figure 34.

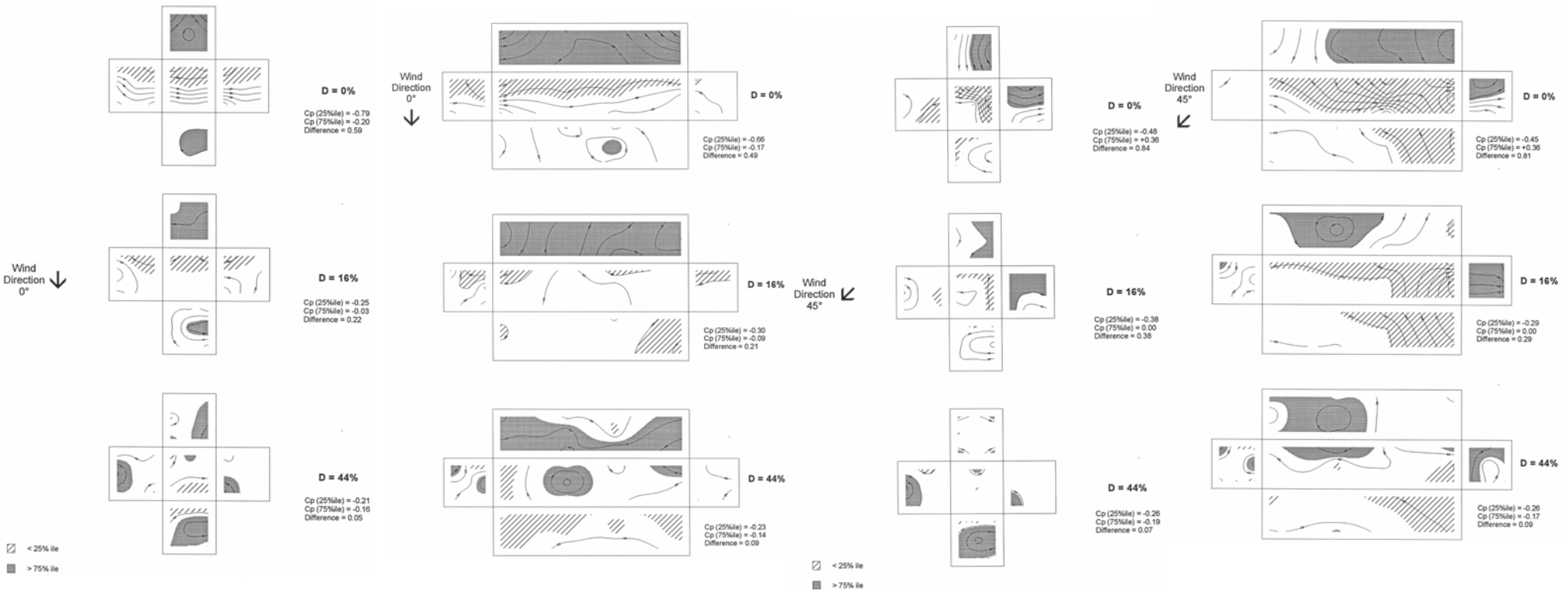

Figure 16. **Pressure Patterns on Cubical and 4x1 Building Forms in Varying Array Densities and Two Wind Directions. The Building Walls Are Folded Outwards in the Plan Views.**
Shaded areas show pressures above 75%ile of area weighted mean on surfaces.
Hatched Areas Show pressures below 25%ile of area weighted mean on surfaces.
Upper row: Isolated Building.
Middle Row: 16% Area Density.
Bottom Row: 44% Area Density.
From Hall et al(1999a), the matching concentration patterns are in Figure 34.

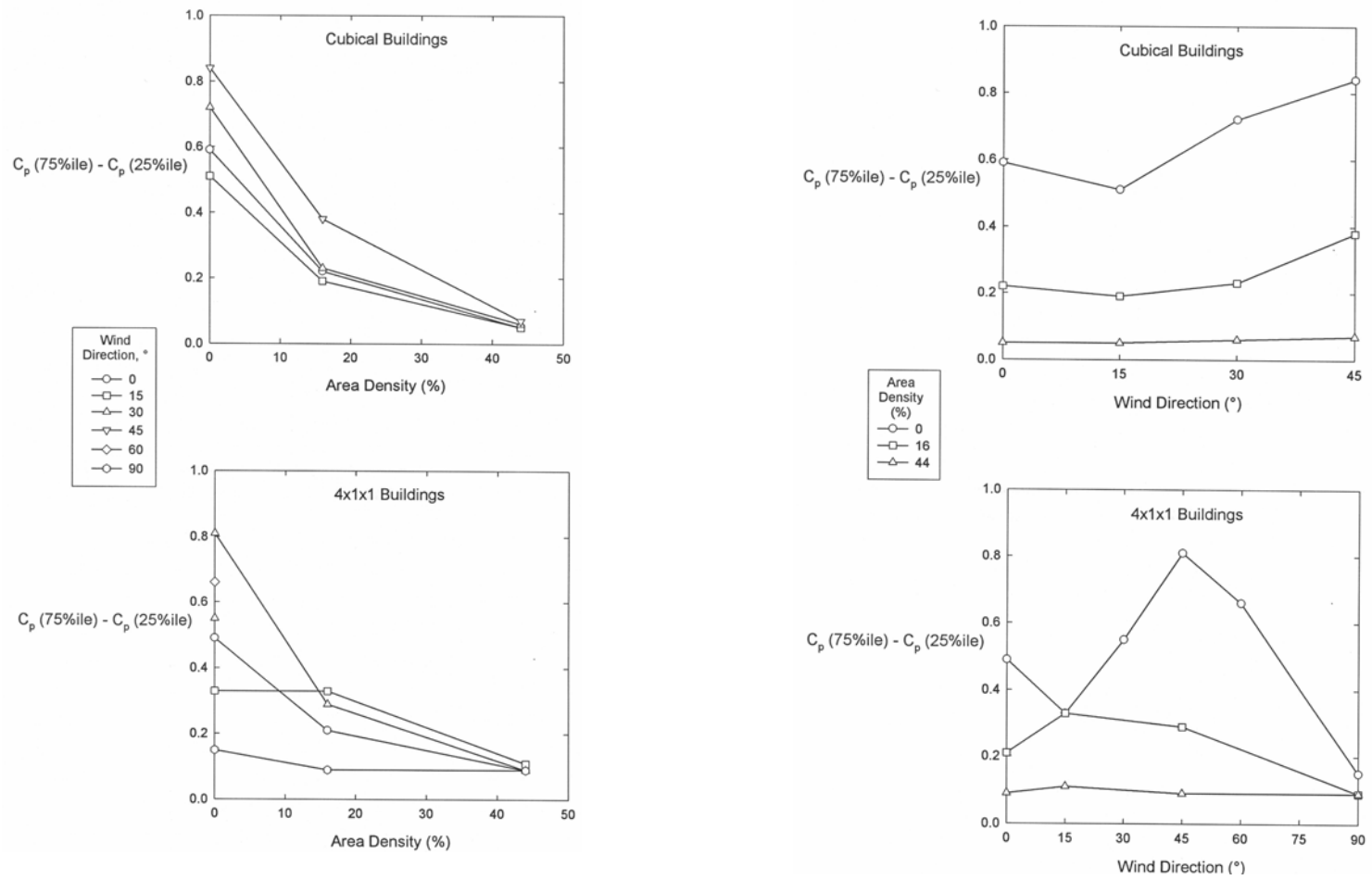

Figure 17. Pressure Differences Over Building Faces (As 75%ile-25%ile of C_p) for the Measurements of Hall et al(1999a) Shown in Figures 15 and 16.
LHS: Effects of Area Density.
RHS: Effects of Wind Direction.

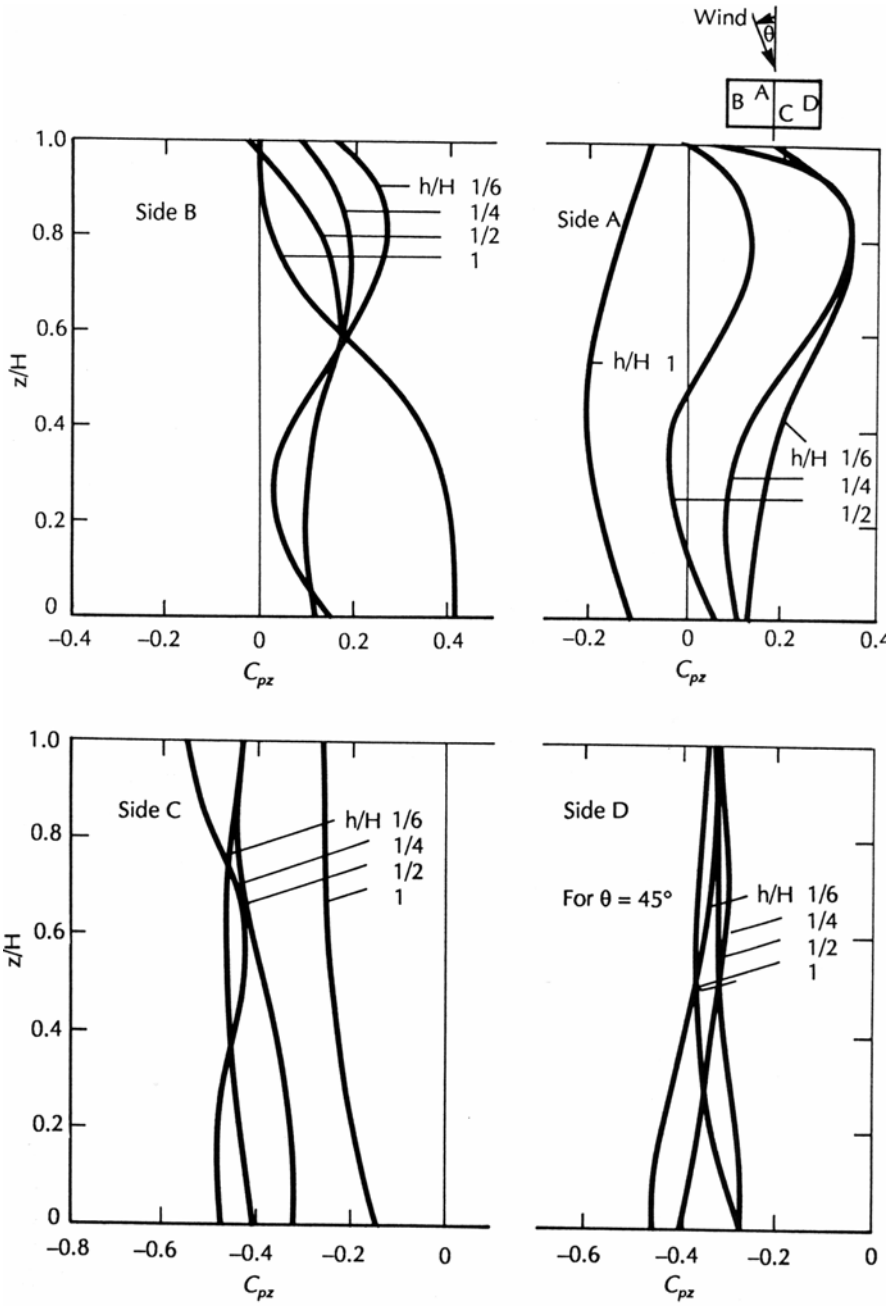

Figure 18. **Vertical Distributions of Weighted Mean Wind Pressure Coefficients C_{pz}, For Various Surrounding Obstruction Heights (at a Wind Angle of 45°). From Bowen's(1976) Data as Reanalysed by Orme et al(1994).**

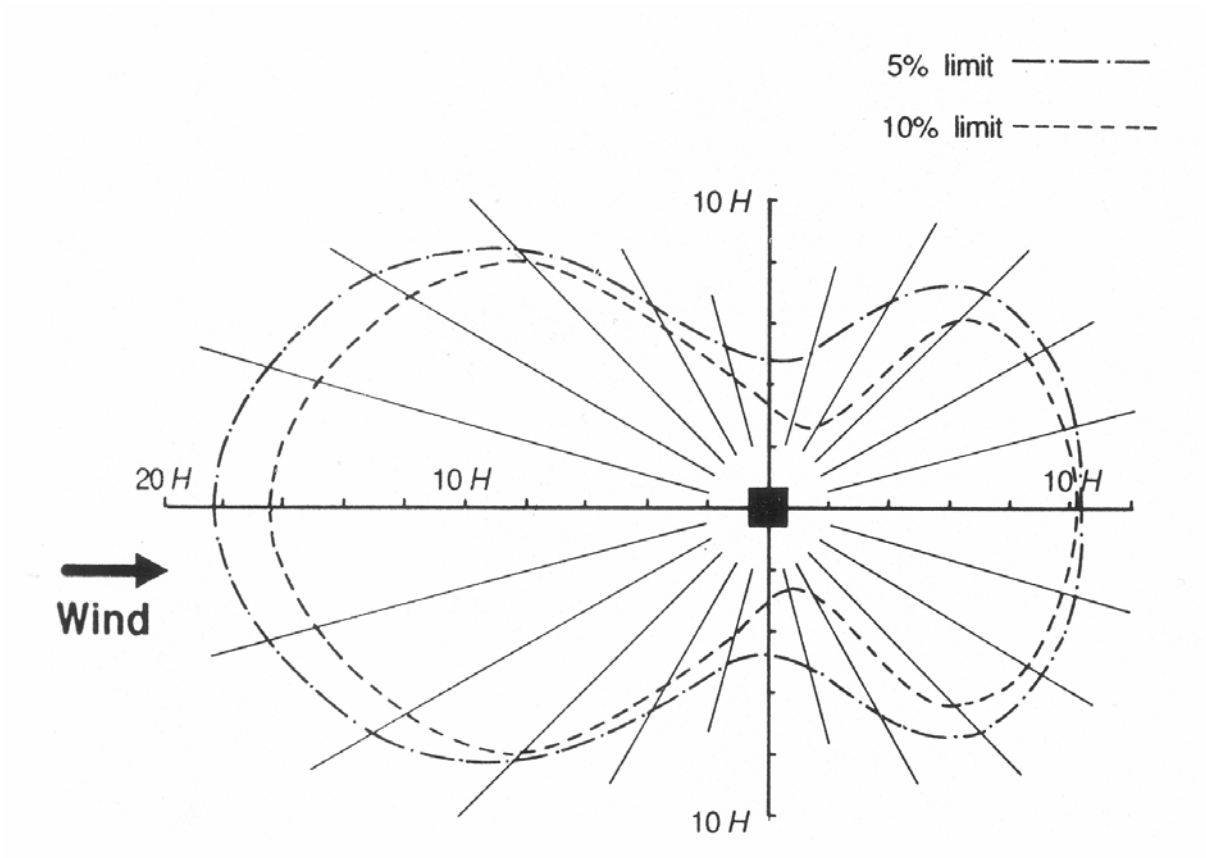

Figure 19. 'Influence Areas' for 5% and 10% Change in Loading on a Cube in an Obstacle Array with 10% Area Occupancy. From Cook(1990), Originally Due to Lee et al(1979).

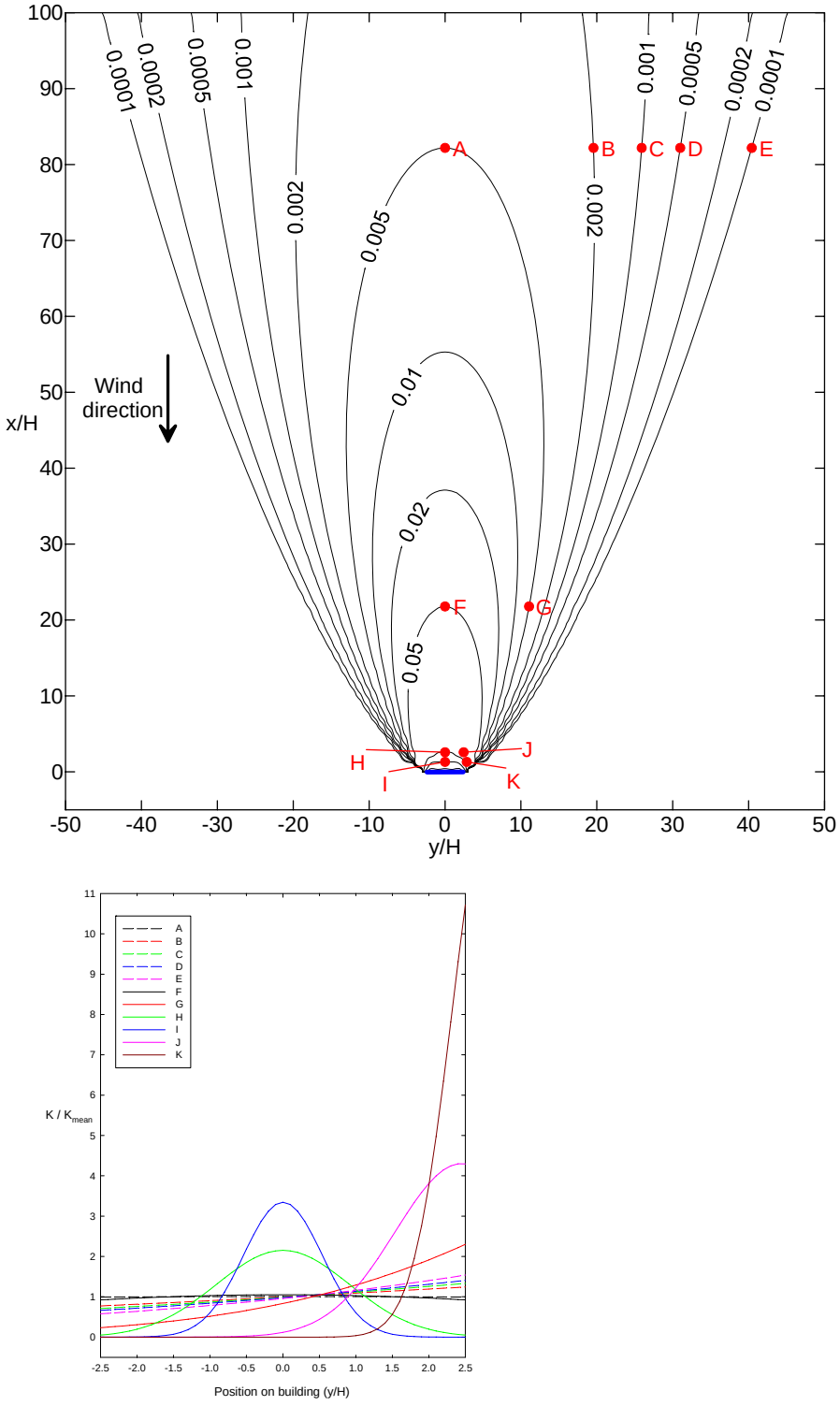

Figure 20. 'Influence' Areas for Exposure to Dispersion: from Within Which Point Sources of Contaminant Will Impinge on the Line Representing a Building.
Upper: Inverted ADMS Model Calculation for a 5H Wide Line Source Representing a Building. Neutral Stability, $z_0/H = 0.01$.
The Contours are of Mean Non Dimensional Concentration, K_{mean}, across the 'Building' for Sources in the Upwind Area.
Lower: Calculated Concentration Contours Across the 'Building' from the Labelled Source Positions in the Upwind Area.
The Mean Value of K, Across the 'Building' is within 5% of the value of K_{mean}, on the contour, except for Case I (12%).

16% Area Density Array **44% Area Density Array**

Mean Dimensionless Concentration, K, on the Building.

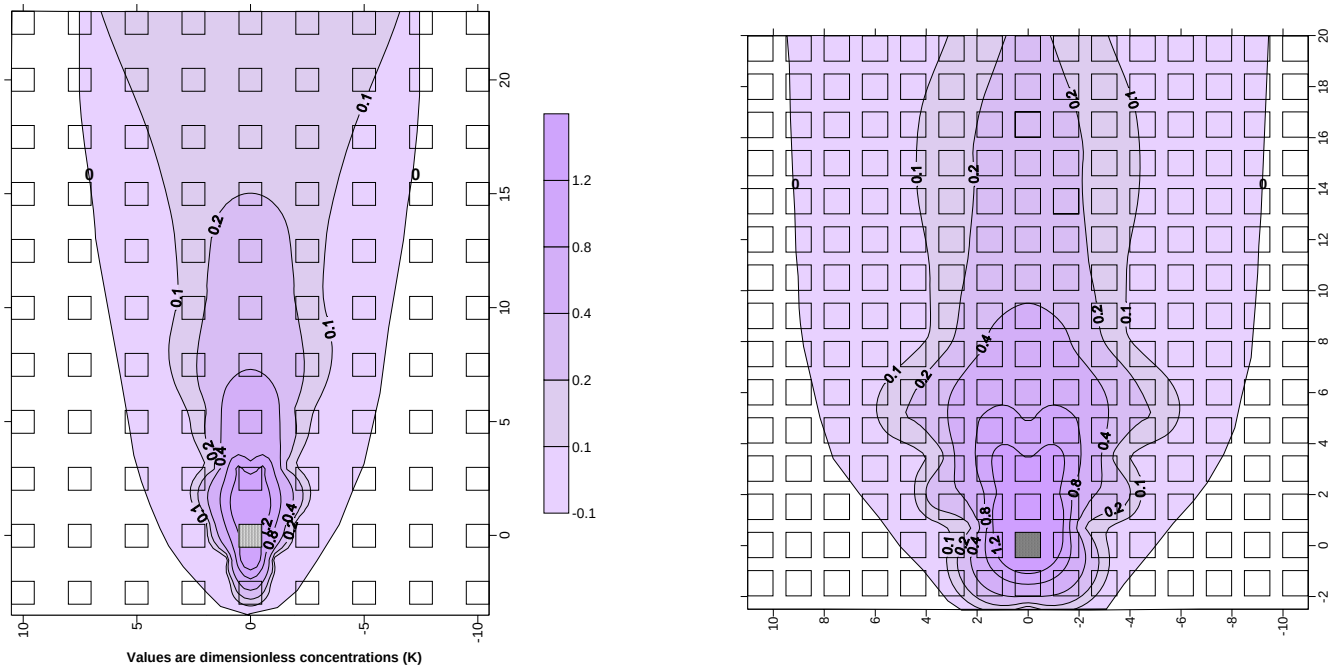

(Max - Min)/Mean

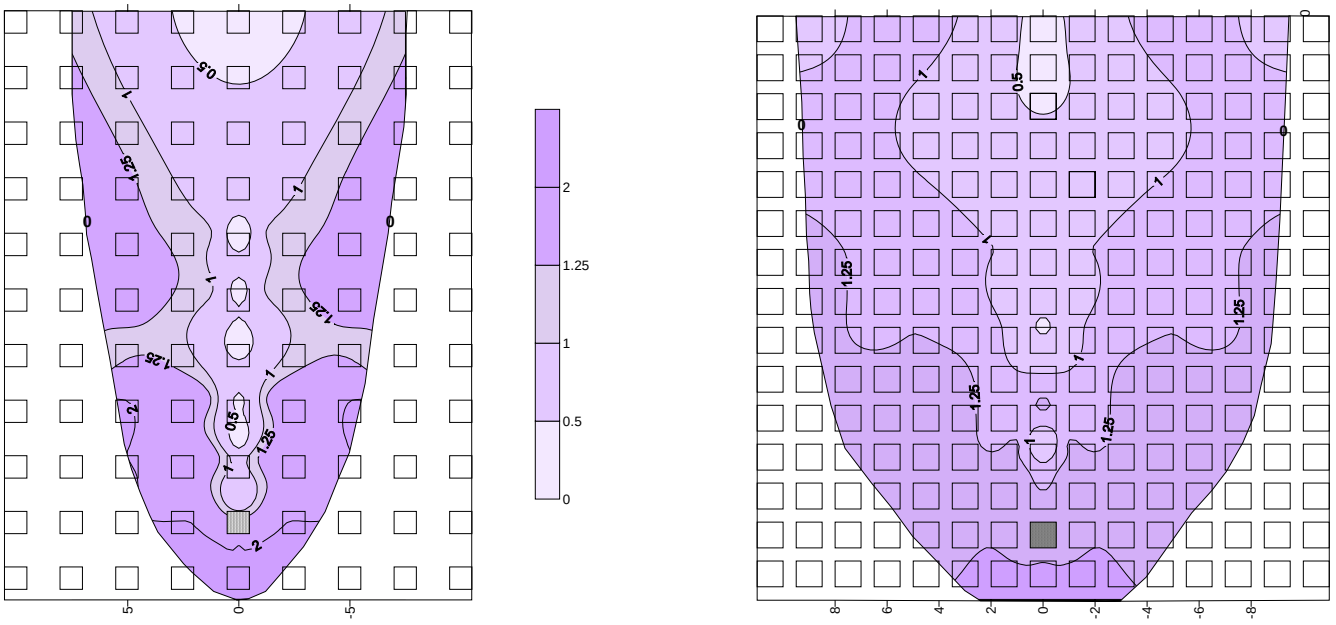

Figure 21. 'Influence' Areas for Dispersion; from within which Sources of Contaminant Will Impinge on the Shaded Building in the Array.
Upper Row: Contours of Mean Concentrations (as K) on all Faces.
Lower Row: Contours of Largest Concentration Difference Across Faces.
In Hall et al(2002), from Wind Tunnel Experiments of Mfula(2004).

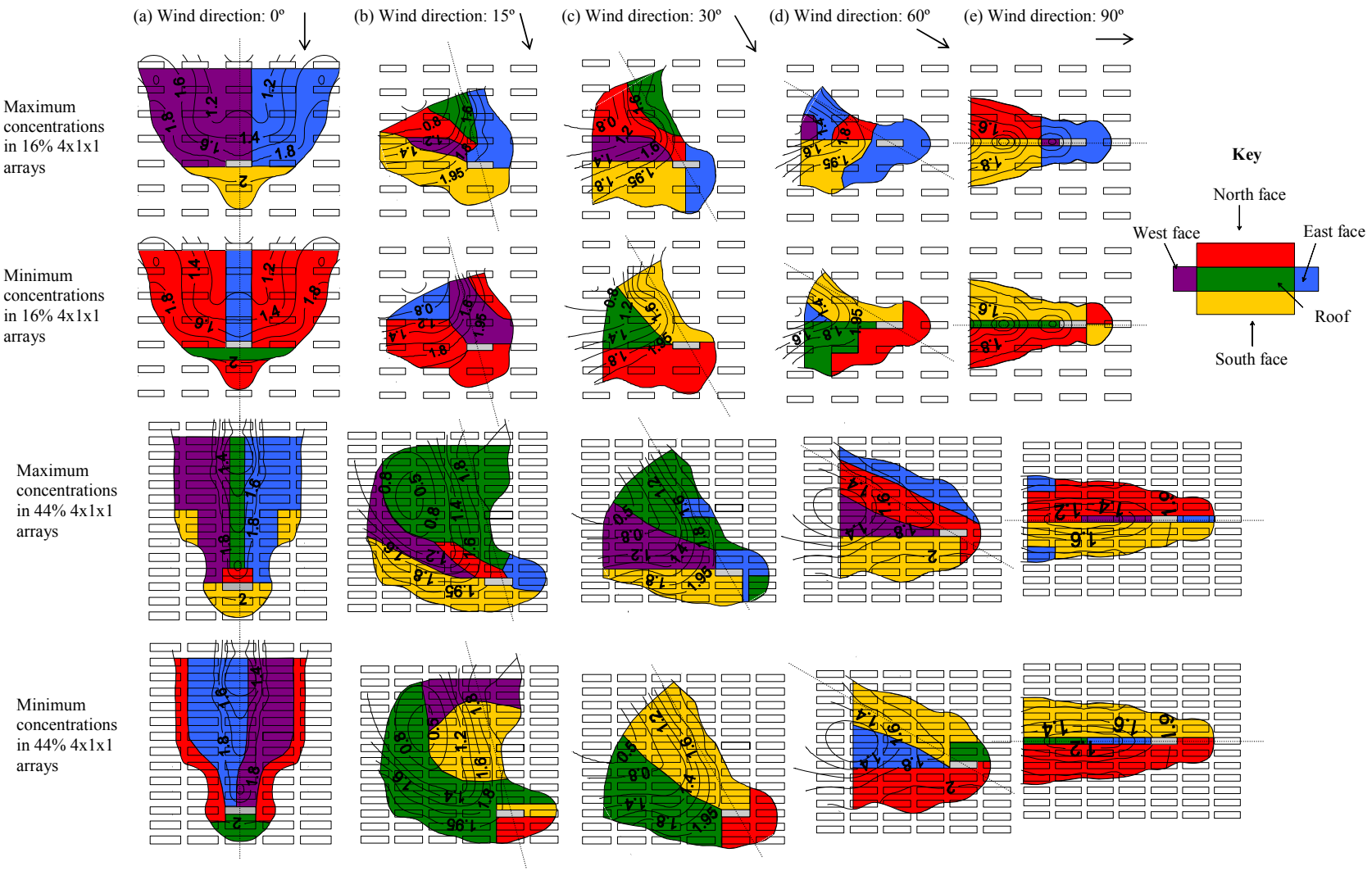

Figure 22. Regions Within which Maximum and Minimum Concentrations are Generated on Given Faces of a Test Building Model (Shaded Grey in the Contour Maps) in 16% and 44% Area Density Arrays of 4x1x1 Buildings. From Wind Tunnel Experiments at BRE. From Mfula (2004). The Line of Wind Direction Through the Building is Shown by a Dotted Line.

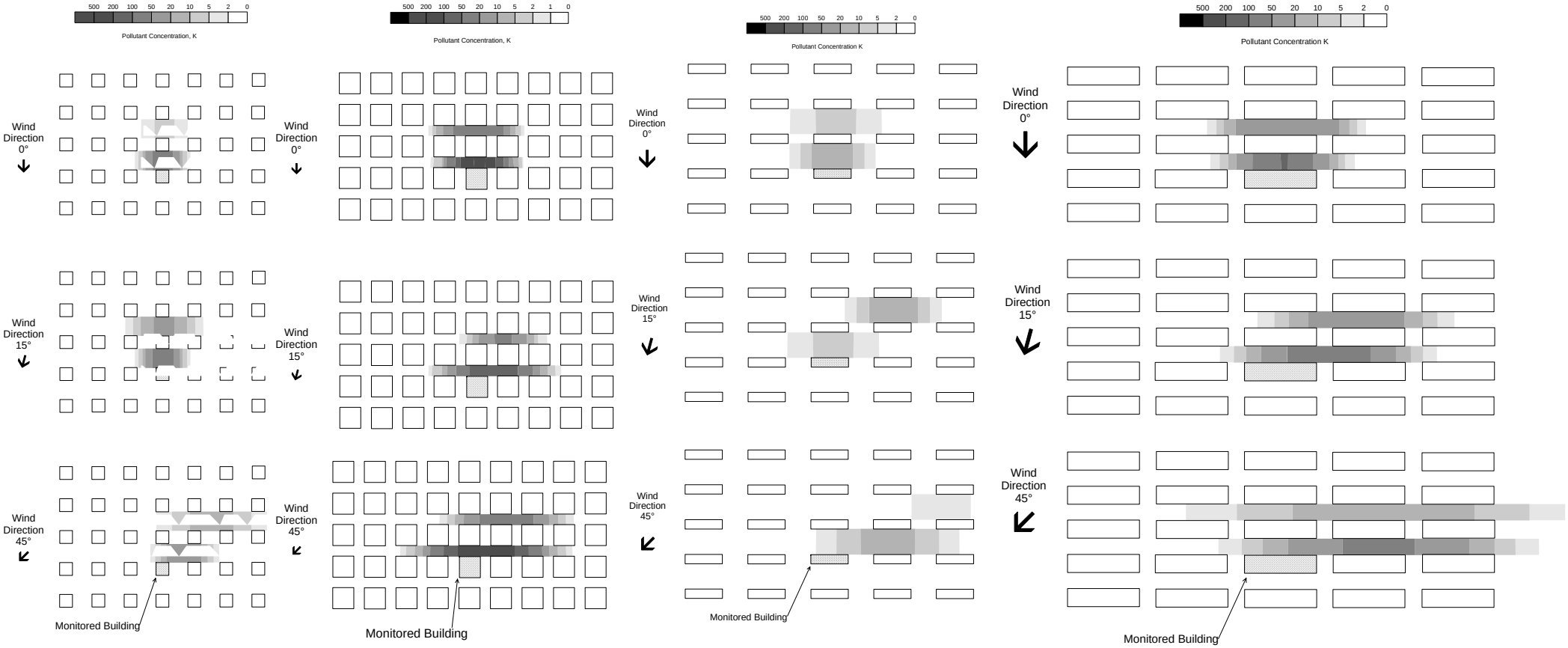

Figure 23. Proportionate Contribution of Line Sources to Exposure of the Shaded Building in the Urban Array.
Left: 16% and 44% Area Density Cubical Building Arrays.
Right: 16% and 44% Area Density 4x1x1 Building Arrays.
From Hall et al(2000).

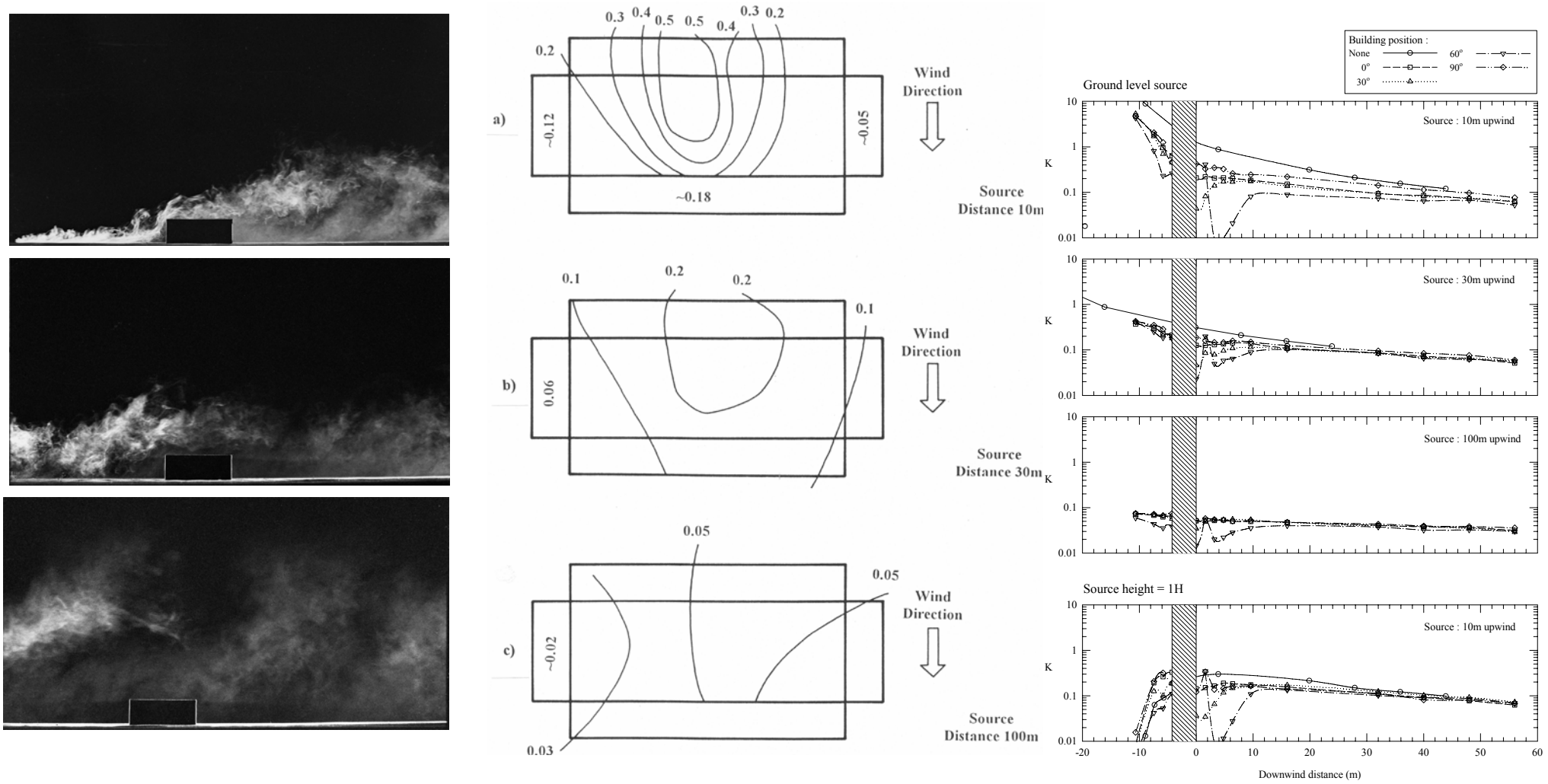

Figure 24. **Concentrations Due to Impact of a Ground-Based Plume on an Isolated Building. The Building Walls Are Folded Outwards in the Plan Views.**
Upwind Source Distances: 6H (Upper), 20H (Middle) and 65H (Lower) (H = Building Height).
Left: Visualised Plumes, Centre: Concentrations on Building (as K).
Right: Centreline Concentrations at Ground (as K, Building Location Shaded).
From Hall et al(1996c).

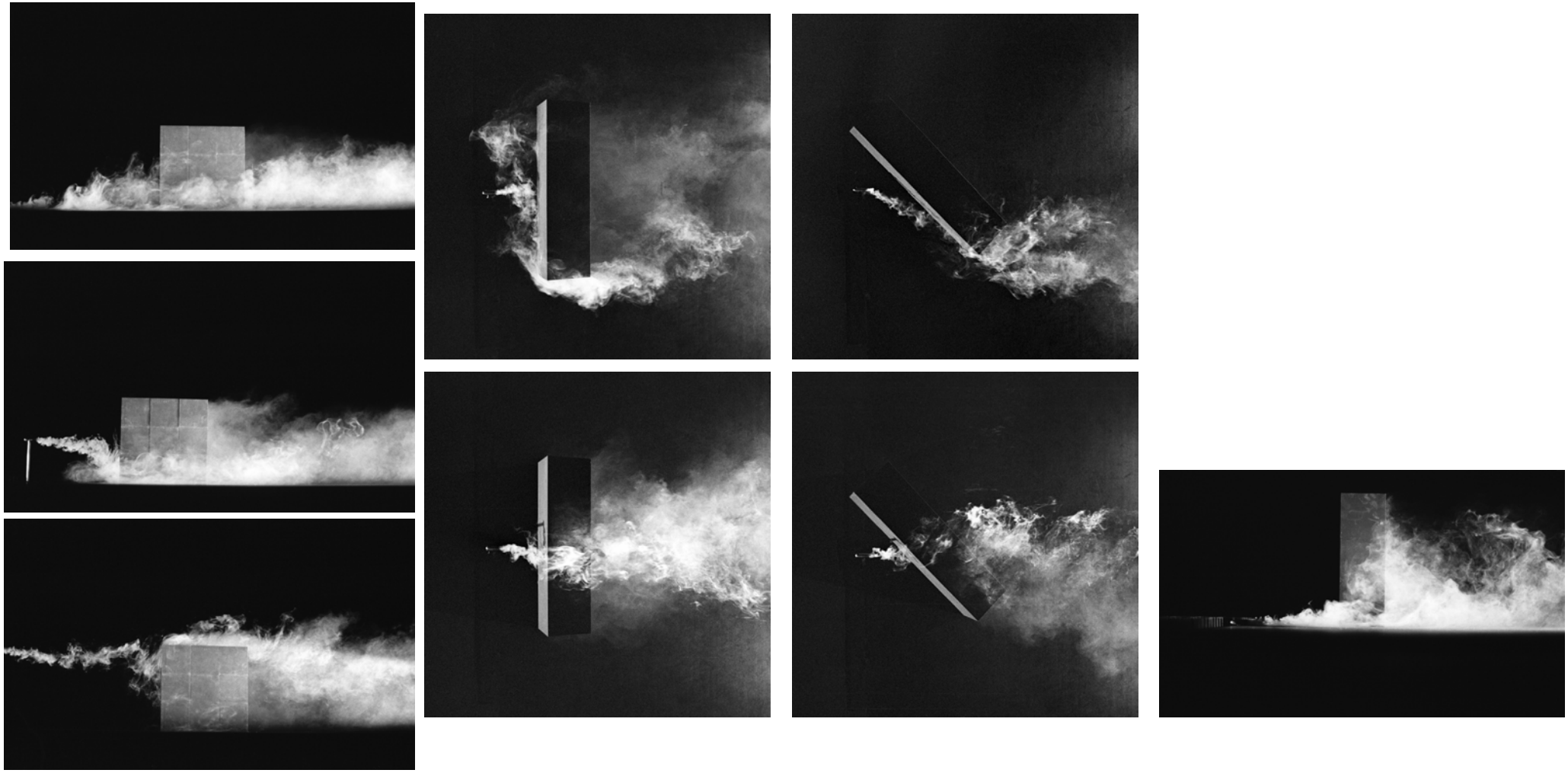

Figure 25. Flow Visualisation Images of Plume Impactions on Single Buildings. From the Dstl UDM Data Archive.
Left: Plumes at Three Heights Impacting on a Cubical Building Normal to the Wind.
Centre: Plumes at Two Heights Impacting on a Low, Wide Building Normal and Skewed at 45° to the Wind.
Right: Ground Based Plume Impacting on a Tall Narrow Building, Showing Vertical Mixing in the Downstream Wake.
From Hall et al(1997).

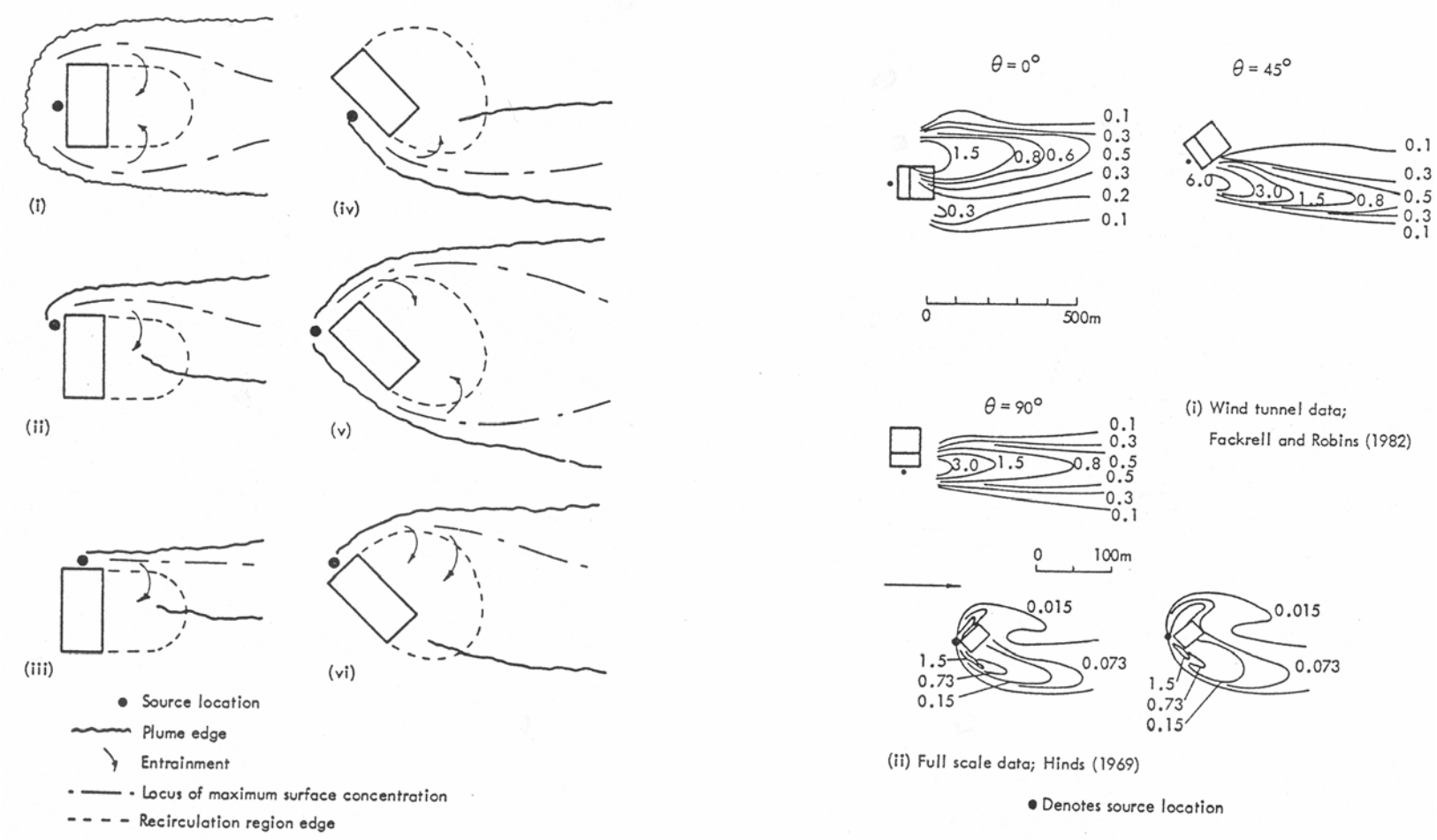

Figure 26. Contours of Flow and Dispersion Patterns Around Buildings from Ground Level Sources. From Robins and Fackrell(1983), as reproduced in Hall et al(1996b).

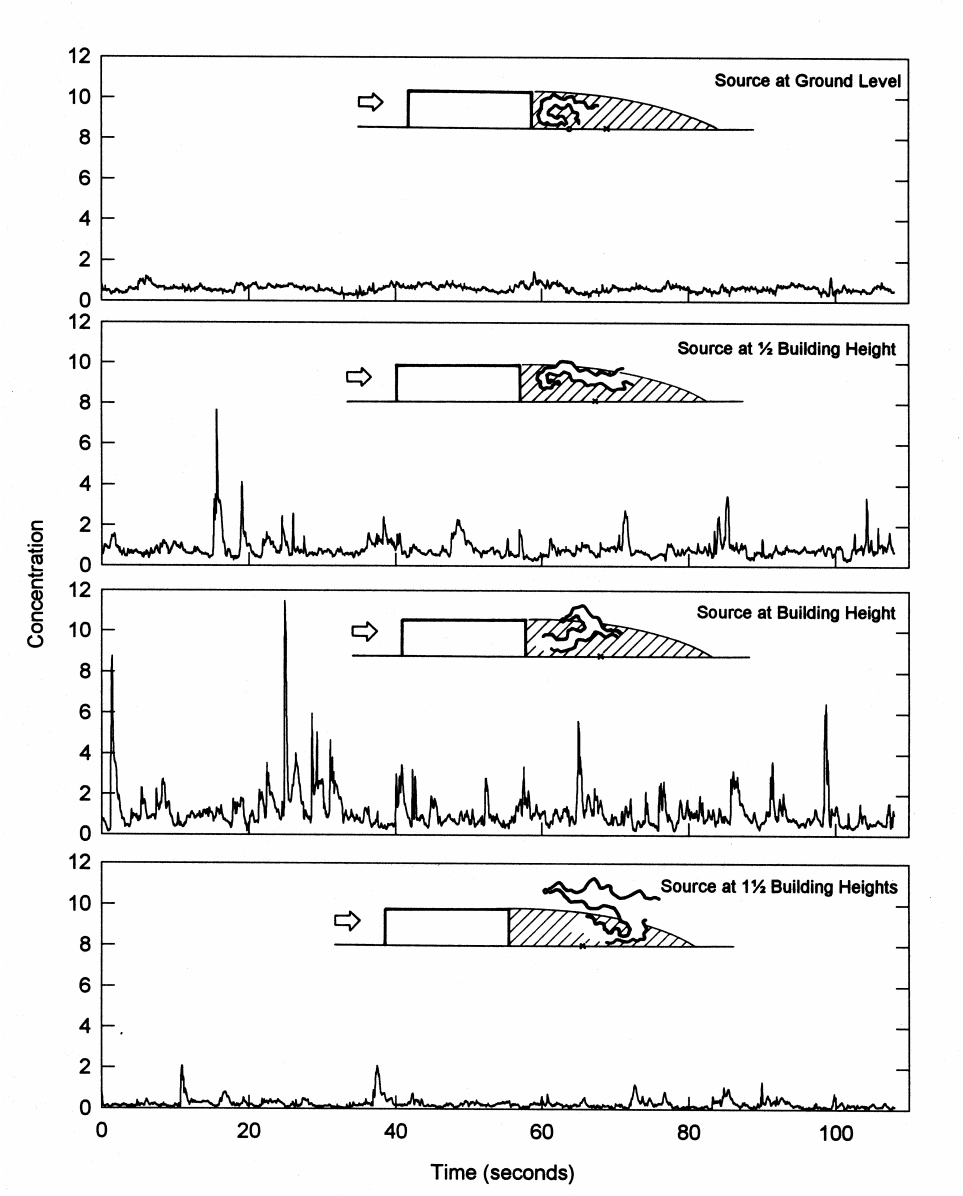

**Figure 27. Short Term Measured Concentrations in a Building Wake with Different Source Positions.
The Measurement Point is at the Ground Half Way Along the Separated Wake.
From Hall et al(1997).**

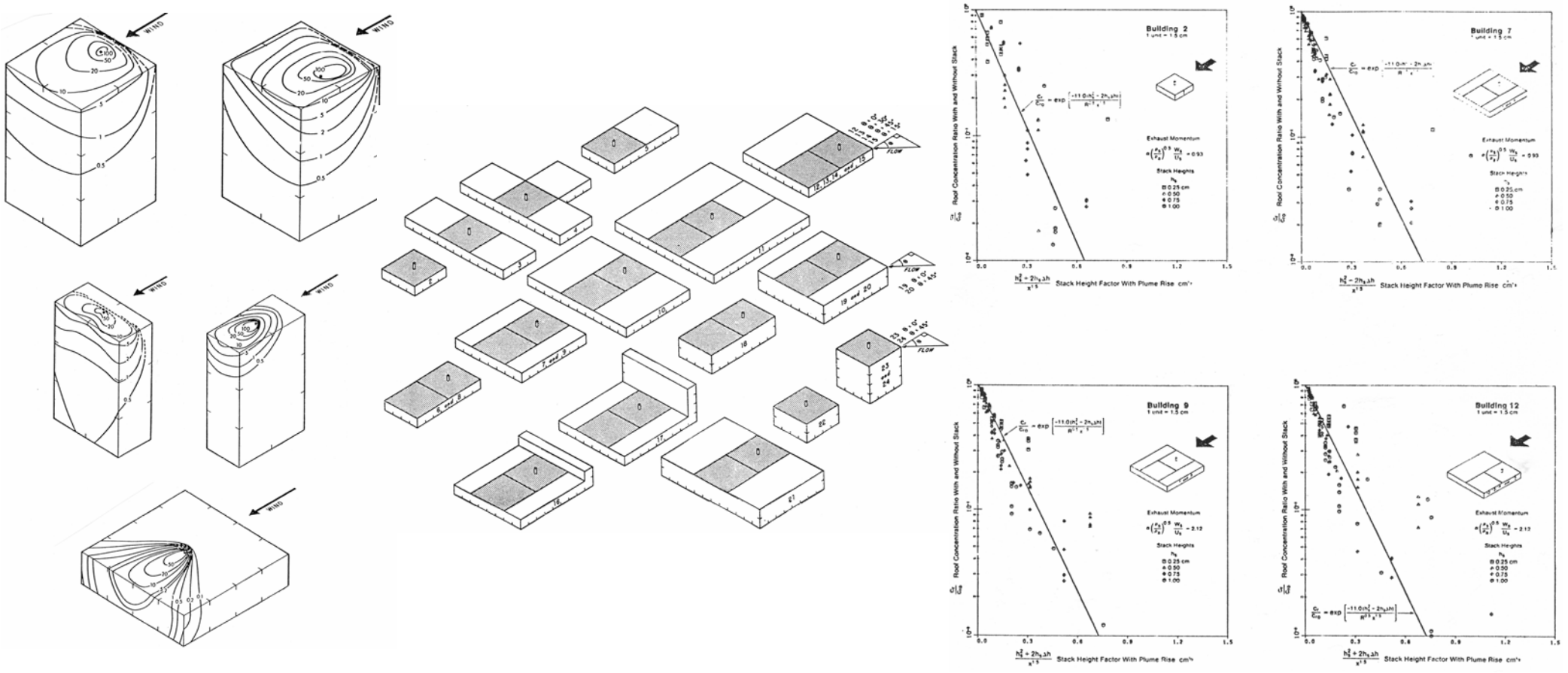

Figure 28. Left: **Concentration Contours on a Single Building Due to a Flush Vent on the Roof. From Wilson (1976).**
Centre: **The Range of Building Shapes Used in Wilson and Winkel's(1982) Experiments on Concentrations on a Building from Elevated Sources on the Building.**
Right: **Some Results of Wilson and Winkel's(1982) Work, Showing Bulk Plots of the Data and Empirical Data Fits.**

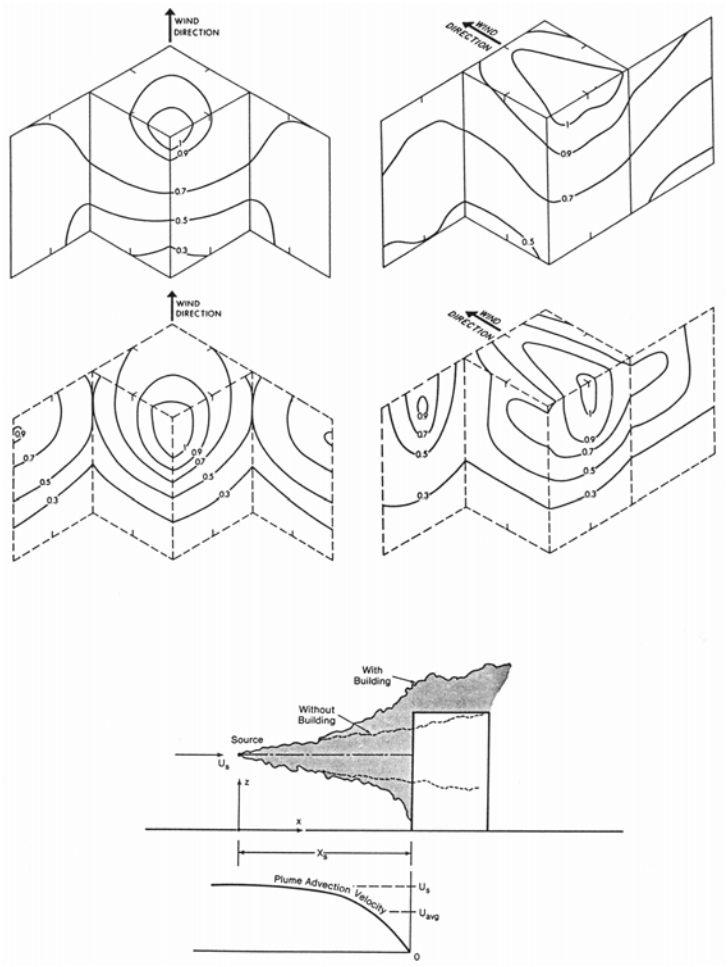

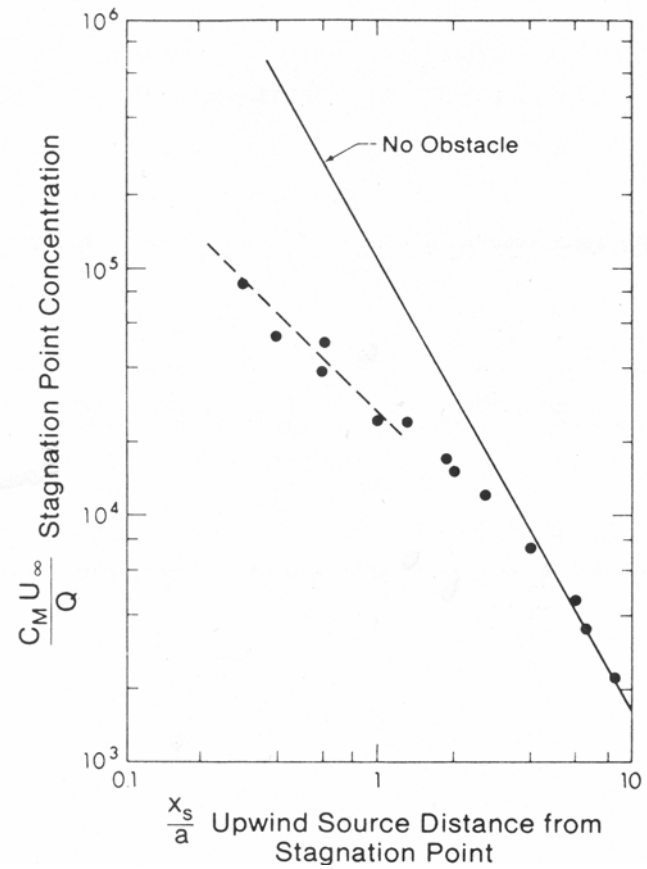

Figure 29. Effect of Source Distance on Maximum Concentrations on a Building Due to an Impacting Plume.
Left: Example of Building Concentration Patterns from an Elevated Plume Impacting on a Building Normal and at 45° to the Wind.
Right: Maximum Concentrations on the Building from Sources at Varying Upwind Distances.
Results from Wilson and Britter(1982), using data from Wilson and Netterville(1978).

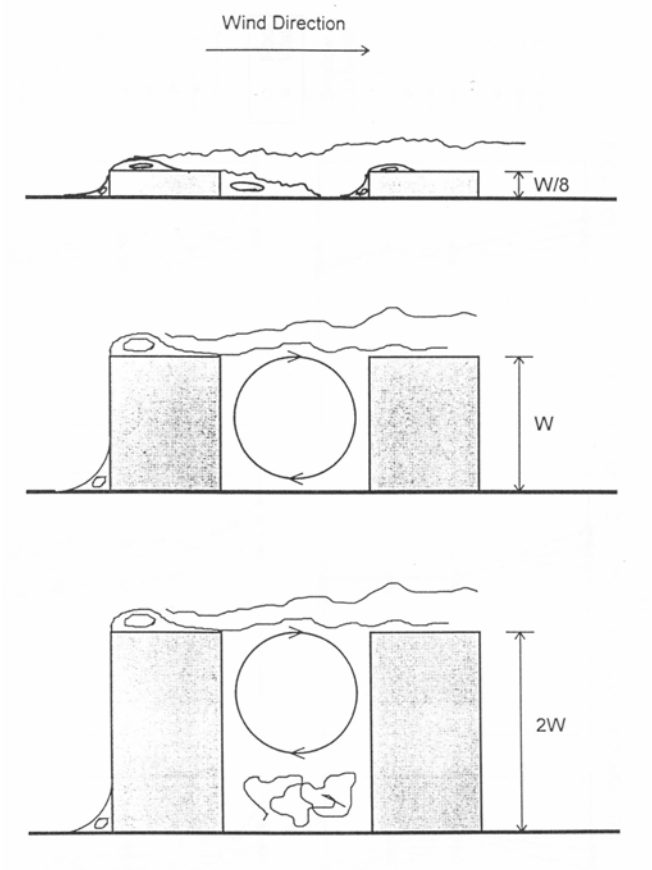

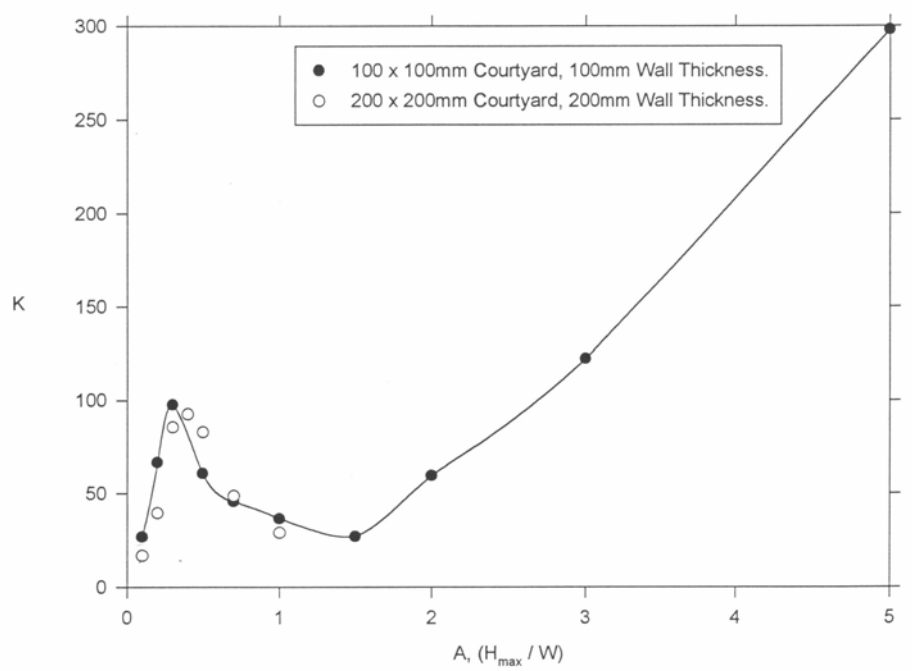

Figure 30. Flow Patterns in Courtyards of Different Depth/Width and the Resultant Concentrations at the Base of the Courtyard for a Release within it at the Base.
The Sketches are not to Scale and the Separations Have Been Exaggerated.
From Wind Tunnel Experiments of Hall et al(1999c).

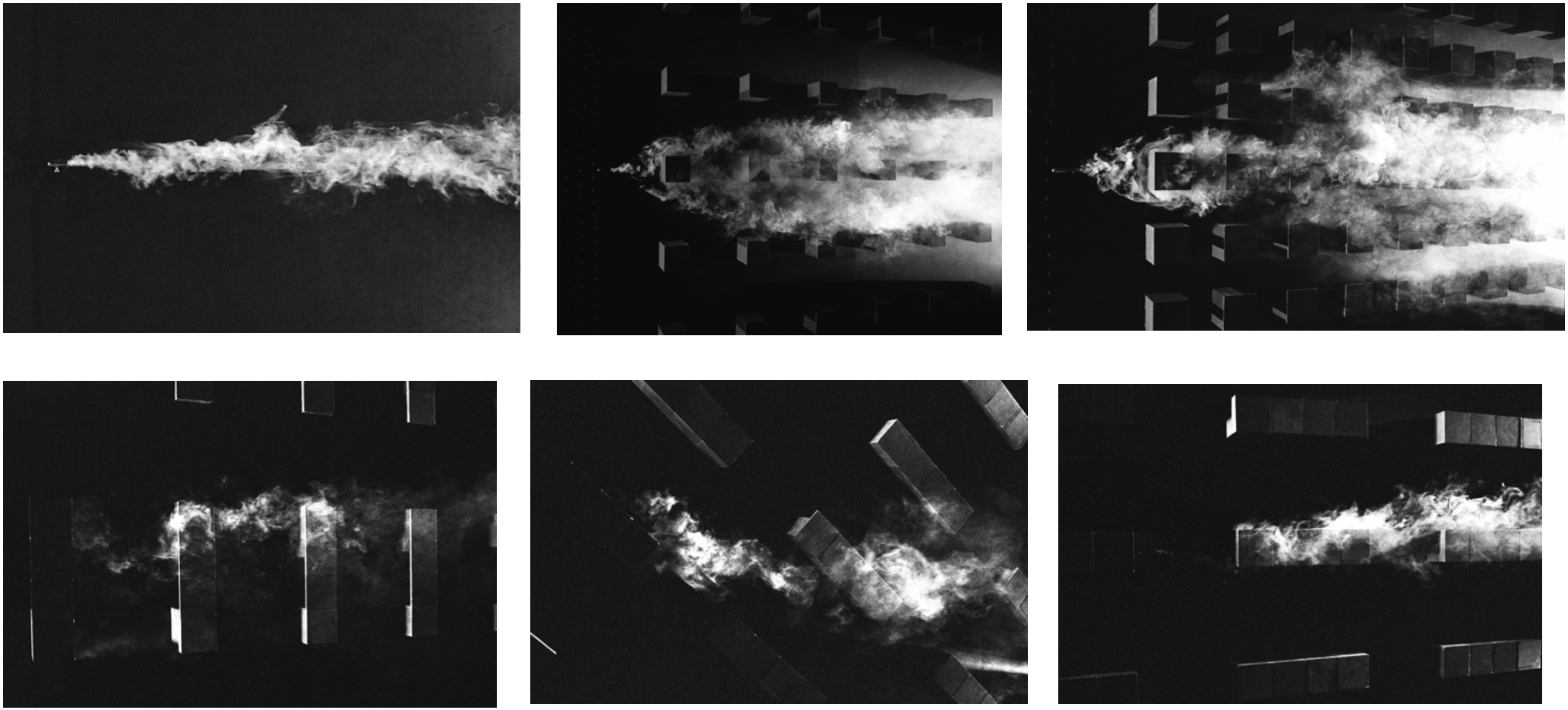

Figure 31. Flow Visualisation Images (Plan Views) of Plume Dispersion From Ground Level Releases Over Urban Building Arrays.
Upper: From Left, Over Smooth Terrain, Over a Cubical Building Array of 16% and 44% Area Densities.
Lower: Over 16% Area Density Arrays of 4x1x1 Building Forms, from Left Set Normal to, Skewed at 45° and Along the Wind.
From the Dstl UDM Data Archive.

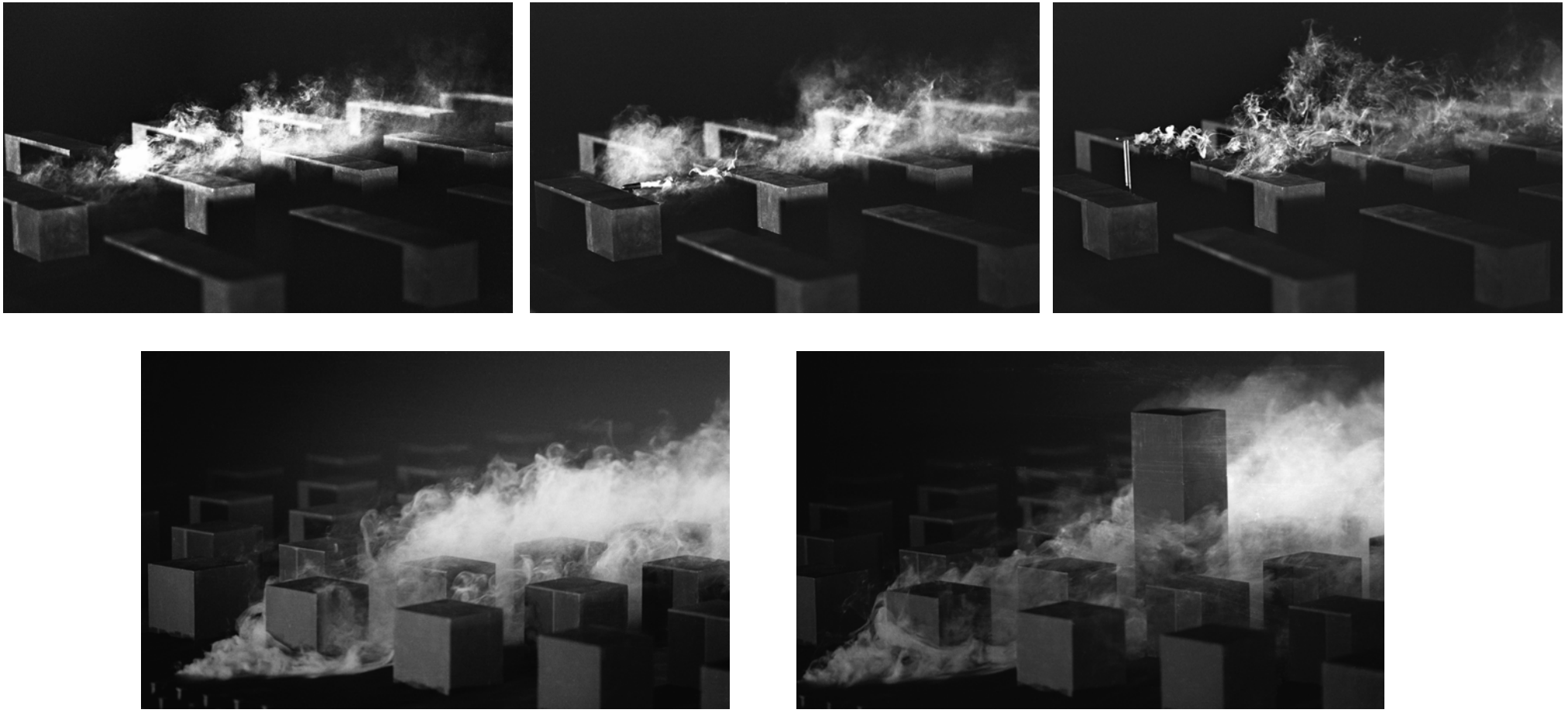

Figure 32. Flow Visualisation Image Showing the Effects of Source Height and Tall Obstacles in Urban Building Arrays.
Upper: Source Heights at the Ground (Left), Obstacle Height (Centre) and Two Obstacle Heights (Right), in an Array of 4x1x1 Building forms Set Normal to the Wind.
Lower: The Effect of a Single Tall Building within a Uniform Array, Showing the Rapid Vertical Plume Mixing in the Tall Building Wake.
From the Dstl UDM Data Archive.

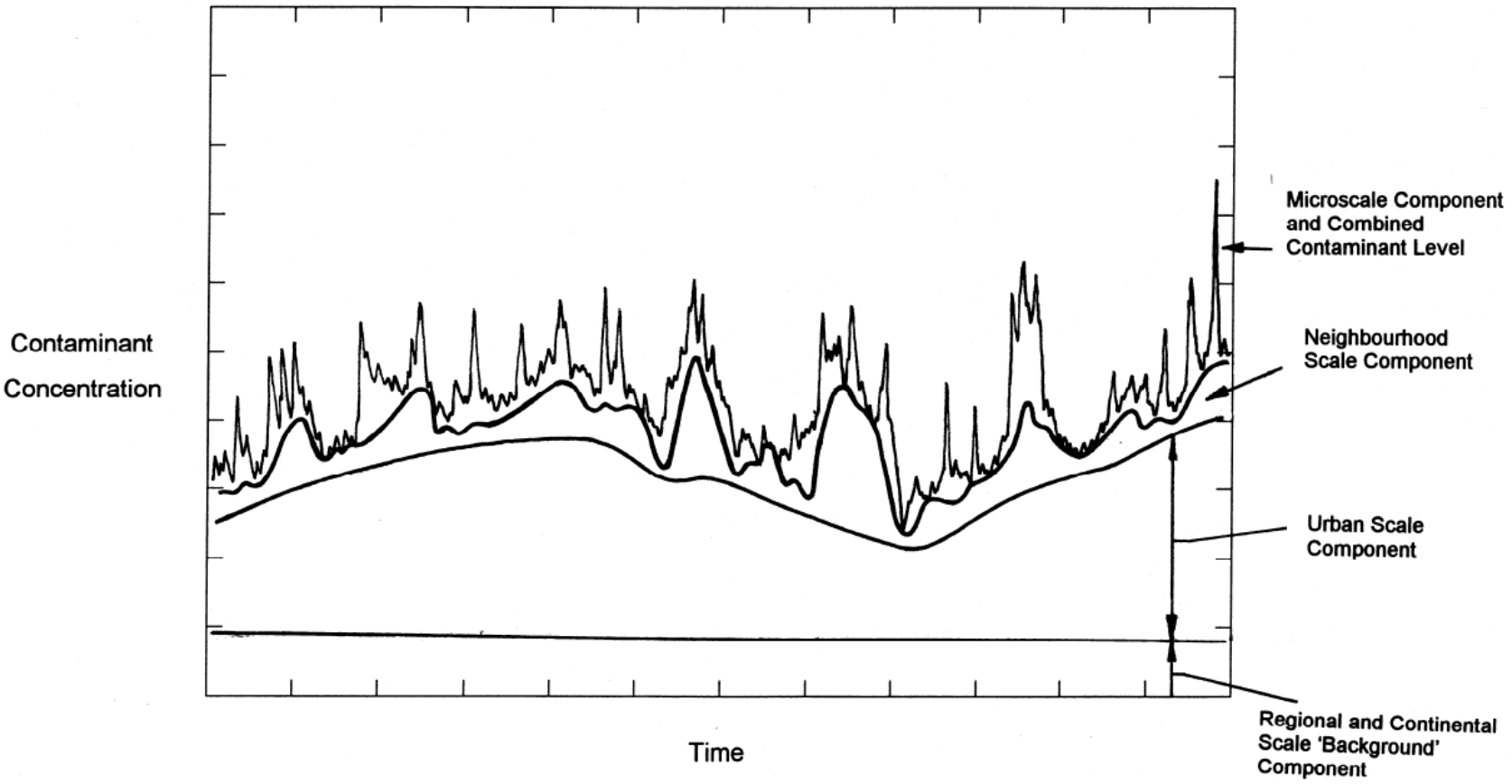

Figure 33. Representation of Local Exposure in an Urban Area from Sources at Different Distances From Hall et al(1996b).

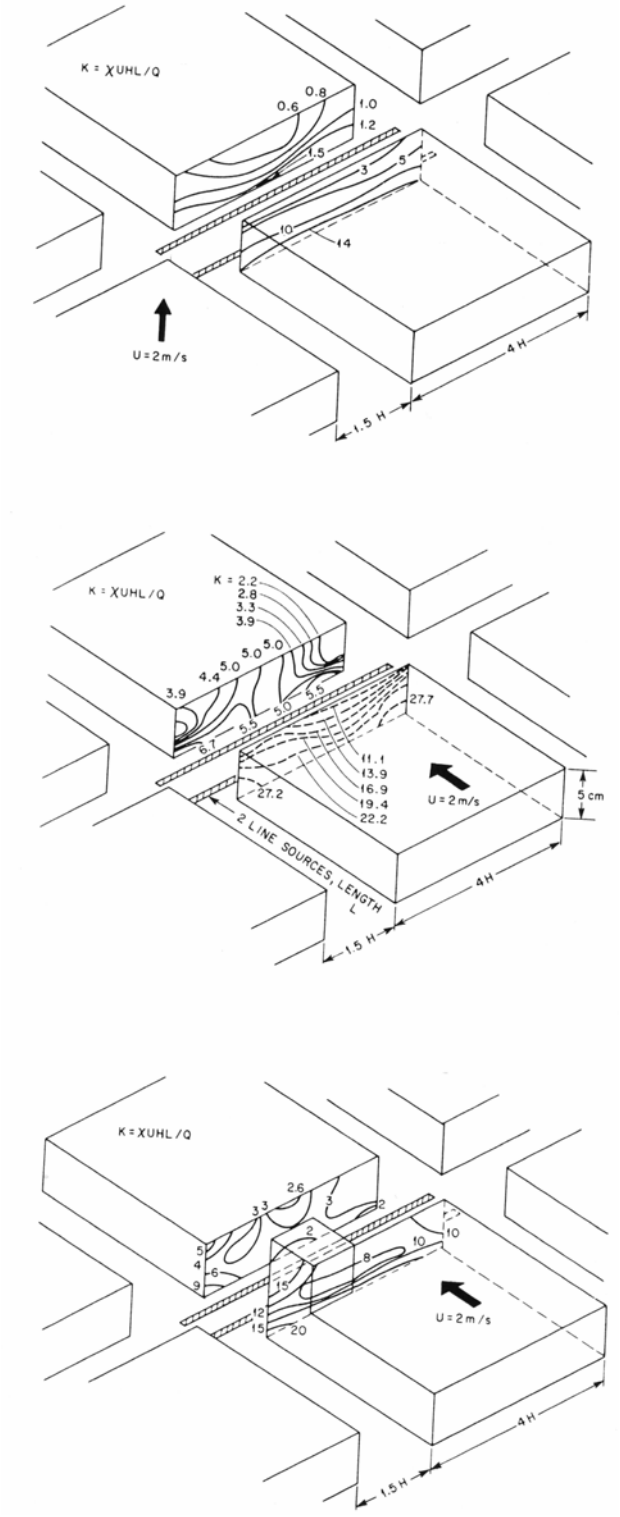

Figure 34. Concentration Patterns on Building Blocks in an Urban Array, for Two Wind Directions and a Modified Block Shape. From Cermak et al(1974).

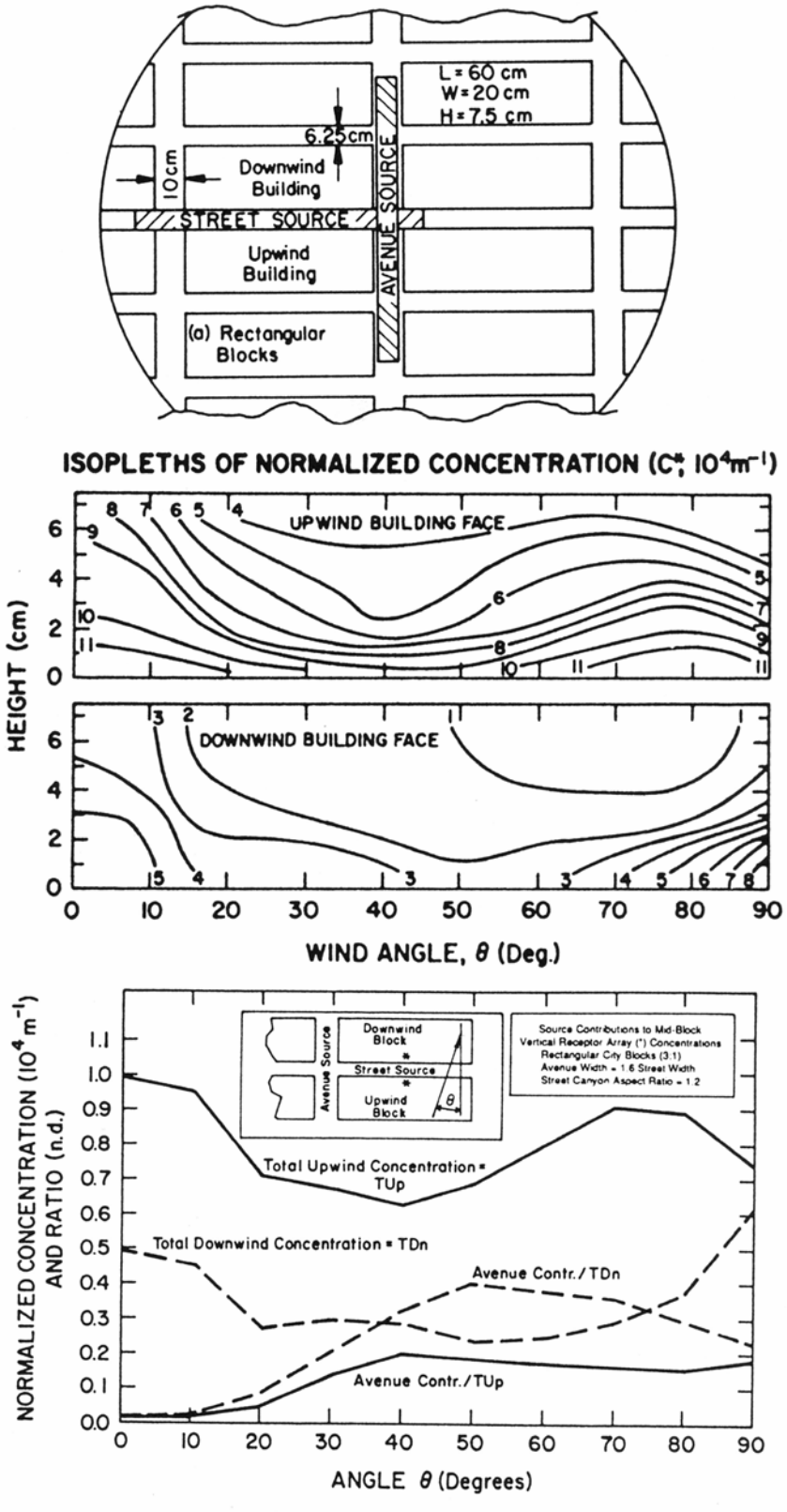

Figure 35. Concentration Patterns on Building Faces in a Dense Urban Array. From Dabbert and Hoydysh(1991).

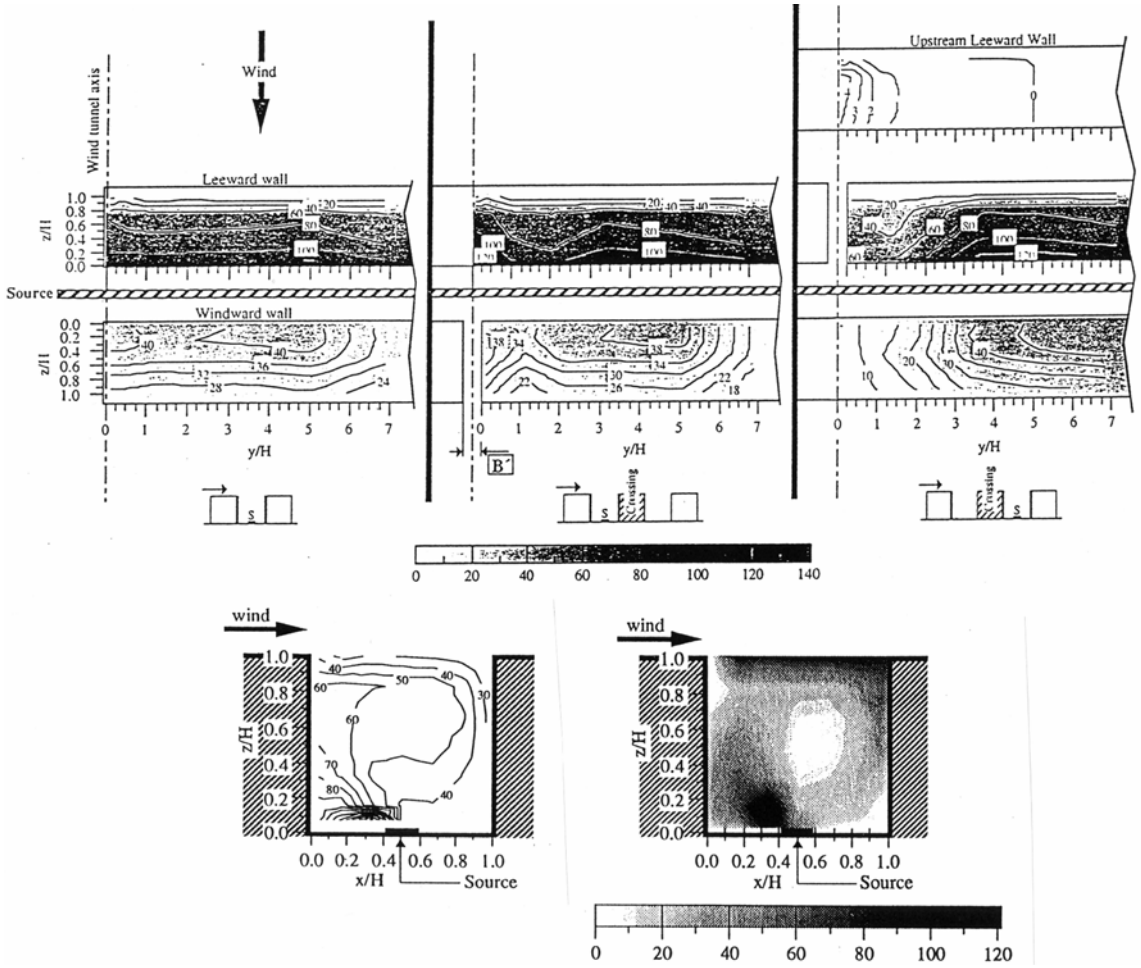

Figure 36. Concentration Patterns in the Street Cross Section and on the Building Faces in a Two Dimensional Urban Canyon. From Pavageau et al (1996).

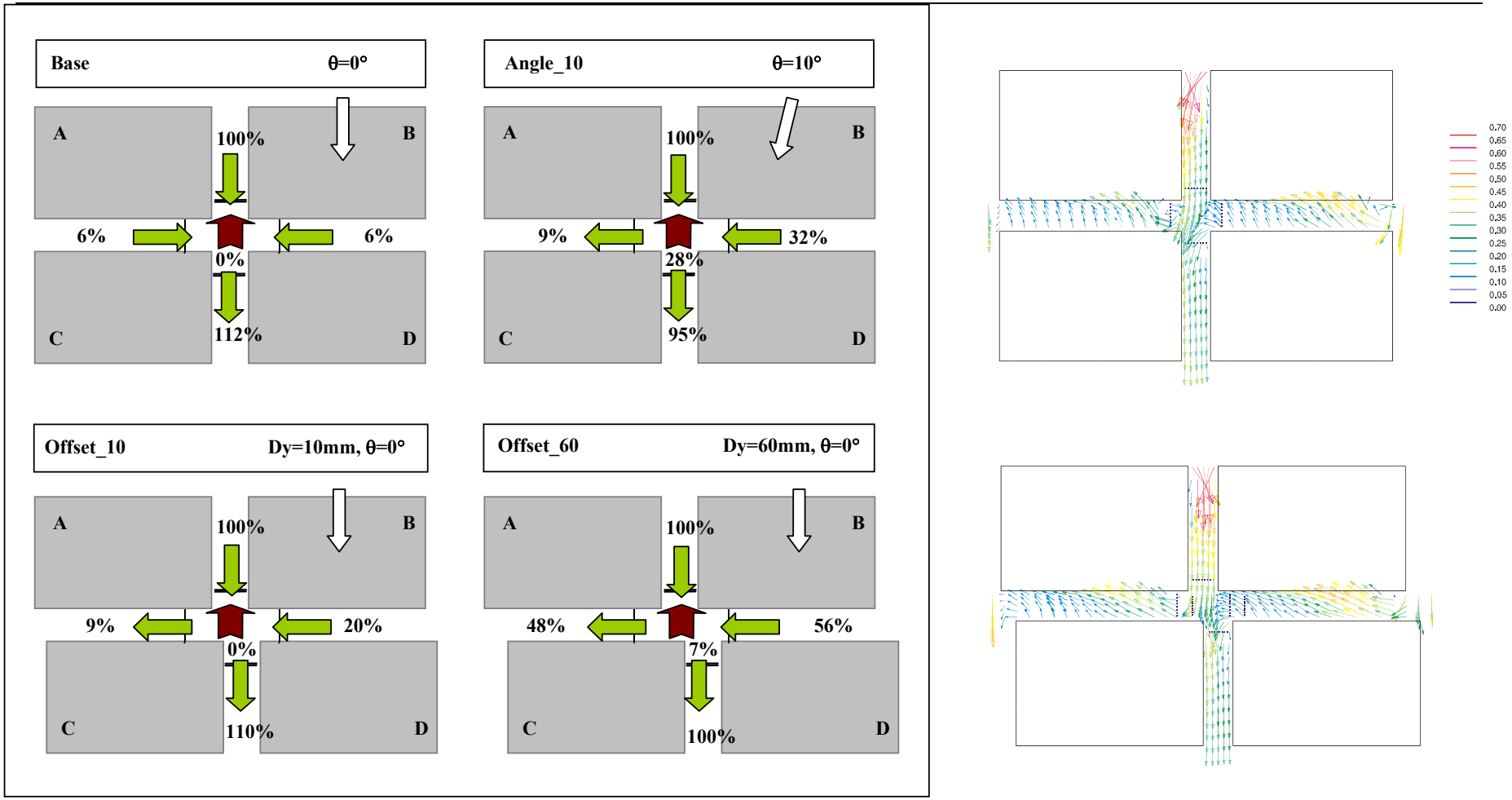

Figure 37. Diagrams Showing the Division of the Flow Around a Street Junction with Small Changes in Wind Direction and Street Alignment.
Left: Mass Flow Balances.
Right: Mean Vectors from LDA Scans Relating to the Two Right Hand Mass flow Balances.
From Wind Tunnel Experiments by Scaperdas(2000), in Robins et al(2002).

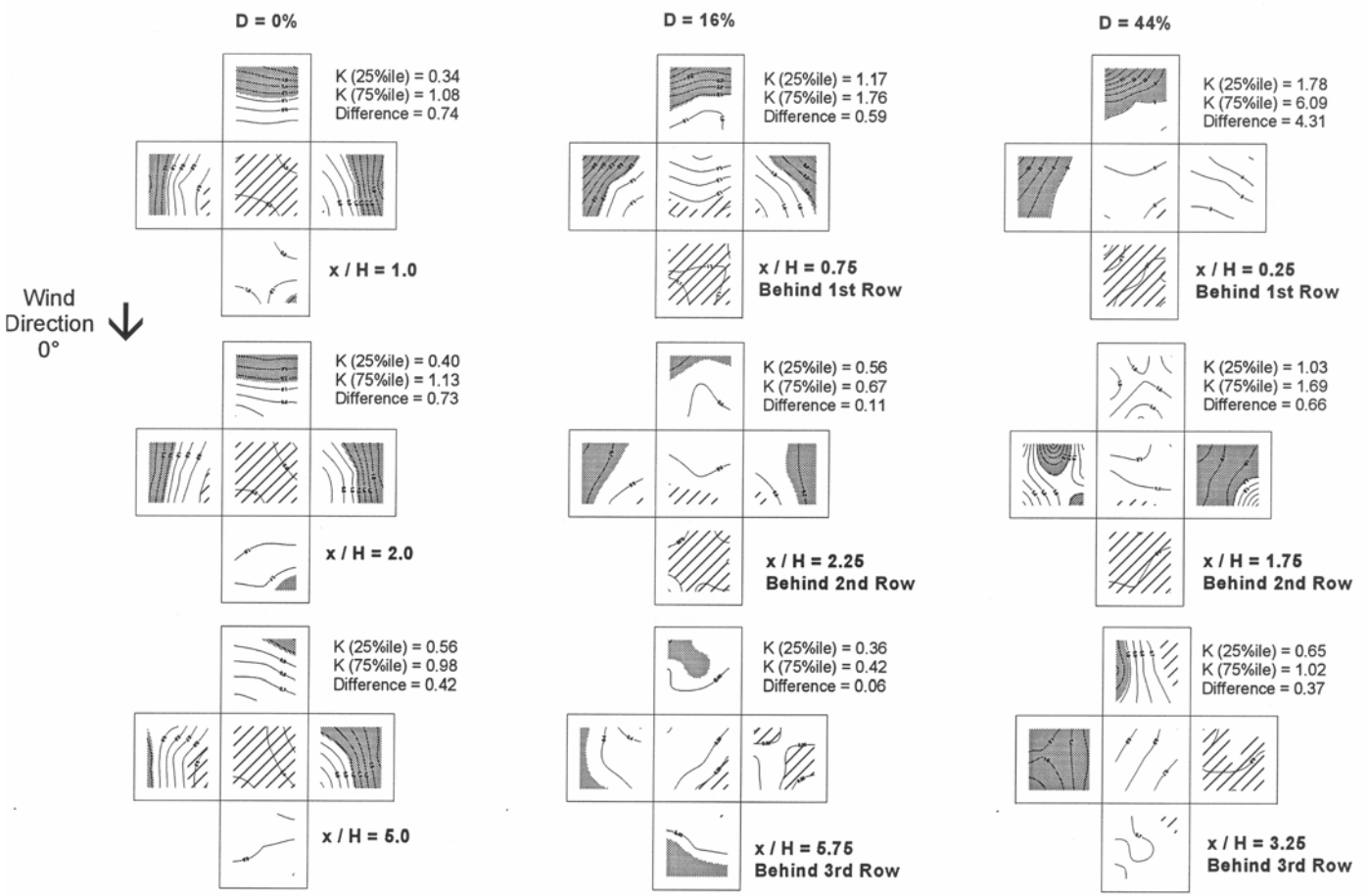

Figure 38. Concentration Patterns on Cubical Building Forms in Urban Arrays Due to Sources at Different Upwind Distances. The Building Walls Are Folded Outwards in the Plan Views.
Left: Open Terrain. Centre: 16% area Density. Right: 44% Area Density.
Top: Source in Street Immediately Upwind.
Centre: Source One Building Row Upwind
Bottom: Source Two Building Rows Upwind.
Shaded areas Show Pressures Above 75%ile of Area Weighted Mean on Surfaces.
Hatched Areas Show Pressures Below 25%ile of Area Weighted Mean on Surfaces.
From Hall et al (1999a), Matching the Building Pressure Patterns in Figure 16.

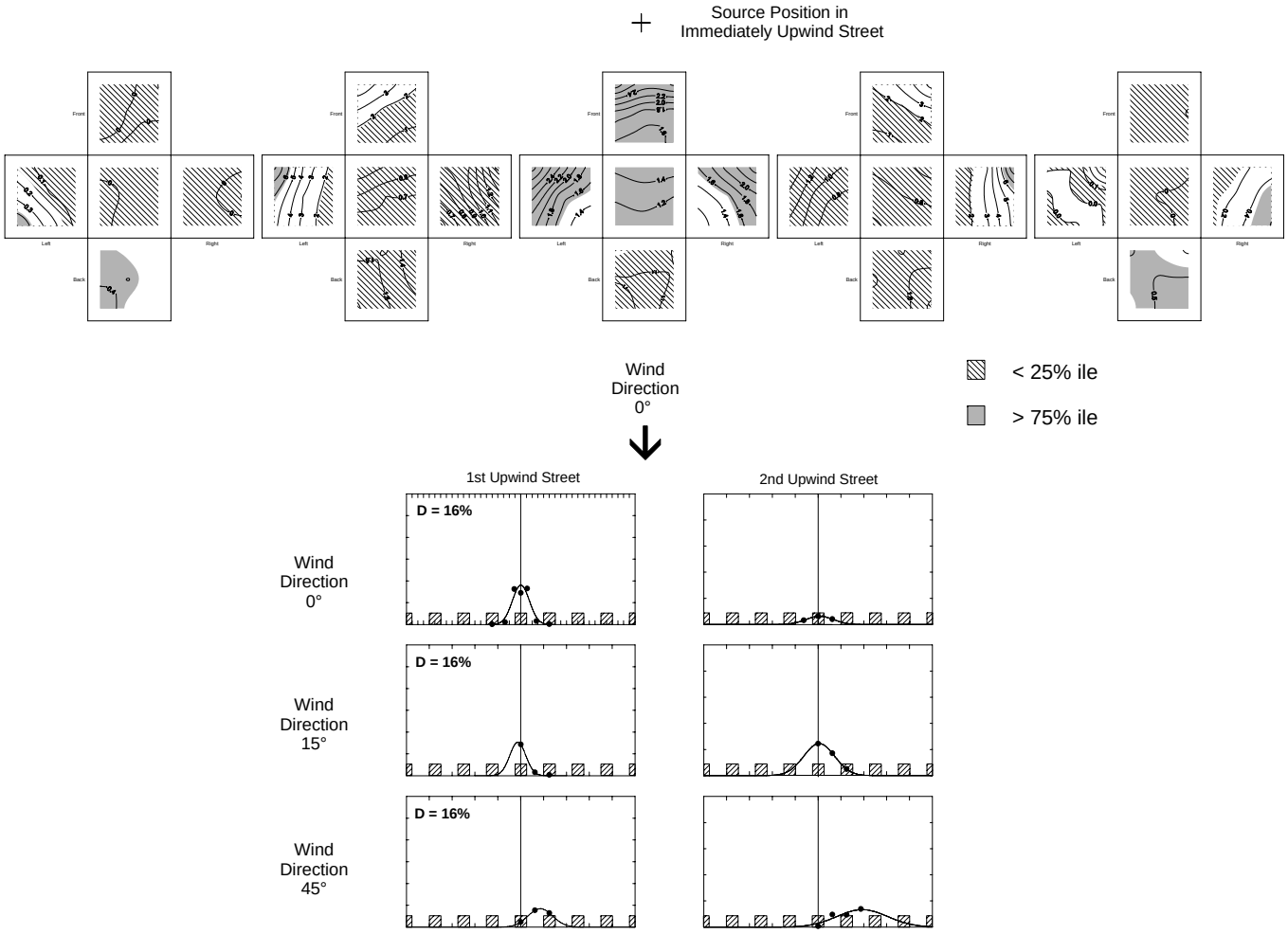

Figure 39. Effect of Source Lateral Displacement on Concentration Patterns on Cubical Buildings in an Array of 16% Area Density.
Upper: Surface Concentration Patterns on Buildings Laterally Displaced from a Source in the Street Immediately Upwind.
Lower: Proportionate Mean Concentration on Buildings from Laterally Displaced Sources in the First and Second Upwind Streets in the Array. The Limited Data is Fitted to the Nearest Gaussian Form.
From Hall et al(2000), Derived from the data in Hall et al(1999a).

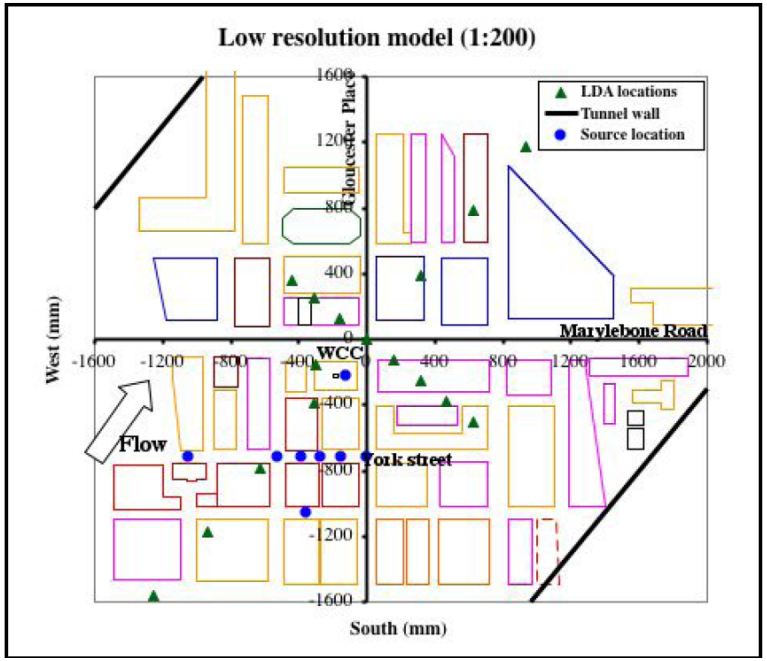

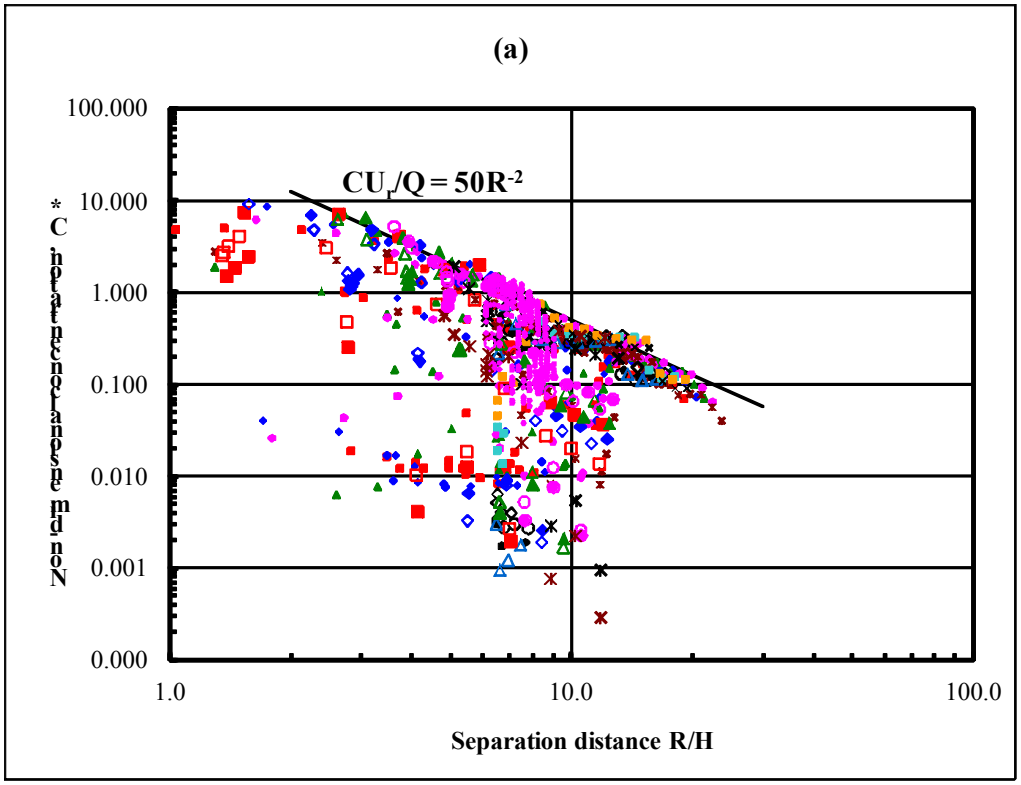

Figure 40. Example of the Range of Concentration Measurements from a Large Number of Releases and Measurement Points Around the Marylebone Road Area.
From Wind Tunnel Experiments of Robins and Cheng(2005).

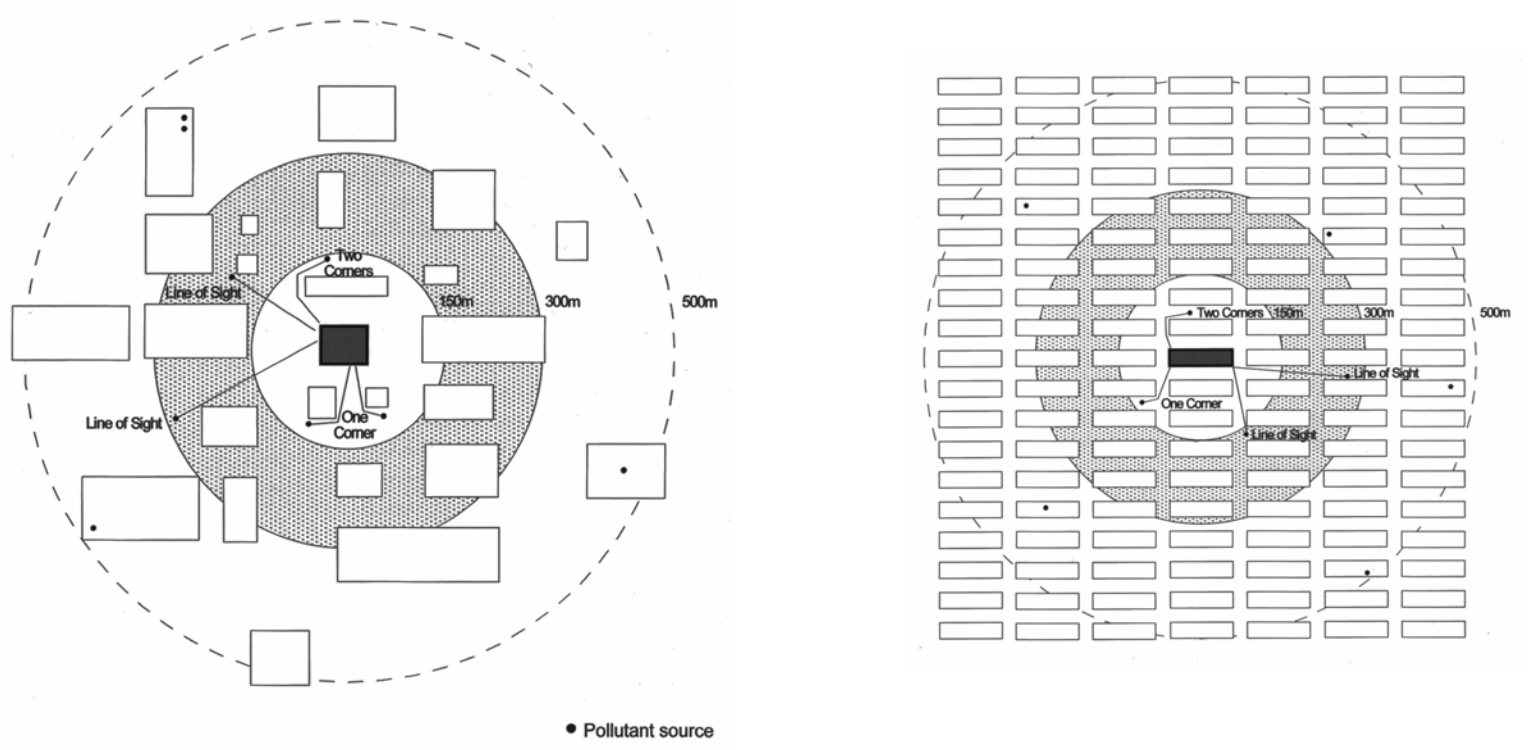

Figure 41. Examples of Assessment of Potential Building Exposure. From Kukadia and Hall (2011).

Pressure	Concentration	Outcome	Code	Key
High	**High**	Ingress of Pollutants	**IP**	
Average		Some Ingress of Pollutants	SIP	
Low		No Air Ingress	NAI	
High	Average	Some Ingress of Pollutants	SIP	
Average		Some Ingress of Pollutants	SIP	
Low		No Air Ingress	NAI	
High	Low	Natural Cleaner Air Intake	**NCAI**	
Average		Mechanical / Natural Cleaner Air Intake	**MCAI / NCAI**	
Low		Mechanical Cleaner Air Intake	**MAI**	

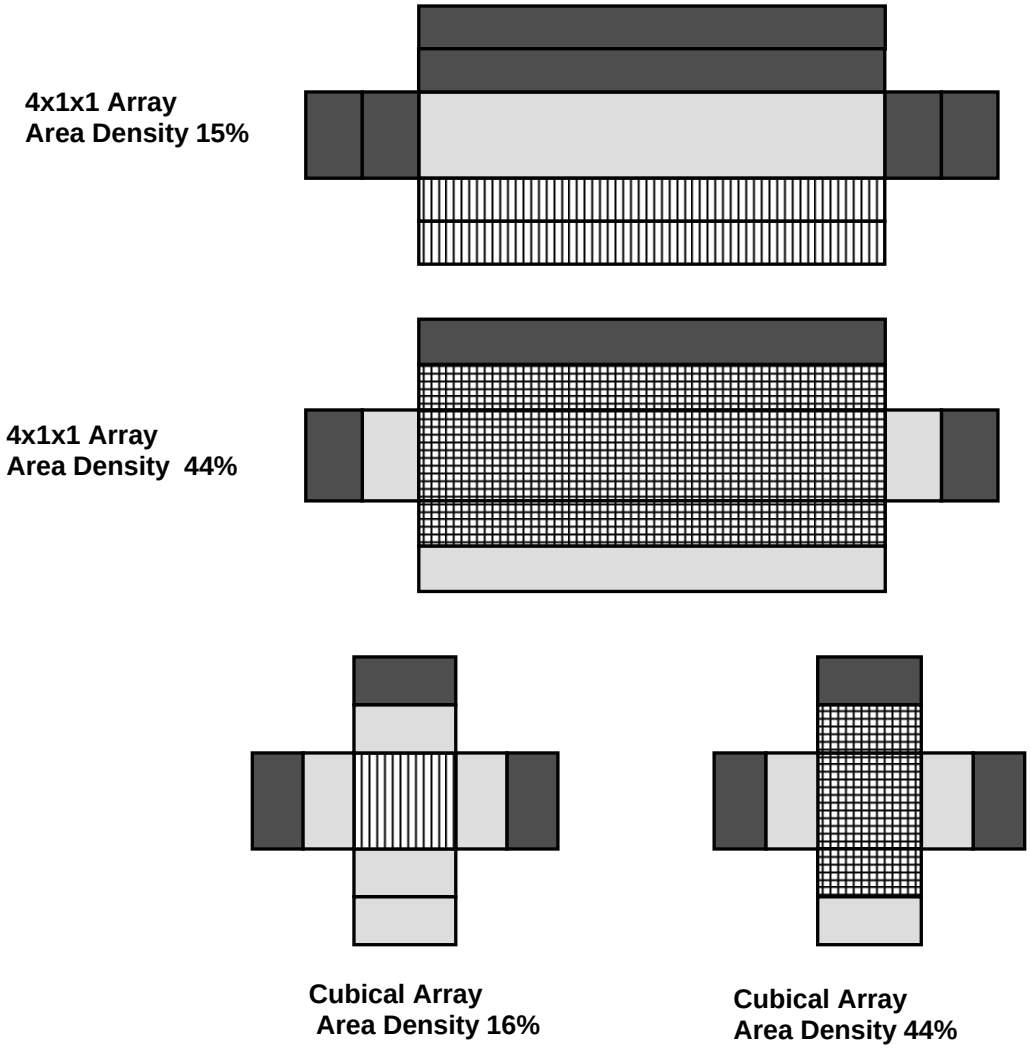

Figure 42. Bulk Estimates of Areas on Some Building Surfaces (Folded Outwards in Plan View) of Different Probable Levels of Exposure to a Source in the Immediately Upwind Street.
The Wind Direction is from Top to Bottom and the Immediately Upwind Street is Adjacent to the Upwind Face.
From Hall et al(2000).

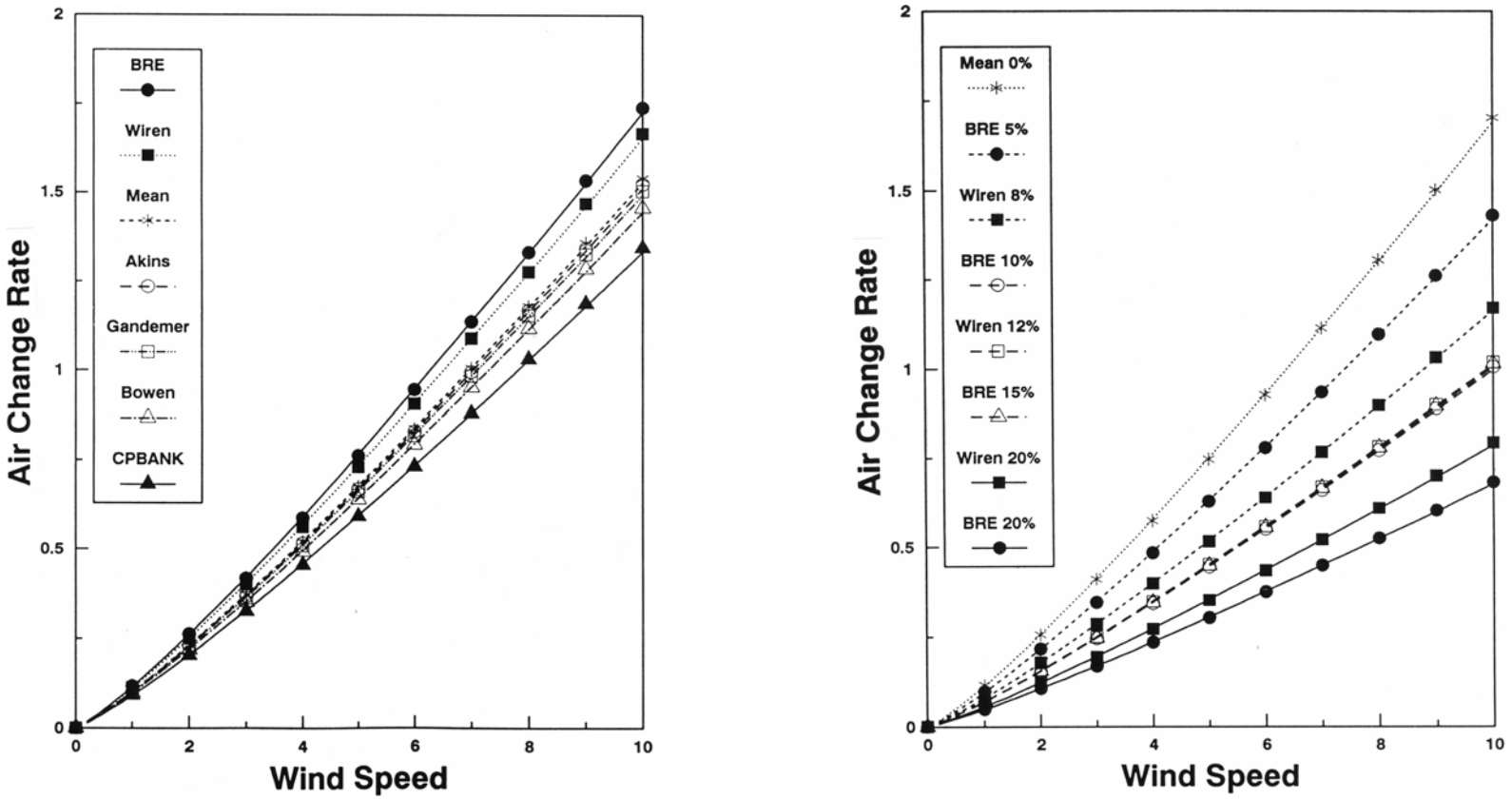

Figure 43. Variation in Air Change Rate with Wind Speed for Buildings of L/W Ratio Between 1:1 and 2:1.
Left: Open Terrain, No Surrounding Buildings.
Right: With Different Surrounding Building Densities. BRE and Wiren Data.
The Wind Speed is in m s^{-1} and the Air Change Rate is h^{-1}.
From Piggins (1991).

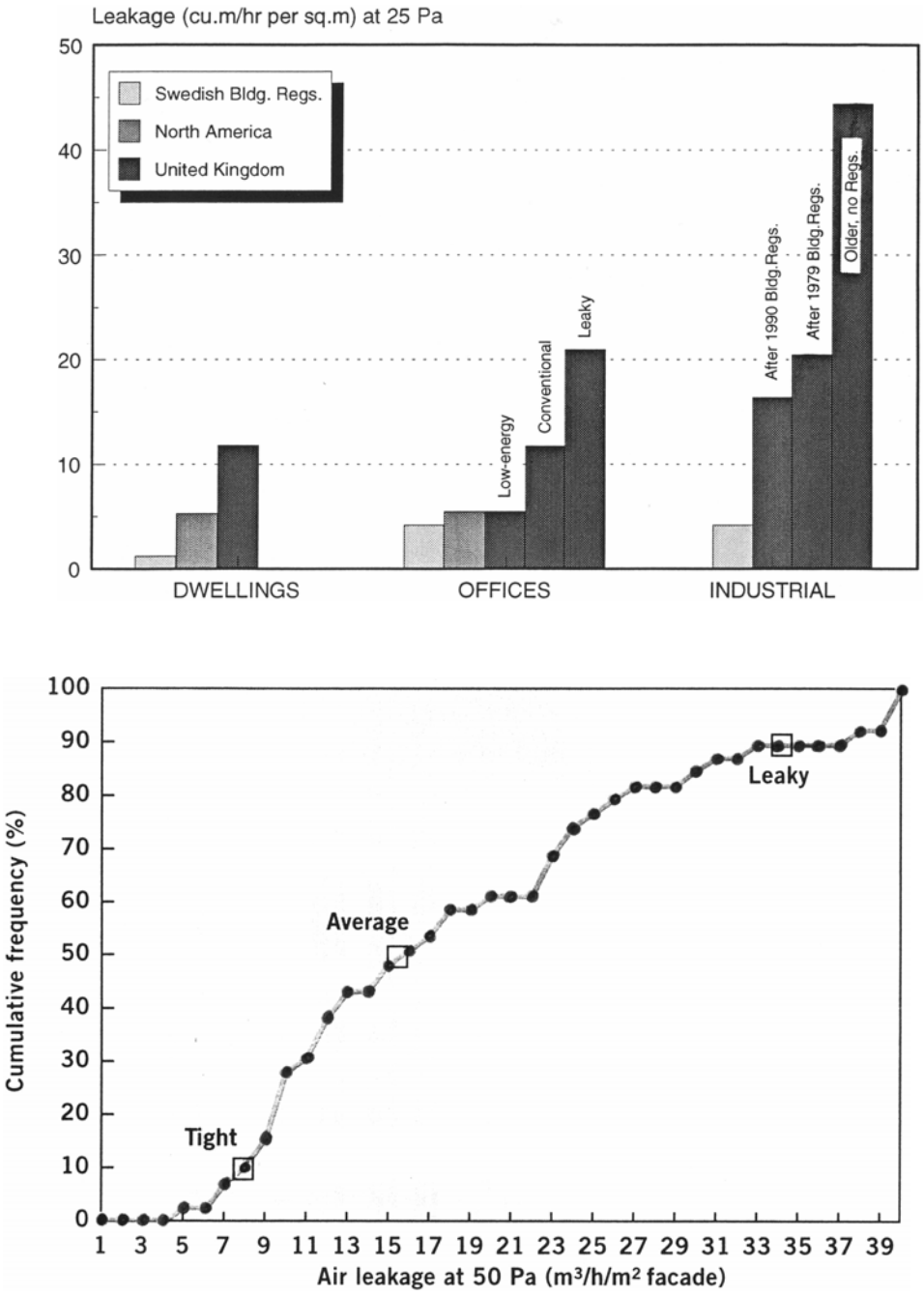

Figure 44. Measurements of Air Leakage Rates in Non-Domestic Buildings.
Upper: From Perera and Parkins (1992).
Lower: Compiled from BRE and BSRIA pressure Test Data (From Building Services Journal(1997)).

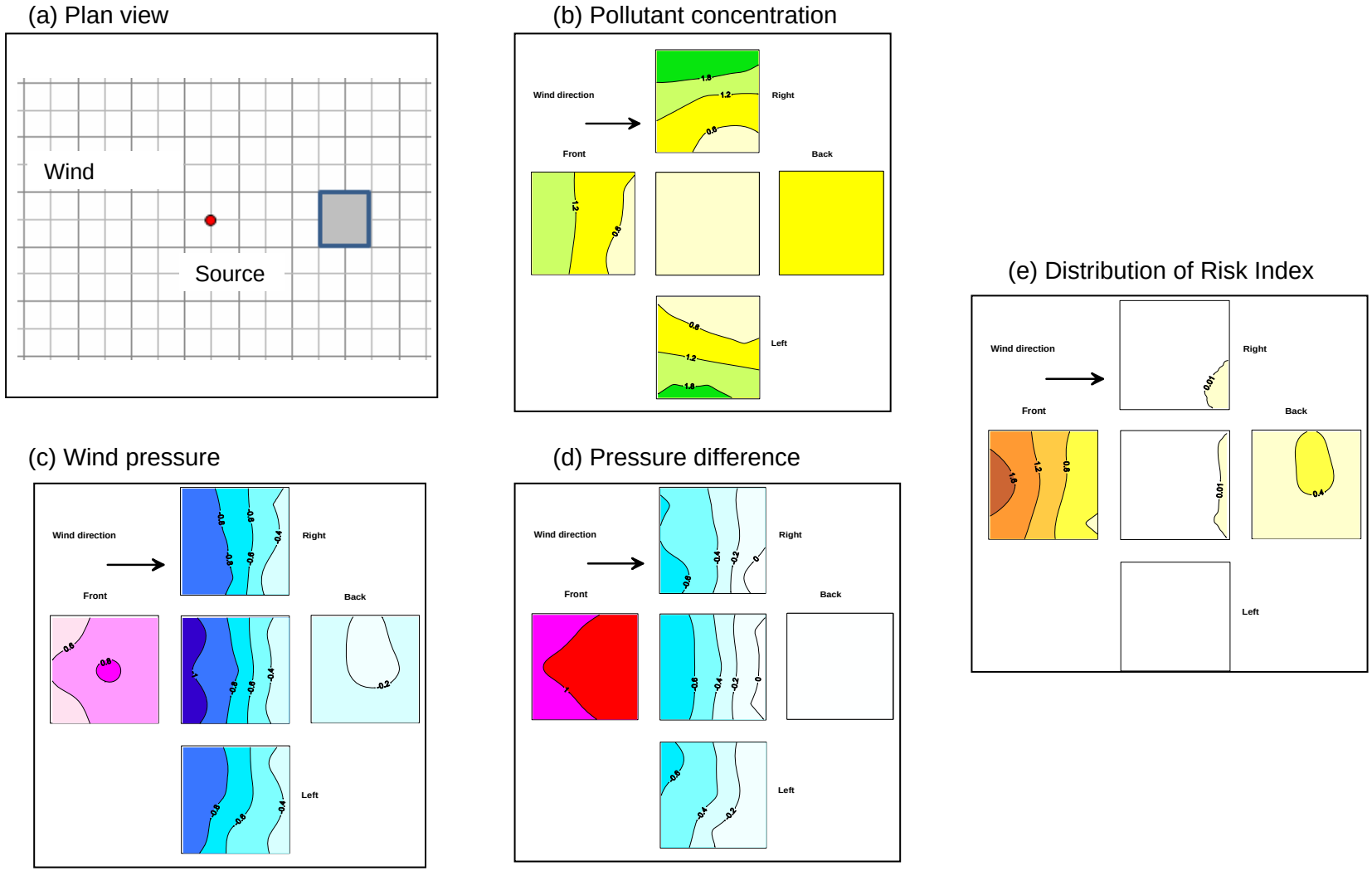

Figure 45. Example of Calculation of Risk of Ingress of Contaminants. Cubical Building in Open Terrain. From Cheng et al(2012a), Using Data From Hall et al(1999a).

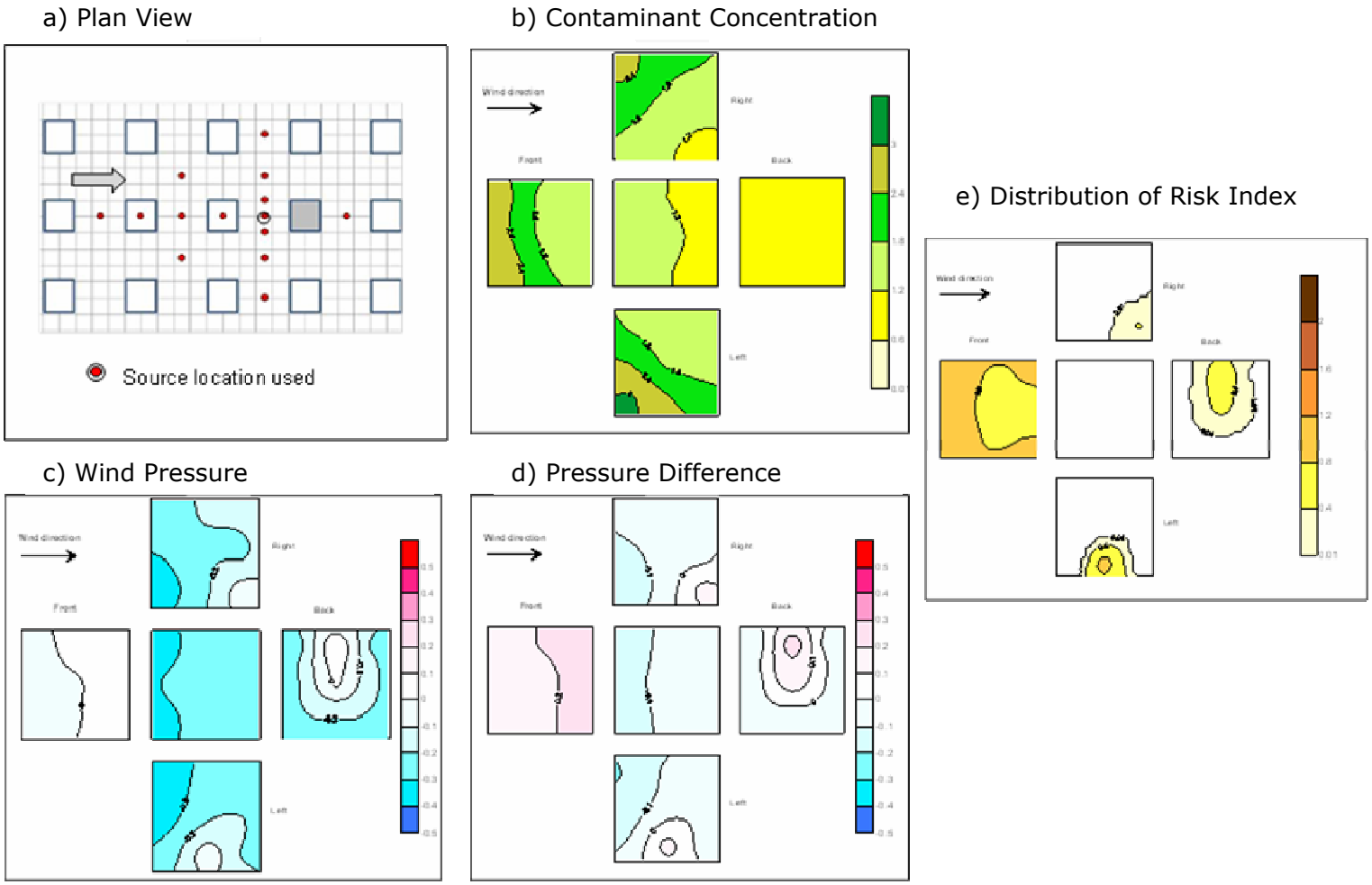

Figure 46. Example of Calculation of Risk of Ingress of Contaminants.. Cubical Building in Array of 16% Area Density. From Cheng et al(2012a), Using data From Hall et al(1999a).

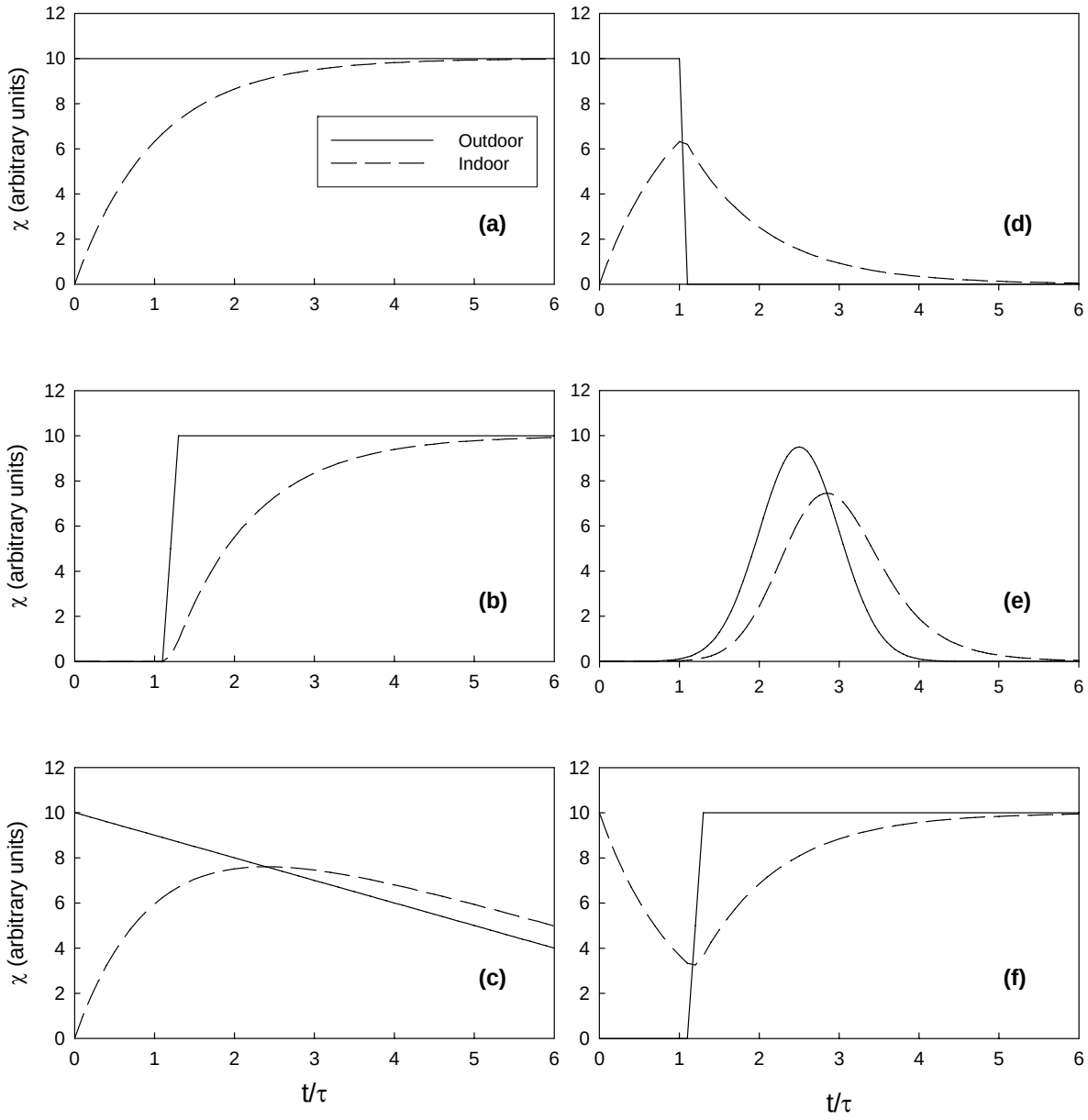

Figure 47. Examples of Internal Changes in Contaminant Concentration in a Well Mixed Internal Environment Due to External Changes in Concentration. See Text for Details.
The External Concentration is Assumed to be Uniformly Distributed Around the Building.
Following Wilson(1990).

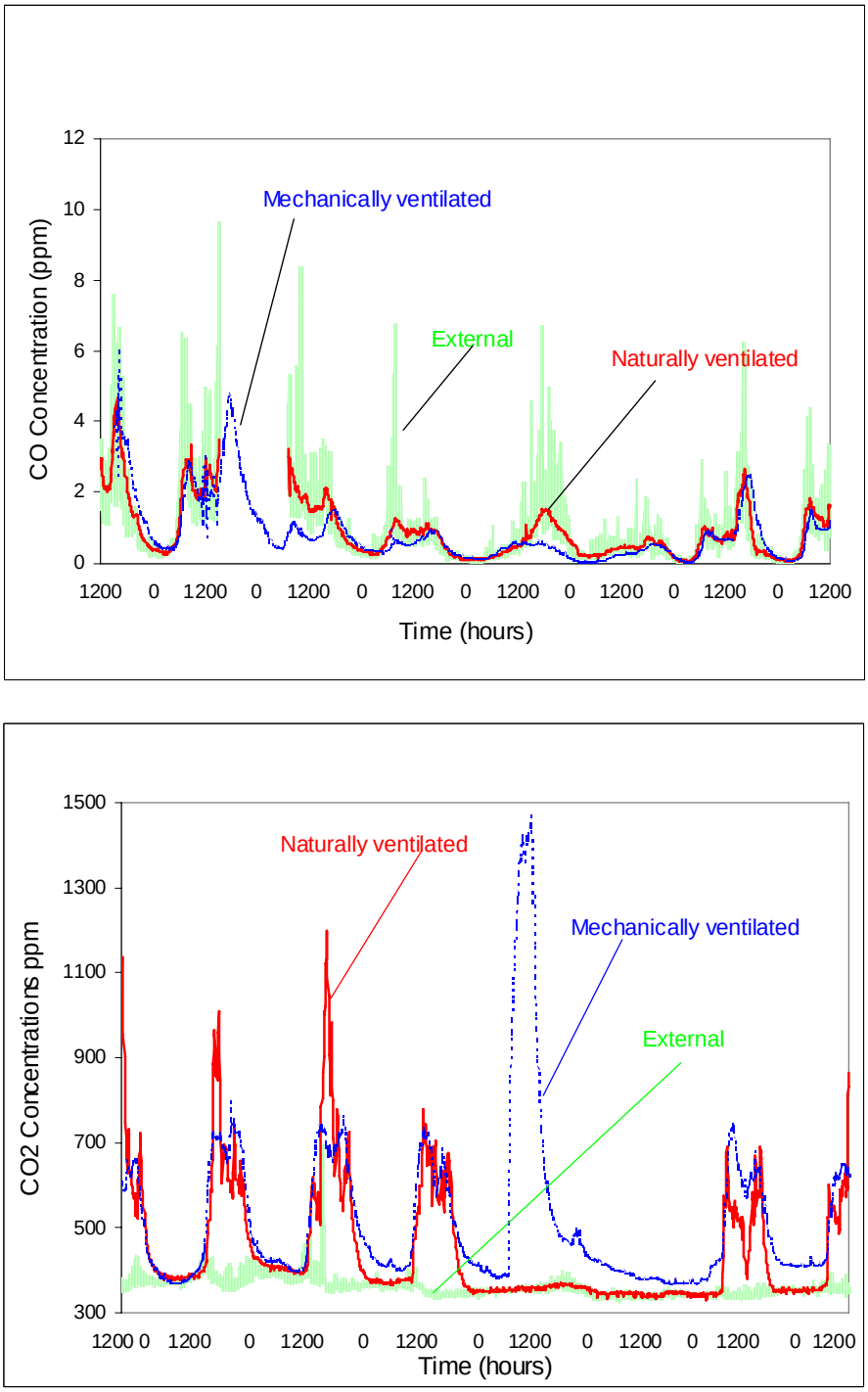

Figure 48. Examples of Measurements of Internal and External Concentrations of Unreactive Pollutants.
Upper: Externally Generated Carbon Monoxide.
Lower: Internally Generated Carbon Dioxide.
From Kukadia et al(1996).

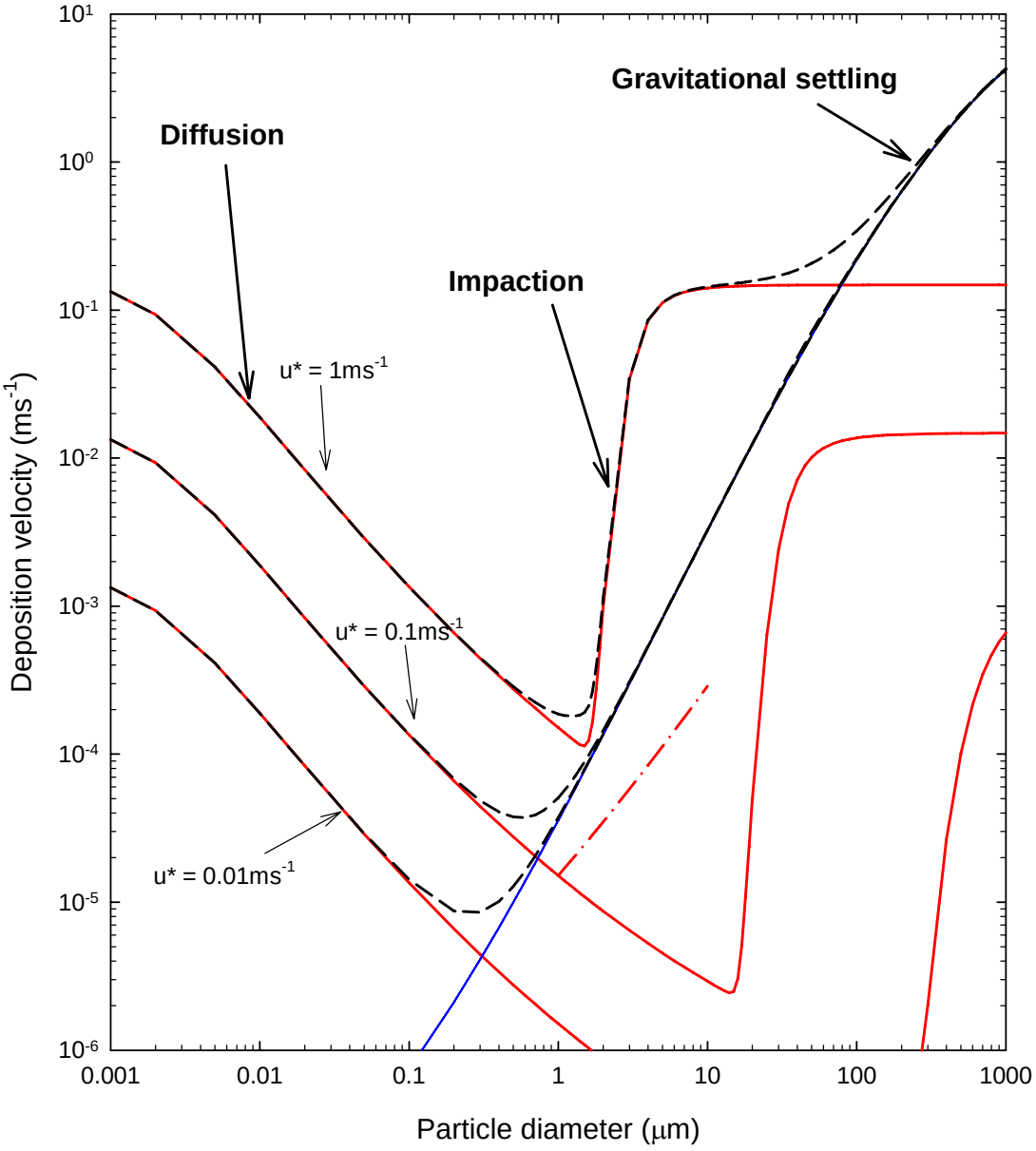

Figure 49. The Variation of Particle Deposition Velocity with Aerodynamic Diameter and the Different Processes Governing the Deposition. The Broken Line Shows the Overall Deposition Velocity. From Hall and Spanton(2004).

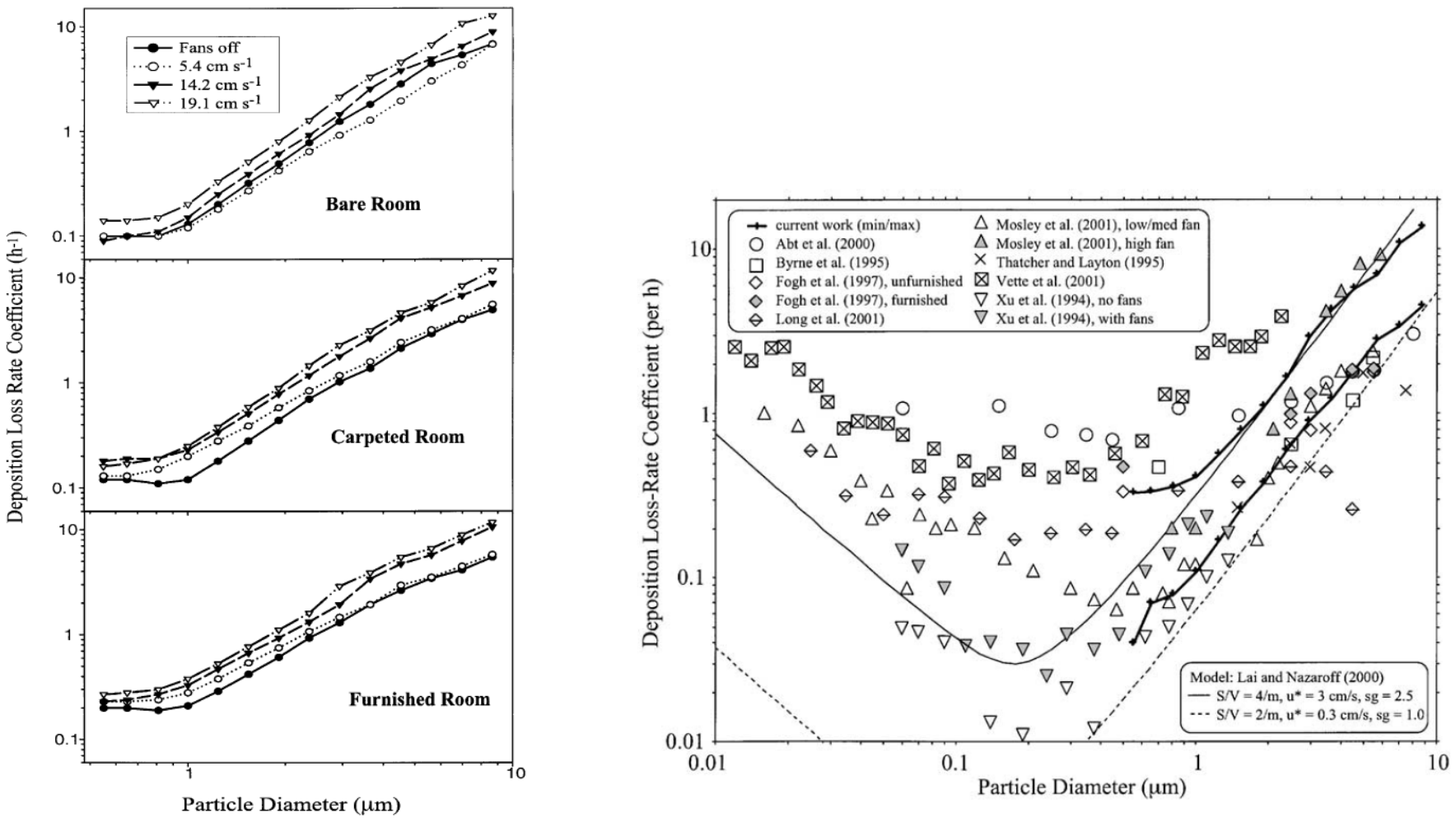

Figure50. Particle Loss rate Coefficients in Domestic Rooms.
Left: Data of Thatcher et al(2002).
Right: Data from Various Sources quoted by Thatcher et al(2002).
The Deposition Loss Rate Coefficient is the Time Equivalent of $1/\tau$ in Equation (13).

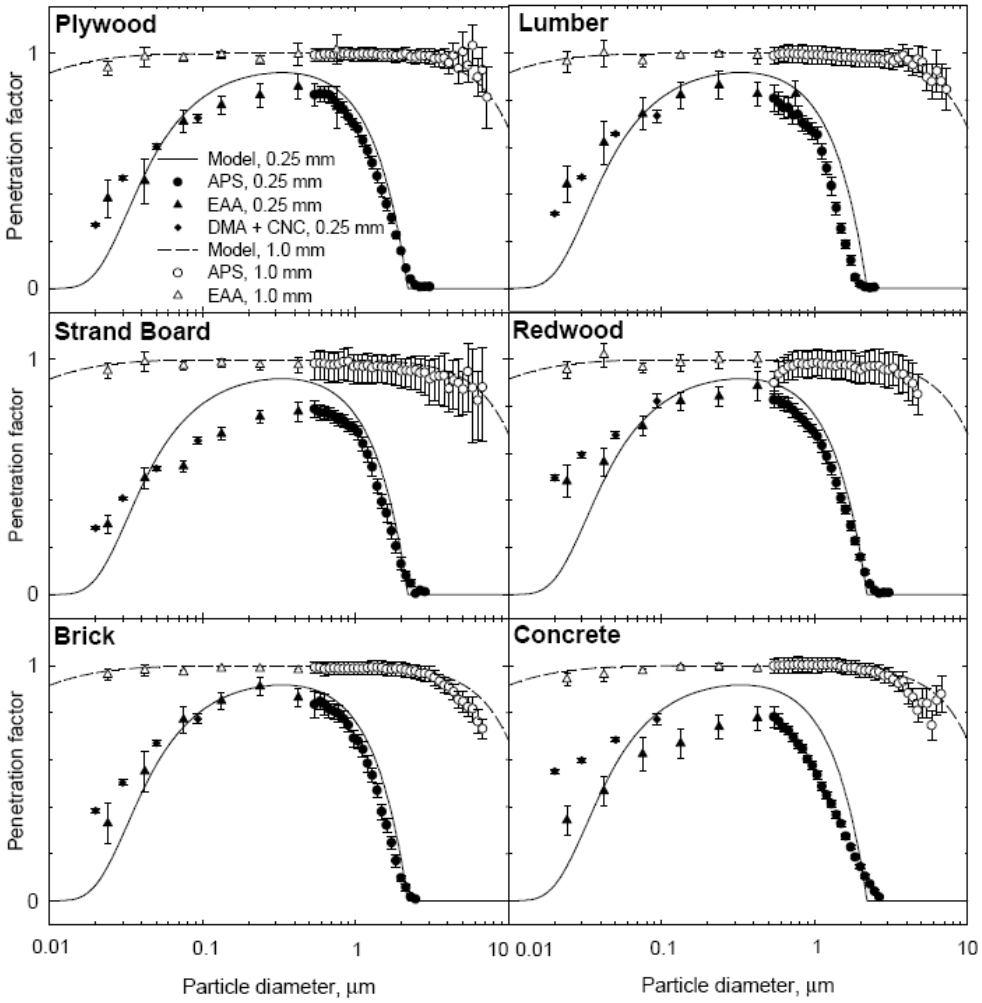

Figure 51. Particle Penetration Through Standard Cracks in Different Materials. From Liu and Nazaroff(2003).

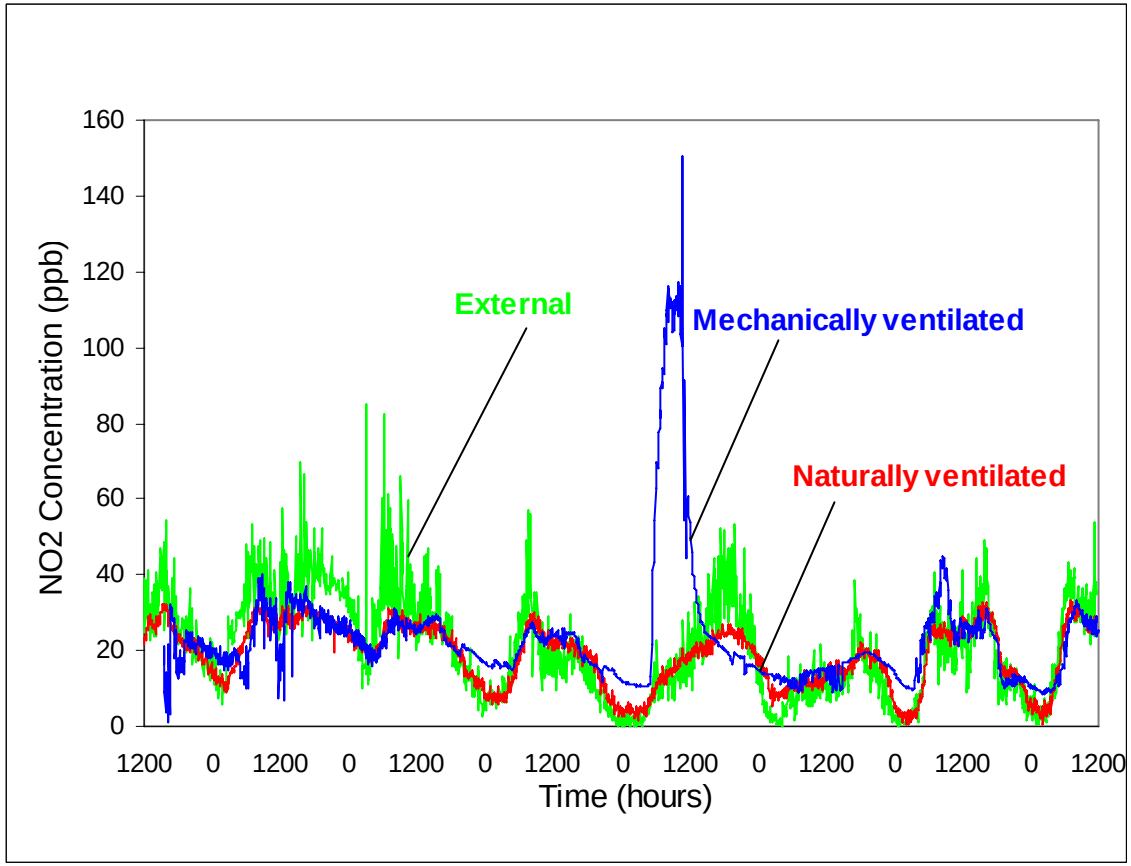

Figure 52. Internal and External Concentrations of a Reactive Pollutant (NO_2) From the Same Experiments as Figure 48. From Kukadia et al(1996).

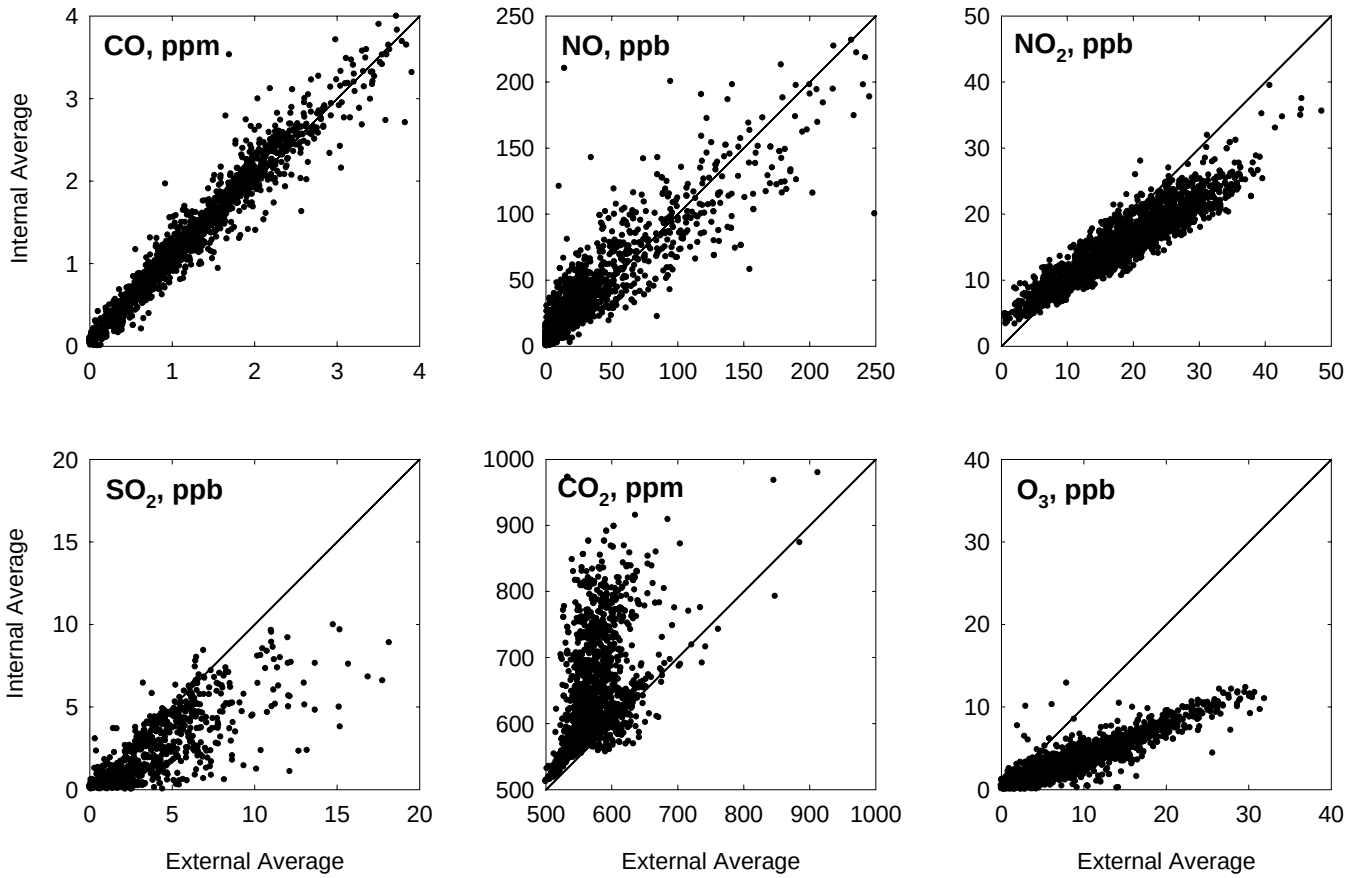

Figure 53. Paired Measurements of Mean Concentration of Air Pollutants Inside and Outside a Naturally Ventilated Laboratory Building in Manchester. From Kukadia et al(2000).

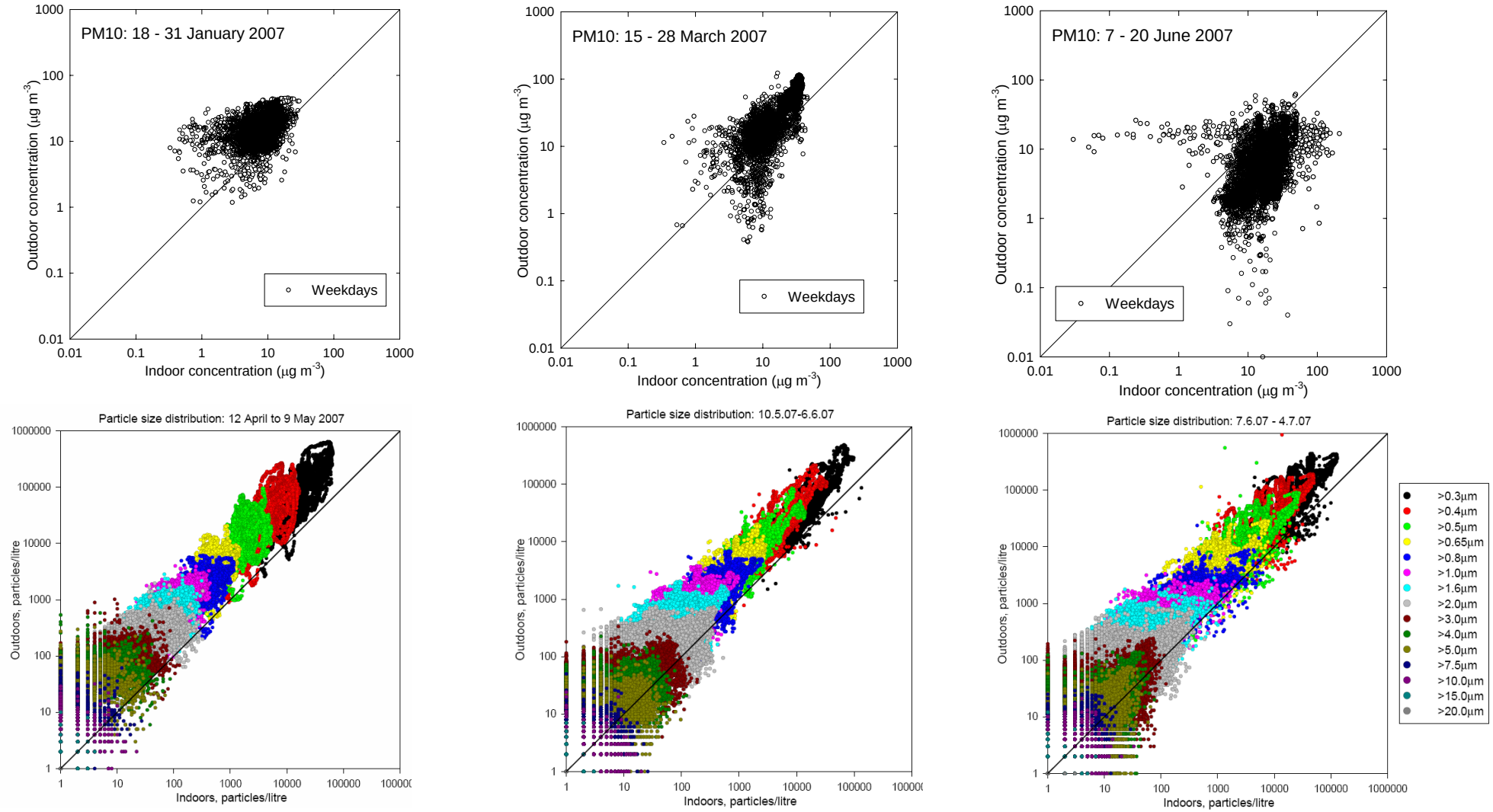

Figure 54. Paired Indoor and Outdoor Particle Mass Concentration (PM_{10}, Top) and Size Distribution (Bottom). Left to Right: Winter, Spring, Summer. From Measurements on a Commercial Office Building in London by Kukadia et al(2011b)).

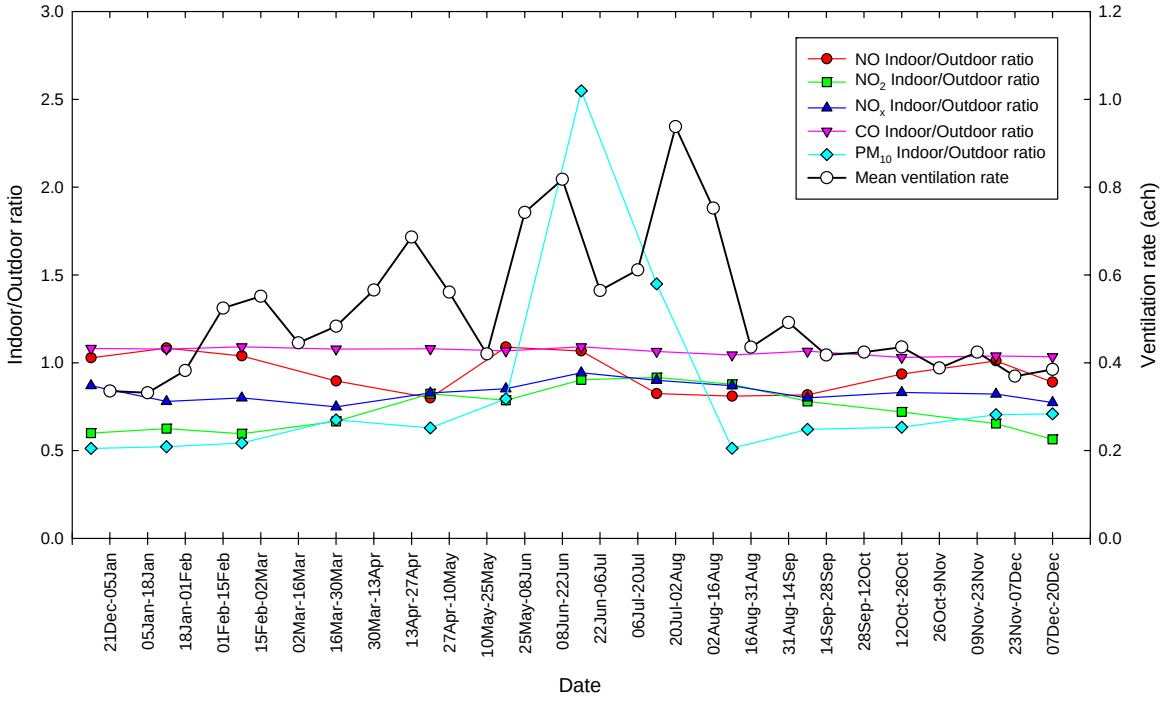

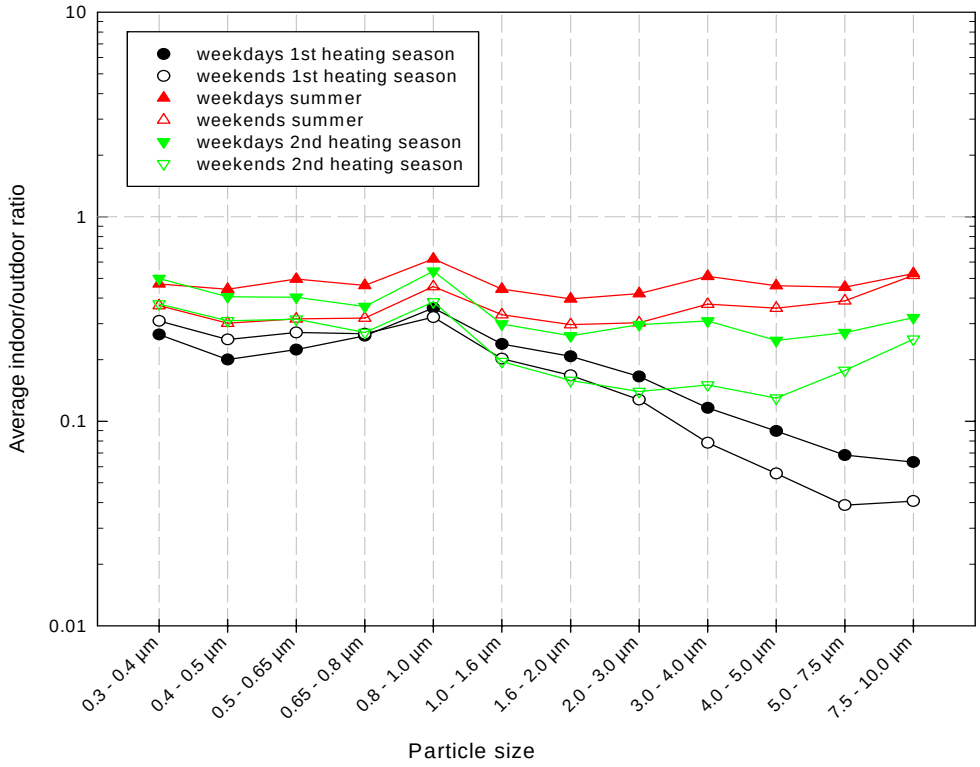

Figure 55. Averaged Ratios of Indoor/Outdoor Concentrations of Pollutant Gases (Top) and Particles by Size Range (Bottom). From Measurements on a Commercial Office Building in London by Kukadia et al(2011b).